NATIONAL CENTER FOR EARTHQUAKE ENGINEERING RESEARCH
Headquartered at the State University of New York at Buffalo

ISSN 1088-3800

PB98-153455

Seismic Evaluation of Frames with Infill Walls Using Quasi-static Experiments

by

Khalid M. Mosalam, Richard N. White and Peter Gergely
Cornell University
School of Civil and Environmental Engineering
Ithaca, New York 14853

Technical Report NCEER-97-0019

December 31, 1997

This research was conducted at Cornell University and was supported in whole or in part by the National Science Foundation under Grant No. BCS 90-25010 and other sponsors.

NOTICE

This report was prepared by Cornell University as a result of research sponsored by the National Center for Earthquake Engineering Research (NCEER) through a grant from the National Science Foundation and other sponsors. Neither NCEER, associates of NCEER, its sponsors, Cornell University, nor any person acting on their behalf:

a. makes any warranty, express or implied, with respect to the use of any information, apparatus, method, or process disclosed in this report or that such use may not infringe upon privately owned rights; or

b. assumes any liabilities of whatsoever kind with respect to the use of, or the damage resulting from the use of, any information, apparatus, method, or process disclosed in this report.

Any opinions, findings, and conclusions or recommendations expressed in this publication are those of the author(s) and do not necessarily reflect the views of NCEER, the National Science Foundation, or other sponsors.

NATIONAL CENTER FOR EARTHQUAKE ENGINEERING RESEARCH
Headquartered at the State University of New York at Buffalo

Seismic Evaluation of Frames with Infill Walls Using Quasi-static Experiments

by

K.M. Mosalam[1], R.N. White[2] and P. Gergely[3]

Publication Date: December 31, 1997
Submittal Date: July 21, 1997

Technical Report NCEER-97-0019

NCEER Task Numbers 93-3111, 94-3111, 94-3112 and 95-3111

NSF Master Contract Number BCS 90-25010

1 Assistant Professor, Department of Civil and Environmental Engineering, University of California, Berkeley; former Lecturer, School of Civil and Environmental Engineering, Cornell University
2 James A. Friend Family Professor of Engineering, School of Civil and Environmental Engineering, Cornell University
3 Professor of Structural Engineering (deceased), School of Civil and Environmental Engineering, Cornell University

NATIONAL CENTER FOR EARTHQUAKE ENGINEERING RESEARCH
State University of New York at Buffalo
Red Jacket Quadrangle, Buffalo, NY 14261

PREFACE

The National Center for Earthquake Engineering Research (NCEER) was established in 1986 to develop and disseminate new knowledge about earthquakes, earthquake-resistant design and seismic hazard mitigation procedures to minimize loss of life and property. The emphasis of the Center is on eastern and central United States *structures*, and *lifelines* throughout the country that may be exposed to any level of earthquake hazard.

NCEER's research is conducted under one of four Projects: the Building Project, the Nonstructural Components Project, and the Lifelines Project, all three of which are principally supported by the National Science Foundation, and the Highway Project which is primarily sponsored by the Federal Highway Administration.

The research and implementation plan in years six through ten (1991-1996) for the Building, Nonstructural Components, and Lifelines Projects comprises four interdependent elements, as shown in the figure below. Element I, Basic Research, is carried out to support projects in the Applied Research area. Element II, Applied Research, is the major focus of work for years six through ten for these three projects. Demonstration Projects under Element III have been planned to support the Applied Research projects and include individual case studies and regional studies. Element IV, Implementation, will result from activity in the Applied Research projects, and from Demonstration Projects.

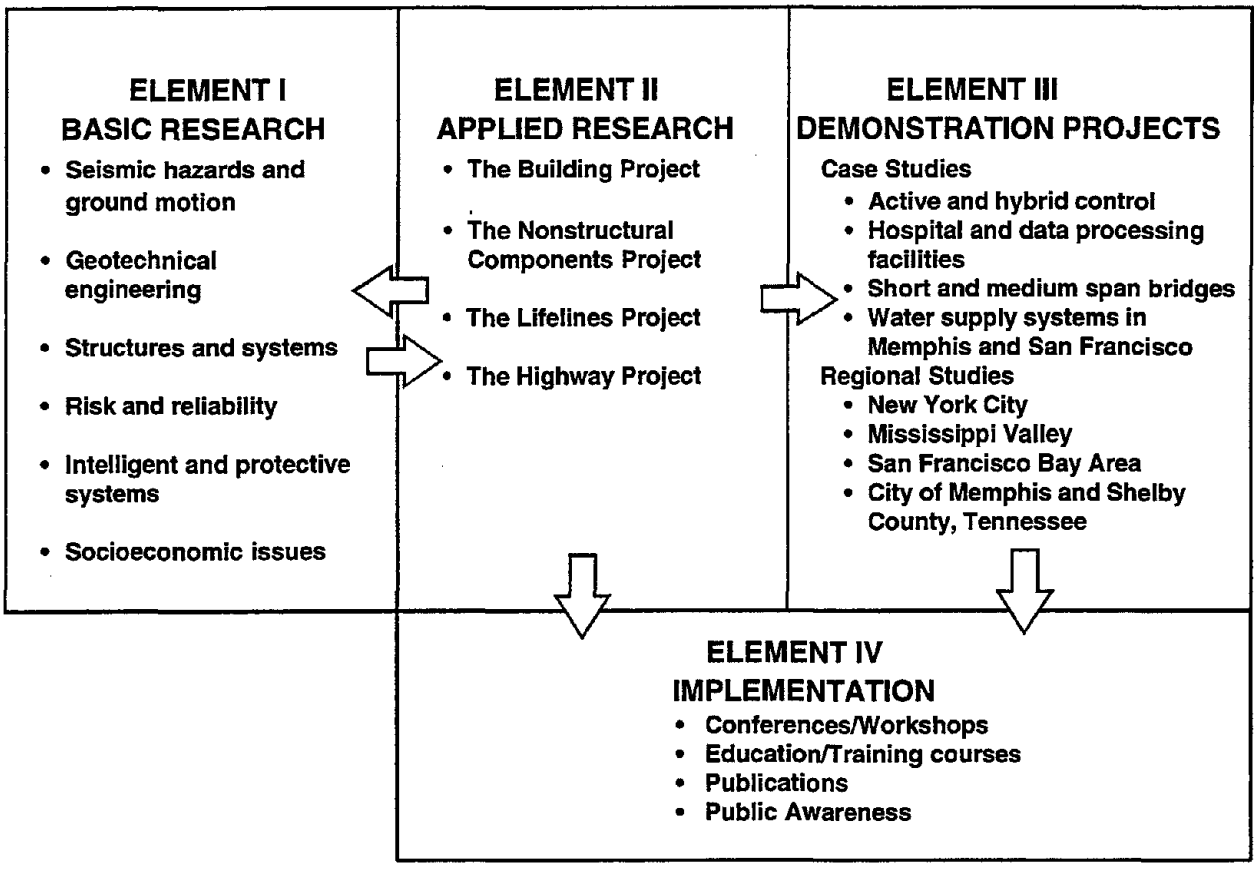

Research in the **Building Project** focuses on the evaluation and retrofit of buildings in regions of moderate seismicity. Emphasis is on lightly reinforced concrete buildings, steel semi-rigid frames, and masonry walls or infills. The research involves small- and medium-scale shake table tests and full-scale component tests at several institutions. In a parallel effort, analytical models and computer programs are being developed to aid in the prediction of the response of these buildings to various types of ground motion.

Two of the short-term products of the **Building Project** will be a monograph on the evaluation of lightly reinforced concrete buildings and a state-of-the-art report on unreinforced masonry.

The **structures and systems program** constitutes one of the important areas of research in the **Building Project**. Current tasks include the following:

1. Continued testing of lightly reinforced concrete external joints.
2. Continued development of analytical tools, such as system identification, idealization, and computer programs.
3. Perform parametric studies of building response.
4. Retrofit of lightly reinforced concrete frames, flat plates and unreinforced masonry.
5. Enhancement of the IDARC (inelastic damage analysis of reinforced concrete) computer program.
6. Research infilled frames, including the development of an experimental program, development of analytical models and response simulation.
7. Investigate the torsional response of symmetrical buildings.

This work proposes a model of behavior of mortar joints including fracture after a peak of nonlinear strength is achieved. The model is calibrated using information from rigorous testing of masonry subcomponents and materials. The model was used in a finite element analysis using a complex computational platform, DIANA, to determine the contribution of masonry infills to the behavior of framed structures. The analytical method of super-convergent path recovery is compared with a smeared crack model approach and with experiments (pseudo-dynamic and seismic simulation using the shaking table). The model was then used to generate fragility curves for infill frames with various properties resulting from variability of materials and modeling parameters. The work presents a comprehensive analytical and experimental approach which allows a complete picture of advanced analysis of masonry structures. The work integrates the efforts of NCEER in seismic loss assessment, providing reliable fragility curves for the probabilistic cost analysis. The work was part of phase one of "Loss Assessment of Memphis Buildings," and provides a strong engineering basis for the evaluation.

ABSTRACT

This report treats an experimental investigation of gravity load designed steel frames, *i.e.* steel frames with semi-rigid connections, infilled with unreinforced masonry walls and subjected to slowly applied cyclic lateral loads. An investigation of the mechanical properties of the materials used in constructing the masonry infill walls is included. Various geometrical configurations of the frame and the infill walls, and different material types of the masonry walls, are considered. Based on the results, a hysteresis model for infilled frames is formulated and discussed. All parameters in the model have physical meaning and are calibrated with experimental data.

ACKNOWLEDGEMENTS

The financial support of the National Center for Earthquake Engineering Research, Buffalo, New York is gratefully acknowledged. The experimental work of this study was conducted in the George Winter Structural Laboratory at Cornell University. The assistance of Timothy K. Bond, the laboratory manager, are acknowledged.

TABLE OF CONTENTS

TABLE OF CONTENTS (Cont'd)

LIST OF ILLUSTRATIONS

LIST OF ILLUSTRATIONS (Cont'd)

LIST OF ILLUSTRATIONS (Cont'd)

LIST OF TABLES

SECTION 1

INTRODUCTION

A common type of construction in urban centers is low-rise and mid-rise building frames with unreinforced masonry walls filling the spaces bounded by their structural members. The walls, usually referred to as infill walls, are built after the frame is constructed as partitions or as cladding. Unreinforced masonry infill walls are usually classified as non-structural components, *i.e.* their structural contribution is neglected during the design process of the frames. Under this assumption, the bounding structural frame should be designed to withstand *all* forces: vertical due to gravity loads and lateral due to wind pressure and/or seismic ground motion.

Ignoring the contributions of infill walls during the design of the bounding frames may lead to erroneous design as the frame/wall interaction under extreme loading conditions always occurs. The effects of neglecting the infill walls are accentuated in high seismicity regions where the frame/wall interaction may cause substantial increase of stiffness resulting in possible changes in the seismic demand due to the significant reduction in the natural period of the structural system. Also, the composite action of the frame/wall system changes magnitude and distribution of straining actions in the frame members, *i.e.* critical sections in the infilled frame differ from those of the bare frame, which may lead to unconservative or poorly detailed designs. Moreover, these designs may be uneconomical since an important source of structural strength (particularly beneficial in regions of moderate seismicity) is wasted.

As a matter of fact, there is no resemblance between the responses of the infilled frame and the bare one, as the former is substantially stronger and stiffer than the latter. The performance shown by infilled frames is advantageous especially when the capacity (and ductility) of the frame itself is suspected to be inadequate. This is the case of frames mainly designed for gravity loads without or with little attention to lateral loads (usually due to wind effects) when subjected to moderate or severe lateral loads due to earthquakes.

Lessons from recent damaging earthquakes illustrate the consequence of ignoring the contribution of infill walls. In some cases, the real structure (*i.e.* the infilled frame) is subjected to demands smaller than those considered during design. Unfortunately, in other cases, the contrary occurs, *i.e.* design forces may be significantly exceeded increasing the seismic damage vulnerability of the structure. In all cases, the changes in the distribution of straining actions may render the structural detailing ineffective.

The problem of considering infill walls in the design process is partly attributed to incomplete knowledge of the behavior of *quasi-brittle* materials such as masonry and to a lack of conclusive experimental and analytical results to substantiate a reliable design procedure for this type of structure.

A series of three reports addresses the definition and investigation of experimental and computational strategies to evaluate the behavior of infilled frames subjected to earthquake loading. These reports are based on a study at Cornell University which is divided into three parts as schematically illustrated in Figure 1-1. In **Part I**, the static experiments on infilled frames are presented together with an investigation of the properties of concrete block masonry and its constituents. In **Part II**, the pseudo-dynamic experimentation and the corresponding results for a two-story infilled frame are presented. Finally, in **Part III**, different computational strategies are introduced and critically investigated.

This report, which is the first in the series, outlines the static experiments conducted on masonry and on frames infilled with masonry walls. **SECTION 2** describes the geometrical, physical and mechanical properties of masonry constituents (*i.e.* concrete blocks and mortar), masonry subassemblages (*e.g.* prisms) and the block/mortar joint behavior. **SECTION 3** is devoted to the description of the quasi-static experimental approach for gravity load designed steel frames, *i.e.* steel frames with semi-rigid connections, infilled with unreinforced masonry walls. In this investigation, various geometrical configurations were treated where different shapes of openings were introduced in the wall panels. In **SECTION 4**, the results of the quasi-static experiments on infilled frames are presented and a hysteresis model for infilled frames is formulated and discussed. In this model, all parameters have physical meaning and are calibrated by means of the experimental data. Finally, concluding remarks are given in **SECTION 5**.

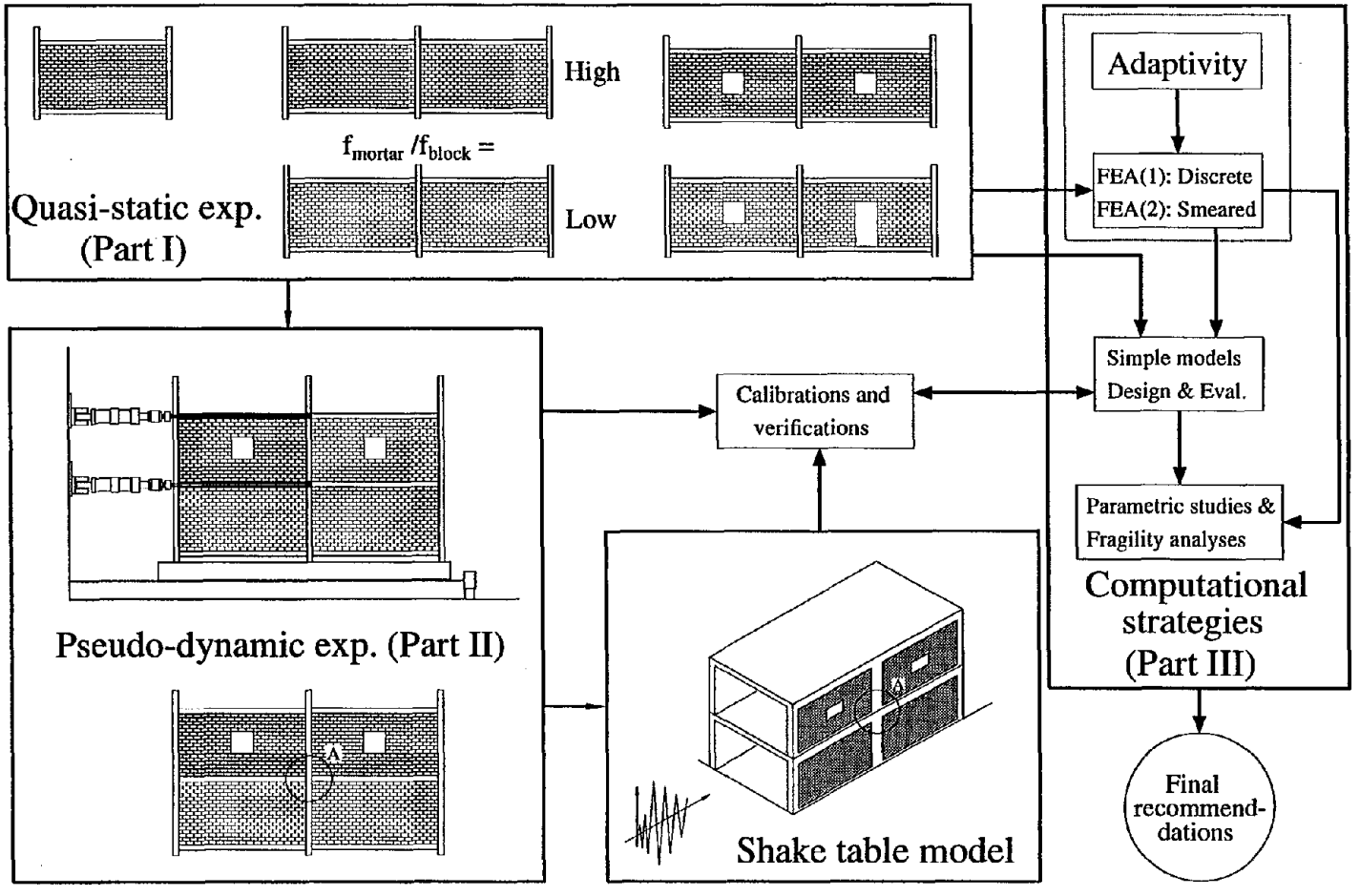

A: Typical lightly reinforced concrete joint detail, f: Compressive strength, FEA: Finite Element Analysis

FIGURE 1-1 Study program of infilled frames.

SECTION 2

PROPERTIES OF MATERIALS

Several reduced scale frames with masonry infill walls were tested in the present study. This section deals with the experimental investigation of the geometrical, physical and mechanical properties of the materials used in constructing the model infilled frames. Properties of masonry constituents (*i.e.* concrete block and mortar) and masonry assemblages are emphasized.

From a theoretical point of view, the optimum modeling technique is the one leading to "true" models[1], *i.e.* models which can predict the *elastic* and the *inelastic* behavior including failure.

The main objectives of testing the reduced scale structures were to understand how frames interact with their infills and to obtain experimental data for calibrating analytical models of the infill walls and/or the infilled frame. Complying with these objectives, it was decided that the sophistication involved in arriving at true models was not necessary. Therefore, the models and their material were intended for pragmatic manifestation of the structural response of infilled frames from a qualitative point of view.

Three groups of masonry constituents were considered in the study of frames infilled with masonry walls, namely,

- Group A: weak blocks/strong mortar joints
- Group B: weak blocks/moderate strength mortar joints
- Group C: moderate strength blocks/strong mortar joints

The present study emphasizes the experimental results obtained using the more typical material combinations of groups B and C. Results of group A are documented in references [82] [25] and [55].

2.1 Concrete Block Masonry

Masonry is normally laid of rectangular units of different materials, shapes and sizes. The common types of units are clay bricks, clay tiles, concrete blocks, light weight cellular concrete blocks, sand-lime bricks and natural building stones. Ungrouted (*i.e.* hollow) concrete block units were used herein.

[1]For true models, all similitude requirements for geometry, materials and loading must be obeyed. For that purpose, the theory of dimensional analysis is usually used. An extensive discussion of the similitude requirements for masonry can be found in references [9], [30] and Section 2.5.2 of reference [62].

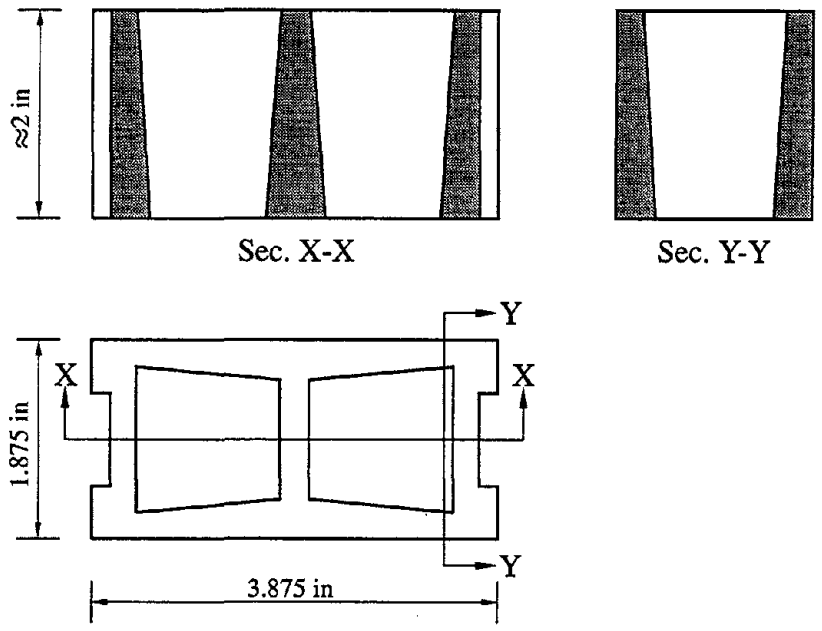

FIGURE 2-1 Typical geometry of the quarter scale concrete blocks.

2.1.1 Block manufacturing

The concrete blocks are made up of mason sand, type I Portland cement and fly ash. The following steps summarize the manufacturing process of the model concrete block masonry[2].

1. The ingredients are mixed in a Hobart mixer and deposited into hand tamped machine which contains the block mold.
2. The block molds are vibrated until the mixture becomes solid.
3. The blocks are put on pallets in a curing chamber where a trough of warm water is placed on the floor to keep the area warm and moist.
4. After the blocks are cured for a specific amount of time (about 24 hours), they are left to dry.

The blocks are one quarter scale models of an eight inch, two core stretcher with mortar grooves. The face shell and the intermediate webs are tapered as shown in Figure 2-1. The block height does not have a control factor and varies slightly.

[2]Information provided by BESSER company of Alpena, Michigan is acknowledged.

2.1.2 Physical and geometrical properties

The physical and geometrical properties of the model concrete block units were obtained according to the ASTM C-140 [2]. The determined properties include the average net and gross areas, the unit weight, the moisture content[3] and the water absorption[4].

Six units were randomly chosen from a sample of 100 units. Width, height and length were measured at mid points and end points of adjoining sides and the average was calculated. Face shell thickness was measured along the perimeter of the upper and lower bearing surfaces. From the measurements, the gross area was 7.4 in^2 whereas the net area was 3.9 in^2, *i.e.* the percent of solids was 53%. The average face shell area was 2.3 in^2 with face shell percentage of 31% of the gross area. Based on the net volume of the block, the unit weight was 128 pcf.

The same six units used for the geometrical measurements were also considered for the determination of the physical material properties. The average properties for the absorption and moisture content were calculated using the mean values of dimensions and weights. The moisture content and water absorption were found to be 12% and 16 pcf, respectively.

2.1.3 Mechanical properties

Compressive strength is usually the most important characteristic of quasi-brittle materials (*e.g.* concrete, mortar, masonry or ceramics). In determining the compressive strength of the concrete block units, the requirements of the ASTM C-140 [2] were followed. Units were capped with Hydrostone[5] at top and bottom for the purpose of achieving uniform stress on the bearing surfaces. The capped model unit was tested under axial compression using a Baldwin universal testing machine (maximum capacity = 60 kips). The loading rate was adjusted such that failure load was obtained within 2-3 minutes. Vertical displacement was measured using 2 LVDT's[6], one mounted at the center of each face shell of the block. These two displacement measurements were converted into axial strains by dividing by the gage lengths of the LVDT's and then the average strain was calculated. The corresponding stress was determined based on the net area of the unit. The experimental scatter of the stress-strain relations of the weak and moderate strength model blocks is shown in Figure 2-2.

[3]Moisture content is the difference between the sampled weight and the dry weight density.
[4]Water absorption represents the difference between the wet weight density and the dry weight density.
[5]Hydrostone is a trade name of the U.S. Gypsum Corporation.
[6]LVDT = Linear Variable inductance Differential Transformer.

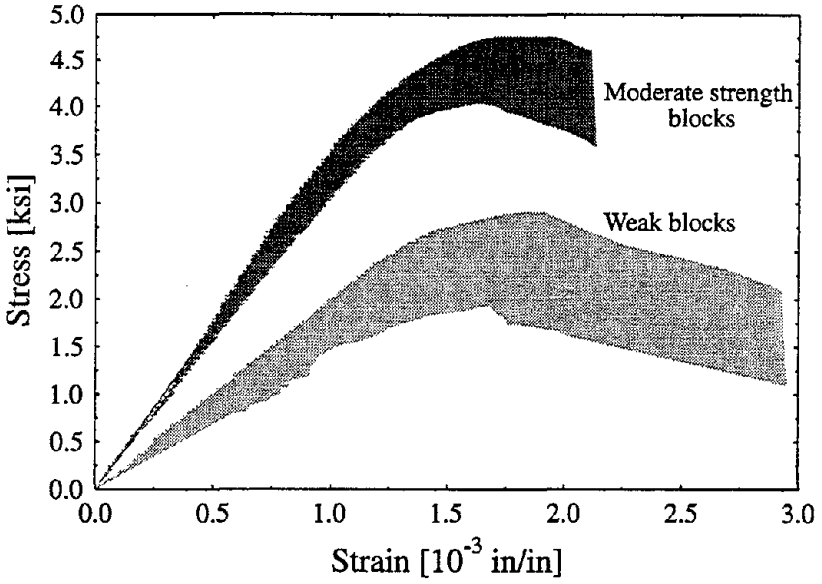

FIGURE 2-2 Stress-strain relations of model concrete blocks.

TABLE 2-I Mechanical properties of concrete blocks.

Type	NS	f_b [ksi]	ϵ_b^{peak}	E_b [ksi]
Moderate strength	10	4.2 ± 0.8	0.0017	3200
Weak strength	34	2.0 ± 0.9	0.0018	1600

The predominant failure mode of the concrete blocks was *compression shear* through the thickness of the webs and face shells. Horizontal splitting of one end web was evident in almost all specimens. This asymmetrical horizontal splitting can be attributed to load eccentricity. Attempts to eliminate such eccentricity were not completely successful. From Figure 2-2, one may observe that there was little warning at ultimate load of impending failure for the moderate strength blocks. This brittle behavior was accompanied by an explosive release of energy. A summary of the compressive strength (f_b), strain at the peak stress (ϵ_b^{peak}) and stiffness[7] (E_b) of the concrete blocks is presented in Table 2-I together with the number of tested specimens (NS) for each type of block. The material properties listed in Table 2-I are given as the mean values except f_b which is listed as the mean $\pm$ the standard deviation. One may clearly notice that the experimental scatter of the weak blocks (COV[8] = 45%) is much higher than the scatter of the moderate strength blocks (COV = 19%). This may be attributed to lower quality control in manufacturing the weak blocks (*e.g.* less vibrations of the molds).

[7]The term stiffness is used rather than the elastic modulus to emphasize the fact that such quantity is highly dependent upon the geometry of the block. Therefore, it is not solely a material parameter.

[8]COV = Coefficient Of Variation = $\frac{\text{standard deviation}}{\text{mean}} \times 100\%$.

TABLE 2-II Mix proportions for the model mortar types.

Type	Cement	Lime	Aggregate
S	1.0	0.21	3.83
N	1.0	0.50	4.50

2.2 Model Mortar

Historically, the original purpose of mortar in masonry structures was to fill the irregularities between the masonry units. Architecturally, mortar joints provide resistance to the penetration of light, wind and water. Structurally, mortar joints bond the masonry units together and help add strength to the masonry structures. The infill walls of the tested structures were constructed using the previously discussed concrete blocks bonded together with cement-lime mortar.

2.2.1 Model mortar proportions

The model mortar materials included Portland cement type III (*i.e.* high early strength) and hydrated lime. The aggregate was commercially obtained natural masonry sand having the gradation curves shown in Figure 2-3. As shown in this figure, two gradation curves were adopted for the two mortar types used in the present study. These mortar types, namely, moderate strength and strong, are basically the respective replicas of types N and S indicated by ASTM C-270 [2]. The method used in scaling the size of the aggregate was to remove the undesired coarse parts of the same aggregate. In the present study, the geometrical scale factor (S_l) was selected to be 4. Accordingly, the particles retained on U.S. sieve #16 (rather than #4) were removed. This modified gradation satisfied the similitude requirements as well as the requirements of ASTM C-144 [2]. Also, these aggregate sizes were appropriate for model joint thickness of 3/32 inch[9] scaled down from the commonly used 3/8 inch thickness.

Based on several trial batches and following the procedures given in ASTM C-270 [2], the mix proportions (given by weight) shown in Table 2-II were used for the two mortar types. Water was added to the dry mixes and a relatively high water/cement ratio (≈ 1.2) was needed to provide sufficient workability.

[9]Although all possible precautions were taken to obtain such small joint thickness, it was realized that the obtained joint thickness was sometimes larger than the required thickness. In general, the joint thickness in the constructed models varied from 3/32 inch to 5/32 inch.

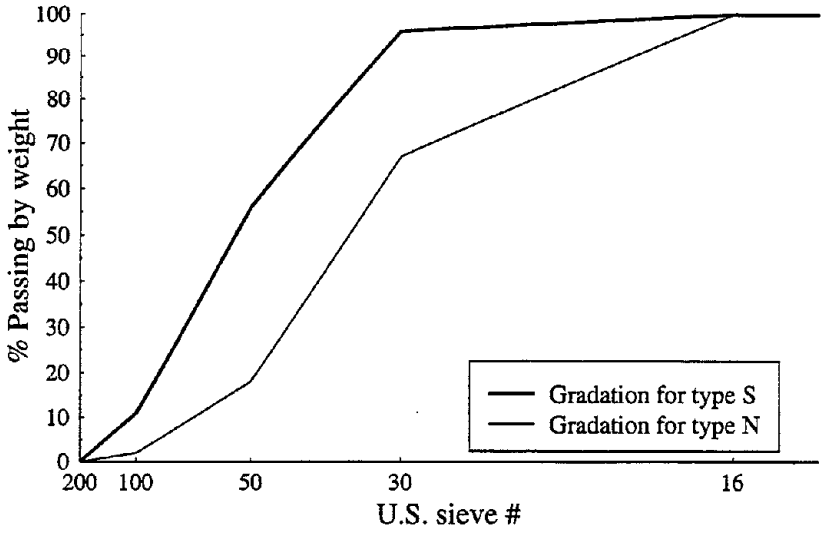

FIGURE 2-3 Aggregate gradation curves for model mortar.

2.2.2 Mechanical properties

For the quality control of the mortar, two types of specimens were cast: 2 inch mortar cubes for compression tests and 2 inch diameter by 4 inch high cylinders for splitting tension tests and also for compression tests. From each batch of the mortar used in the construction of the models, at least 6 cylinders and 3 cubes were cast. Half of the cylinders were tested in compression and the other half in splitting tension. Testing of the quality control specimens was performed at approximately the same age as the corresponding infill walls. All control specimens were air cured in the laboratory under the same conditions as the infill walls. Figure 2-4 shows typical results of a cylinder made of mortar type N. To obtain the complete stress-strain relation in compression, several loading/unloading cycles, under load control experiments, were applied as shown in Figure 2-4. Assuming the same modulus of elasticity in tension as in compression, the results of the splitting tension test are also included in Figure 2-4.

A comparison between the envelopes of the stress-strain relations in compression for mortar types S and N is shown in Figure 2-5, which shows the superior stiffness[10] and strength of the mortar type S. Table 2-III summarizes the mechanical results for both mortar types. The listed properties are the compressive strengths obtained from the cylinders (f_{cyl}) and cubes (f_{cube}), the splitting tensile strength (f_{sp}), the Young's modulus obtained from the mortar cylinders (E_{mor}) and the ratios between f_{cyl} and f_{cube} and that between f_{sp} and $\sqrt{f_{cyl}}$. In this table, the listed values are the mean of all the tested specimens.

[10]It is suspected that for type N specimens, the measured strain was slightly overestimated because it was based on the relative displacement of the testing machine cross heads which implies that the deformation due to the flexibility of the loading frame was included in the measured displacements. This situation was rectified for type S specimens where measurements were directly taken from the specimens using an accurate extensometer.

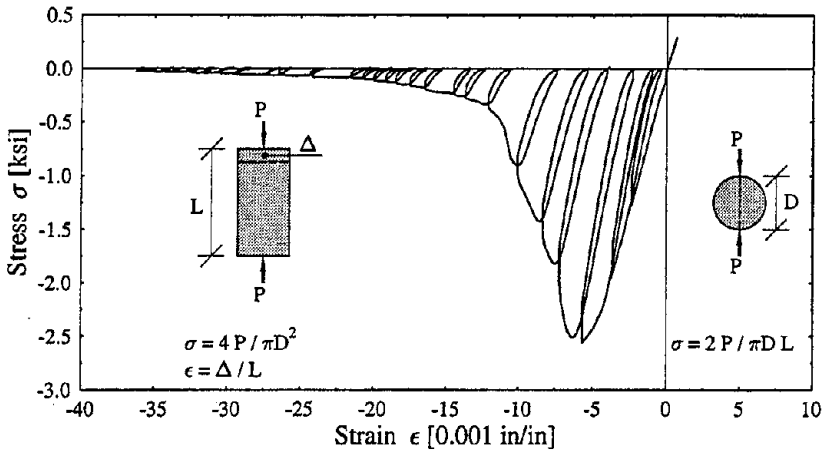

FIGURE 2-4 Typical stress-strain relation for model mortar of type N.

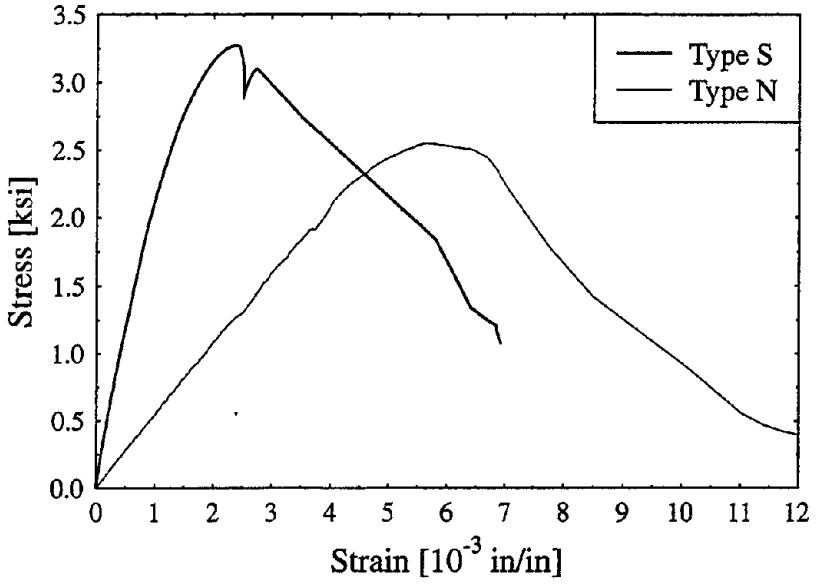

FIGURE 2-5 Stress-strain relations in compression for different mortar types.

TABLE 2-III Mechanical properties of mortar specimens.

Type	f_{cyl} [psi]	f_{cube} [psi]	f_{sp} [psi]	E_{mor} [ksi]	f_{cyl}/f_{cube}	$f_{sp}/\sqrt{f_{cyl}}$
S	3070	3530	240	2000	0.87	4.3
N	1770	2020	190	600	0.88	4.5

2.3 Masonry Assemblages

From the previous sections, it is clear that the two materials, *i.e.* concrete block and mortar, forming the masonry structure *do not* have identical mechanical characteristics. Therefore, one should realize that masonry used in structural components form a *system of composite mechanical action.* In masonry structures, the common modes of failure are:

- Debonding of the bed joints (*i.e* splitting tension failure).
- Crushing of masonry (*i.e* axial compression failure).
- Diagonal tension cracking (*i.e.* splitting tension and joint shear failure).

To understand the causes and effects of these failure mechanisms, it is essential to scrutinize the behavior of masonry assemblages under axial compression, joint shear and diagonal tension.

2.3.1 Axial compression

The most often studied property of masonry, by testing or by theory, is its strength under load perpendicular to the bed joints [64]. The strength of a masonry prism is affected by several factors, including workmanship, thickness of the mortar joints, height of the units and age of the mortar. Sahlin [64] reports that the range of attainable prism strength is very broad, ranging from 100 to 7000 psi. In the present study, the workmanship and the dimensions of the units and mortar joints were kept constant in all the experiments. Most of the following discussions pertain to the material group B because of its susceptibility to crushing.

An attempt was made to *experimentally* measure the stiffness and strength of the masonry and its constituents from the same specimen. Several 5 course prisms with running joints were constructed and instrumented to measure the overall deformation of the prism (Δ_p), the deformation of a single block (Δ_b) and the deformation of a single mortar joint (Δ_m)[11] as shown in the insert of Figure 2-6. Typical results which relate the deformation characteristics of the masonry prism to the deformation characteristics of its constituents are shown in Figure 2-6.

To verify the possibility of theoretically relating the properties of masonry to its constituents, the following approximate relation is used

$$\Delta_p \approx (\Delta_m + \Delta_b)\frac{g_p}{g} \tag{2.1}$$

[11] Δ_m includes deformations of parts of the upper and lower blocks and the mortar joint because it was impossible to measure only the deformation of the small mortar joint.

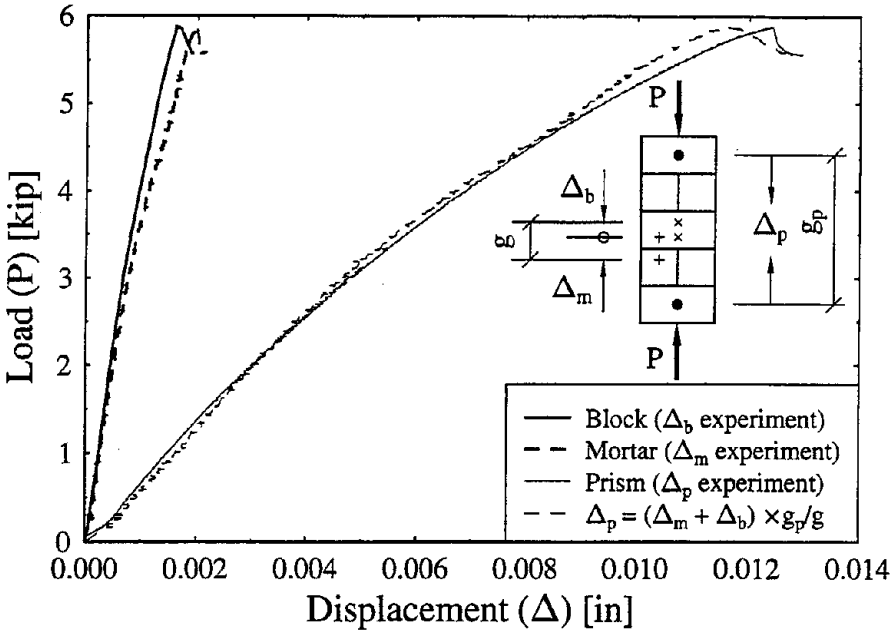

FIGURE 2-6 Deformation of different components of a masonry prism.

where all variables are defined in the insert of Figure 2-6. The previous relation is approximate because the actual relation involves modifying Δ_m to isolate the deformation of the parts of the blocks included in the gage length. This may be performed using simple geometrical arguments but the result can be reasonably approximated by Eq. (2.1). The calculated results for Δ_p using Eq. (2.1) are in a very good agreement with the measurements, as shown in Figure 2-6.

A comparison between the stress-strain relations obtained from a mortar cylinder, a concrete block and the standard masonry prism, *i.e.* 3 courses with stack joints, is illustrated in Figure 2-7. The results shown in this figure are for mortar type N and weak blocks. One notices that the prism strength and stiffness fall between those of the mortar and the concrete block.

Although the ASTM E-447 [2] gives recommendations for determining the compressive strength of masonry using prisms, there is no exact shape specified for the prism to be tested. Therefore, two basic parameters affecting the shape of the prism and consequently the obtained compressive strength were investigated. These two parameters were the type of bond pattern (stack versus running) and the slenderness ratio (height/width) of the prism.

Similar capping and testing procedures used for the individual concrete blocks were followed for the prisms. Figure 2-8(a) illustrates the stress-strain relations for 5 course prisms of the stack and the running bond patterns (2 specimens are shown for each bond pattern). The stiffness of the prism is not affected by the bond pattern whereas the strength differs (about 25% reduction from stack pattern to running pattern). Figure 2-8(b) shows the

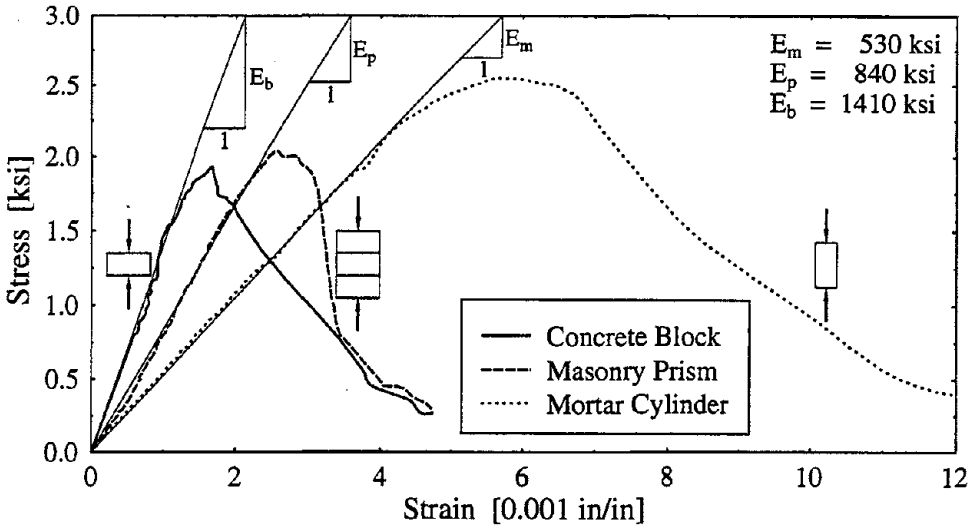

FIGURE 2-7 Comparison between stress-strain relations of masonry and its constituents.

variation of the compressive strength with the slenderness ratio of the prism. The variation and degree of scatter are shown for both the stack and the running bond patterns. From this figure, the higher the slenderness ratio, the lower the compressive strength for both stack and running patterns. This may be attributed to the increase of the influence of load eccentricity with the increase of the slenderness ratio. In the prisms of the running pattern, the mode of failure was usually vertical splitting along the head joints whereas for the prisms of the stack pattern, the failure was either crushing of the face shell or splitting of the intermediate webs. The running pattern always leads to less strength than the stack pattern. This reduction may be attributed to the weak vertical plane introduced by the head joints. One may speculate that the effect of the bond pattern is more pronounced in prism tests than in testing large walls because in the latter case, the number of head joints is independent of the bond pattern.

In the tested infilled frames, window or door openings were introduced in some of the infill panels. This required grouting some of the concrete block cells around the openings. Therefore, 3 course grouted prisms of the stack pattern were prepared for testing under axial compression. In this case, the compressive stress was calculated based on the gross area rather than the face shell area. A comparison between the stress-strain relations of the grouted and ungrouted prisms is given in Figure 2-9. No significant difference is noticed in the response except slight increase of the strength and the initial stiffness followed by decrease in the tangent stiffness for the grouted prism.

Figure 2-10 compares the stress-strain relations for the 5 course prisms of the stack bond pattern made of material groups B and C. It should be noted that the strength of group C is 50% higher than that of group B whereas the stiffness is about 60% higher. The results for prisms of groups A and B were essentially identical. Table 2-IV lists the mean values

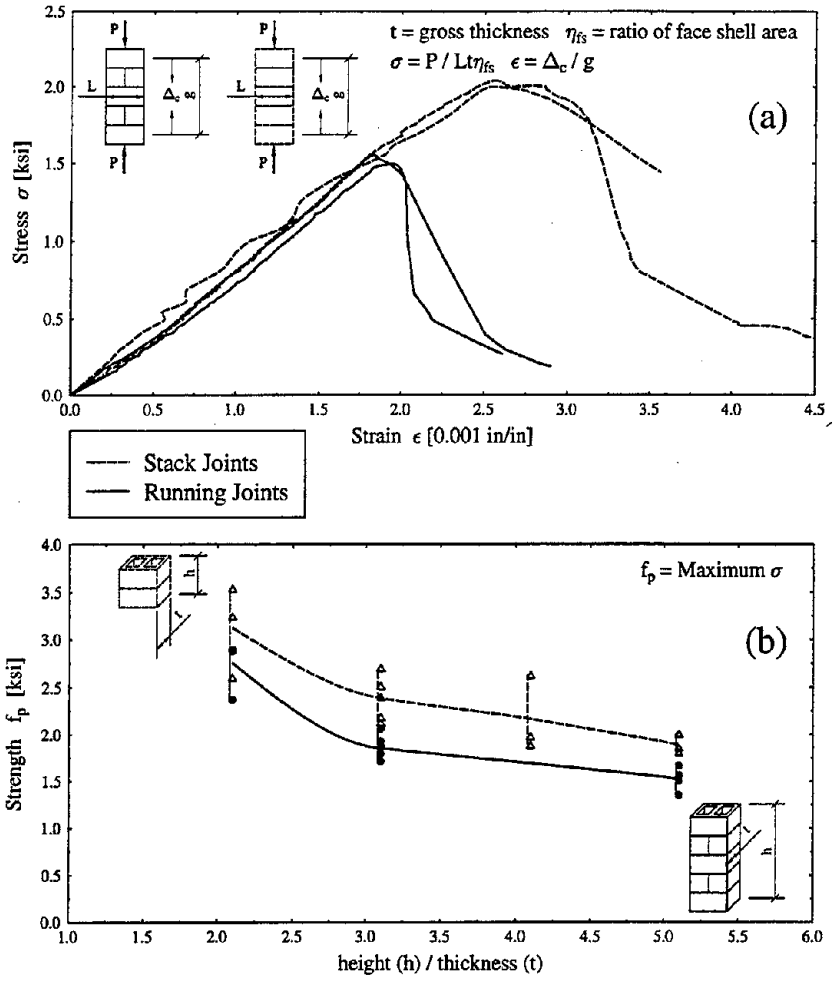

FIGURE 2-8 Effect of the bond pattern and the slenderness ratio on the compressive strength of masonry prisms; (a) Stress-strain relations for different bond patterns; (b) Effect of slenderness ratio.

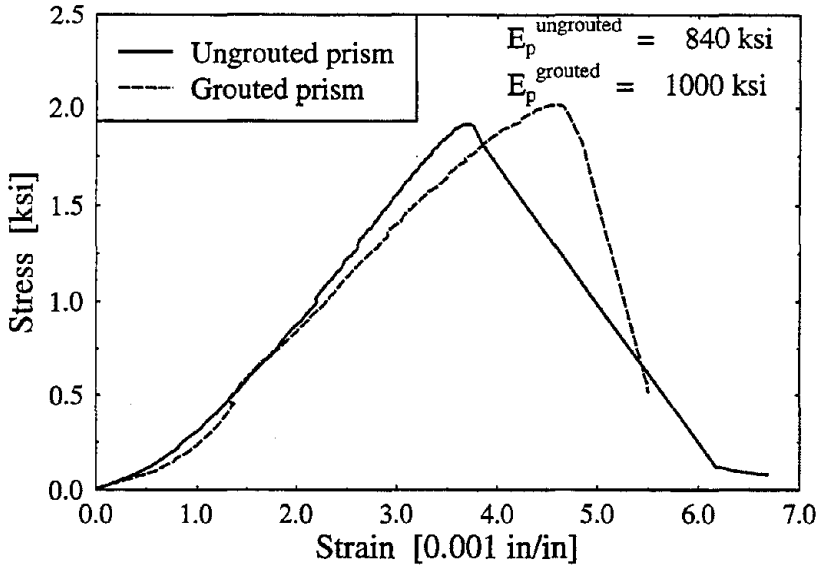

FIGURE 2-9 Comparison between the stress-strain relations for grouted and ungrouted masonry prisms.

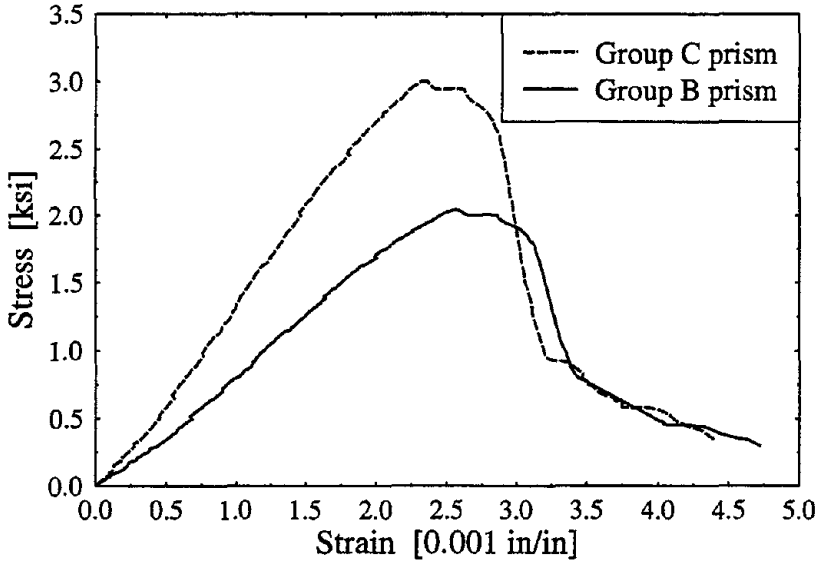

FIGURE 2-10 Comparison between the stress-strain relations of masonry prisms for groups B and C.

TABLE 2-IV Mechanical properties of masonry prisms.

Group	f_p [ksi]	ϵ_p^{peak}	E_p [ksi]
A & B	2.0	0.0026	860
C	3.0	0.0023	1400

of the compressive strength (f_p), the strain corresponding to the peak stress (ϵ_p^{peak}) and the initial stiffness (E_p)[12] obtained from the 5 course prisms of the stack bond pattern for different material groups.

2.4 Mortar Joint Direct Shear

Mortar joints and the interface between the joint and the masonry unit represent planes of weakness and potential sources for crack initiation and propagation in masonry structures. The mortar cracking and mortar/unit debonding produced by slip along the interface under shear loading lead to significant stiffness degradation and material damping. These issues have been recognized by several researchers as documented in many references such as [29] [70] [6] [28] and [26]. It is therefore essential to investigate the shear capacity of the mortar/block interface under direct shear loading.

Masonry researchers have devised numerous shear test methods, including the racking test, the centrifugal force test, the triplet shear test, the four unit assemblage shear test and the couplet shear test. A complete review of literature and evaluation of each of these testing methods can be found in Section 5.2.1 of reference [28]. In the present study the triplet shear test (Figure 2-11(a)) originally proposed by Johnson and Thompson [34] is adopted to mainly investigate the effect of the axial stress normal to the bed joint on the shear capacity of the mortar joint/concrete block interface.

Several specimens were constructed by the same experienced mason who built the infill walls. The delicate nature of these specimens required extreme care in constructing, handling and loading the specimens. The construction position of the specimen is schematically illustrated by Figure 2-11(b) and the procedure of construction is summarized in the following:

1. Two units were placed flush on a wooden plate, spaced 1/8 inch apart.
2. Steel spacers with 3/32 inch thickness were placed on top of one unit (used as a temporary support) and mortar was placed on the face shells of the other unit.

[12]Because the stress conditions near failure of the masonry prisms were not the same as at lower load levels, no strong correlation between prism compressive strength (f_p) and its initial stiffness (E_p) was expected [20].

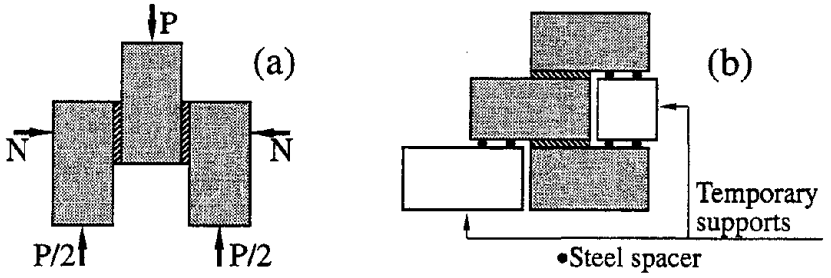

FIGURE 2-11 Triplet specimen for mortar joint direct shear test; (a) Specimen in testing position; (b) Specimen in the position for construction.

3. The central unit of the specimen was positioned in place as shown in Figure 2-11(b).
4. Firm pressure was applied causing excess mortar to squeeze out of the joints.
5. Gentle tapping with the wooden end of the trowel was applied to further consolidate the joints to the required 3/32 inch thickness and to assure horizontal laying of the units with the help of the 3/32 inch steel spacers.
6. The central unit was leveled and plumbed.
7. Another temporary support was made of a half unit and positioned as shown in Figure 2-11(b).
8. A mortar bed joint was placed on top of the central unit.
9. The top unit was placed in position on the mortar joint and plumbed vertically with the lower unit and leveled horizontally to provide the necessary 3/32 inch thick mortar bed joint.
10. The mortar joints were tooled on both sides of the specimen.
11. After 24 hours, when the mortar joints gained reasonable strength, the temporary supports were removed.

Similar procedure to the one listed above was followed by Ghanem [26] for 1/3 scale four unit assemblage shear specimens.

All specimens were made of materials of groups B and C. There were no significant differences between the results of the two groups; all results reported herein are those obtained from group B. At the age of 35 days after fabrication, the top end of the central unit and the bottom ends of the side units were capped using Hydrostone (see Figure 2-11(a) or the insert in Figure 2-12(a) for the specimen in its testing position). The pre-compression normal to the mortar joints was controlled by calibrated springs and kept constant during the shearing of the mortar joints. The force was applied through a spring mechanism where

the spring stiffness was known and by controlling the shortening of the springs, the correct normal compressive force was maintained.

The failure mode for all the specimens, regardless of the material group or the value of pre-compression, was shear slip along one mortar joint. This failure initiated by a debonding at the model concrete block and mortar interface. As noticed by Ghanem [26], in almost all specimens, the failed joints were in one plane which was at the interface between the mortar and the uppermost model block laid during fabrication. Obviously, this implies the sensitivity of the mortar bond at early stages to any pressure normal to the bed joint even if it was produced only by the self weight of the upper courses.

Figure 2-12(a) shows a typical shear stress versus shear slip relation for a particular value of the applied pre-compression (61 psi). The insert in this figure explains how the specimen was loaded and how the shear and normal stresses were calculated. The relation is characterized by a peak (τ_p) and residual (τ_r) values for the shear strength as shown in the insert of Figure 2-12(b). To be able to measure the residual shear strength, loading/unloading cycles were applied in the manner shown in Figure 2-12(a). The envelopes of these cycles are illustrated in Figure 2-12(b) for 5 different values of pre-compression. To illustrate the repeatability of the results, two envelopes are shown at the same pre-compression value for $\sigma = 0$, 41 and 61 psi. The results become more scattered for no pre-compression because of the increase of the sensitivity to any small value of load eccentricity.

From the envelopes shown in Figure 2-12(b), one can determine the relations between the values of the peak and the residual shear strengths and the value of the pre-compression normal to the bed joints. These relations are obtained using regression analysis of the test data and the results are given in Figure 2-13. Linear regression was sufficient leading to Mohr-Coulomb type relations as follows:

$$\tau_p = 0.04 + 1.3\sigma \qquad \& \qquad \tau_r = 0.01 + 0.9\sigma \quad \text{[ksi]} \tag{2.2}$$

where τ_p and τ_r are the peak and residual shear strengths, respectively and σ is the stress normal to the bed joint. In the third report of this series, these relations are used to formulate the post peak behavior of an interface finite element representing the lumped effect of a mortar joint and the interface between the mortar joint and the concrete block.

2.5 Diagonal Tensile (Shear) Test

The diagonal tensile strength or shear strength of masonry is usually determined by applying compression along one of the diagonals of a small square wall. This loading arrangement results in failure by diagonal tension as pointed out by Fattal and Cattaneo [22]. The standard test technique is based on the work by Fishburn [24] and the procedure is determined by the ASTM E-519 [2]. The standard specimen is 4-ft by 4-ft which is scaled down in the present study to 1-ft by 1-ft, *i.e.* 3 units long by 6 units high of the running bond pattern.

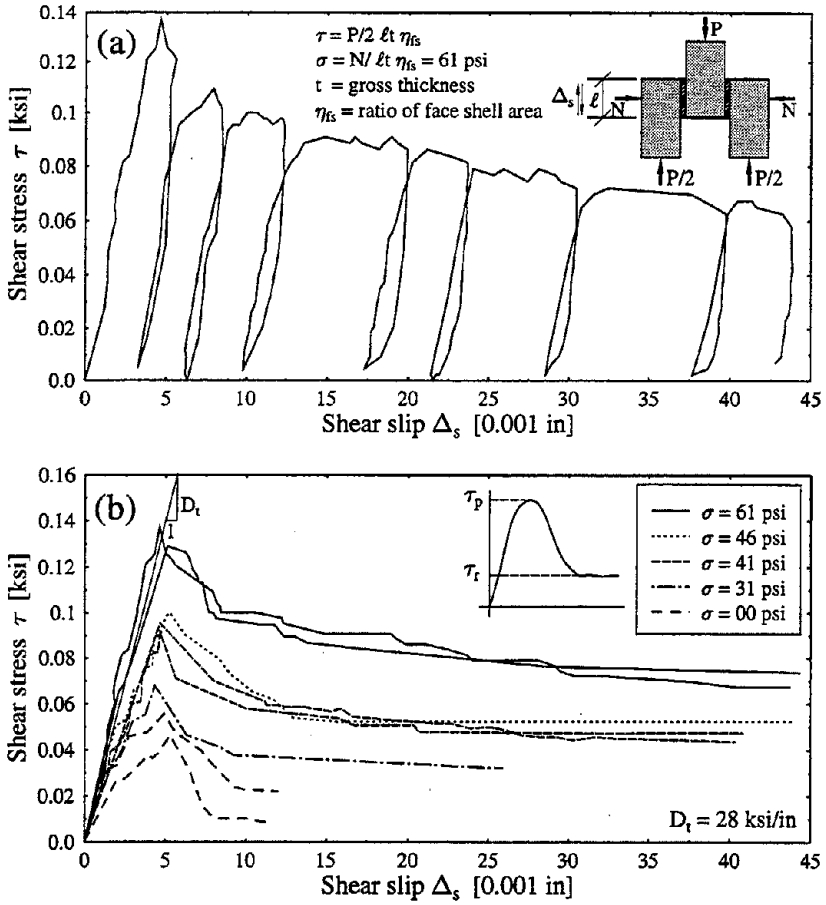

FIGURE 2-12 Mortar joint direct shear test; (a) Applied shear stress versus shear slip relation under certain normal stress; (b) Envelopes of shear stress versus shear slip relations under different normal stresses.

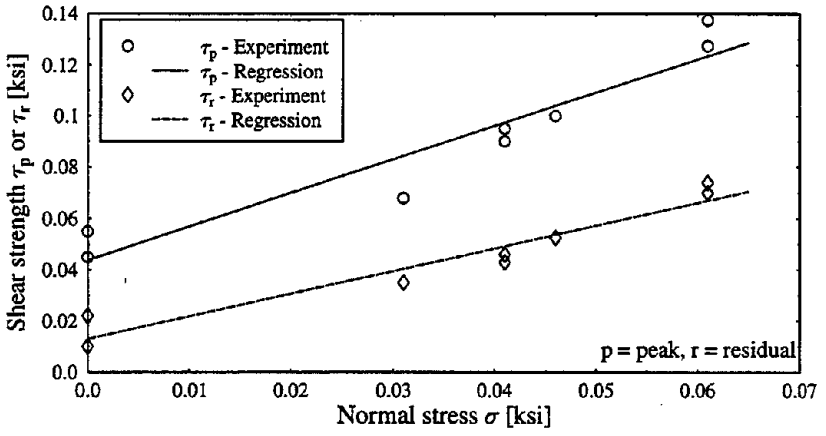

FIGURE 2-13 Effect of pre-compression on joint shear capacity.

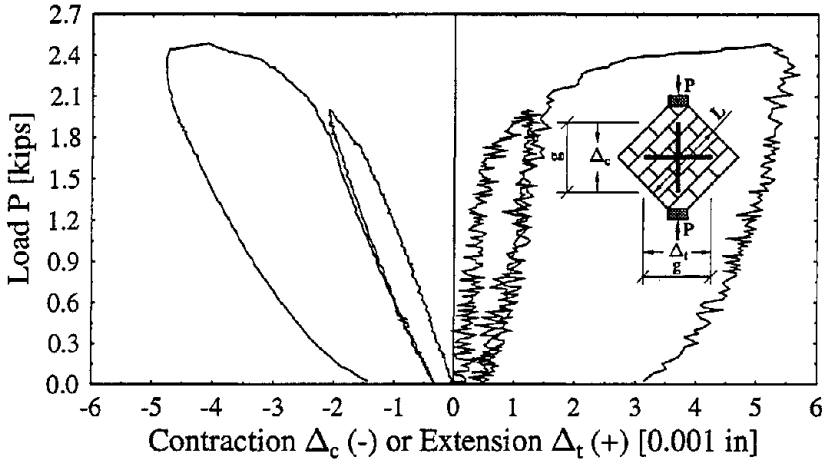

FIGURE 2-14 Typical results for diagonal tension (shear) test.

At least 6 specimens were constructed during the construction of each infill wall model by the same experienced mason who constructed the infill walls.

The specimens were cured under the same conditions as the infill walls. The specimens were instrumented by 2 LVDT's, one on each side of the specimen to measure vertical contraction along one diagonal and horizontal extension along the other diagonal. In lieu of the *loading shoes* recommended by the ASTM E-519 specifications [2], exact 1/4 scale replica shoes were manufactured and used in the tests. These shoes resulted in bearing area encompassed within one unit height (2 inches). The shoes were placed on a leveled surface and filled with a stiff mix of Hydrostone capping material. The insert of Figure 2-14 shows a specimen in the testing position. It should be noted that the gage lengths (g) for the vertical and horizontal LVDT's were identical in compliance with the ASTM E-519 requirements.

The specimens were tested at almost the same age as the infill walls and typical relations for diagonal load (P) versus vertical contraction (Δ_c) and horizontal extension (Δ_t) are shown in Figure 2-14. The results shown in this figure are for material group B. The failure mode for group A specimens shown in Figure 2-15(a) was mainly due to splitting in the weak blocks whereas the mode of failure for groups B and C was caused by sliding along the mortar joints as shown in Figure 2-15(b).

The load and displacement data in Figure 2-14 can be converted into shear stress (S_s) and shear strain (γ) according to the following equations:

$$S_s = \frac{P}{\sqrt{2}A_n} \qquad \text{where} \qquad A_n = Lt\eta \tag{2.3}$$

where A_n is the net area, L is the length of the square specimen (for rectangular specimens, taken as the average of the length and width), t is the total thickness of the specimen and

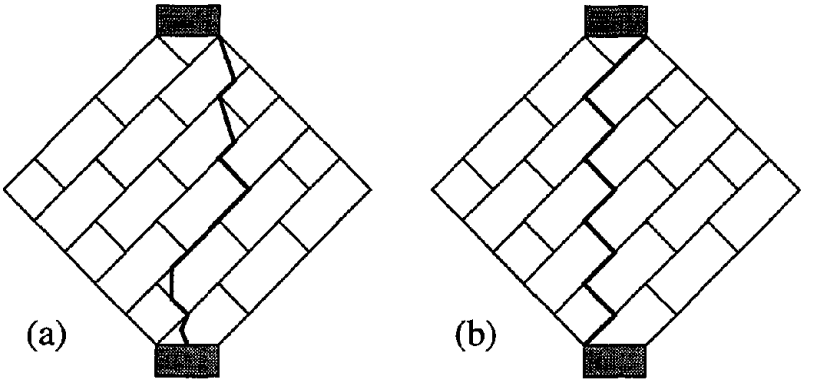

FIGURE 2-15 Modes of failure in the diagonal tension (shear) test of masonry; (a) Group A; (b) Groups B and C.

TABLE 2-V Results of the diagonal tension (shear) test.

Group	S_s [psi]	γ	G [ksi]
A	140	0.00065	215
B	180	0.00045	400
C	250	0.00035	715

η is the ratio of the net area to the gross area.

$$\gamma = \frac{\Delta_c + \Delta_t}{g} \tag{2.4}$$

Parameters in Eqs. (2.3) and (2.4) are defined in the insert of Figure 2-14. The modulus of rigidity (G) is then given by

$$G = \frac{S_s}{\gamma} \tag{2.5}$$

At the ultimate load, the average results obtained from the previous equations are summarized in Table 2-V for all the material groups.

2.6 Summary

The geometrical, physical and mechanical properties of reduced scale masonry assemblages and masonry constituents have been presented. Basic tests on concrete blocks and mortar were carried out to determine the stress-strain characteristics. Shear strength of the

mortar/concrete block interface was evaluated under different values of pre-compression normal to the bed joints. A Mohr-Coulomb failure surface was obtained by regression analysis. Finally, diagonal tension (shear) tests were conducted for mortar/concrete block combinations of different relative strengths.

SECTION 3

QUASI-STATIC EXPERIMENTS ON INFILLED FRAMES

The validation of numerical models for infill walls requires measured results obtained from *realistic* experiments designed for accurate representation of the structural configuration (*i.e.* geometrical and material properties and boundary conditions). Unfortunately, most previous experiments on frames with infills have concentrated on static monotonic load tests performed on the simplest structural configuration, *i.e.* single-bay, single-story infilled frames. The infill walls in most of these frames were solid panels (no openings).

Quasi-static experimentation can be defined as a testing procedure where cyclic loading is slowly applied to the tested structure. In this experimental approach, the definition of a testing program and the associated *load history protocol* is an essential task. As reported by Krawinkler [37], this definition depends on the purpose of the experiment (*e.g.* research or seismic verification) and the type of anticipated failure mode (*e.g.* rapid or slow strength deterioration). Suitable load history protocols for laboratory static and dynamic tests are discussed by White [74]. The specification of loading histories has been extensively studied by the Applied Technology Council (ATC) for cyclic load testing of steel structural elements and configurations [5]. Testing is almost always performed on a deformation-controlled basis to best facilitate interpretation of results in terms of ductility[1] and to permit continued testing beyond the load carrying capacity.

In this section, several quasi-static experiments conducted on infilled frames are discussed. The structures used in these experiments were reduced scale Semi-Rigidly Connected Steel (SRCS) frames infilled with UnReinforced concrete block Masonry (URM). These frames were Gravity Load Designed (GLD) to represent existing design philosophy in low and sometimes moderate seismic risk regions[2].

3.1 Background

Infilled frames have been experimentally investigated by many researchers. Most of this effort has been focused on single-bay, single-story frames infilled with various materials and subjected to monotonic or cyclic (quasi-static) loading. The aim of such experiments was to determine the change in stiffness for different levels of loading and the strength and

[1]From the point of view of earthquake-resistant design, ductility may be defined as the amount of inelastic deformation the structure can sustain without significant loss of strength.

[2]Examples of these regions include the eastern part of North and South America, Australia, Great Britain, ...etc. For discussions on seismically quiet continental areas, the reader is referred to Section 1.2 of *The seismic design handbook* [13].

stiffness evolution upon load reversals. For seismic evaluation purposes, it is not clear how to extrapolate the results of these experimental studies to multi-bay, multi-story infilled frames subjected to realistic earthquake loading.

3.1.1 Monotonic loading

Dating back to the 1950's, the earliest attempt to perform static experiments on infilled frames with monotonically increasing lateral load was conducted in 1952 by Thomas [71]. Since then, several researchers [10] [11] [12] [75] [63] [32] [33] [67] [68] [69] [58] [45] [78] performed experiments on steel or reinforced concrete frames infilled with different materials such as plain or reinforced concrete, mortar, bricks, clinker blocks, hollow, grouted or reinforced concrete block masonry and clay blocks. Important information about the behavior and modes of failure of infilled frames can be obtained from such static experiments. For example, monotonic loading (push-over) experimentation provides the load-displacement relationship, one of the essential pieces of information required in dynamic analysis. Also, this information can be utilized in developing analytical models. Monotonic experiments were aimed at the determination of the effect of infills on the lateral strength and stiffness of the infilled frames.

In the 1970's and 1980's, more interest was directed to numerical modeling of infilled frames. Accordingly, experimental efforts on monotonically loaded infilled frames were performed to reveal the effect of specific parameters, such as,

- Openings [47].
- Shear connectors [47] [41] [43].
- Contact length between the wall and the frame members [44] [8].
- Initial gap arrangement and sizes between the infill walls and the bounding frames [61].

The test program conducted at the University of New Brunswick may be considered as one of the most intensive experimental programs on infilled frames tested monotonically. In this program, McBride [51], Yong [77], Amos [3] and Richardson [60] examined the frame/infill interface conditions, column to infill ties, initial gaps, frame connection types, infill openings, reinforced bond beams and loading conditions. Their experimental program consisted of 34 large-scale single-bay, single-story steel frames infilled with concrete masonry. The results of this experimental program were further investigated by Pook and Dawe [59] and by Dawe and Seah [17].

One of the rare studies on the behavior of GLD frames with URM infills was recently conducted by Harris *et al.* [31]. Four 1/6-scale single-bay, three-story Lightly Reinforced Concrete (LRC) frames were tested. One was tested as a bare frame and the other three

were infilled with concrete block masonry (one with infill in the first story only, one with infills in the first and second stories only and one with infills in all three stories). Inverted triangular monotonically increasing loading pattern was applied to all frames. Details of the testing program and results are given by Ballouz [7]. The major conclusions and recommendations of this study include:

1. Retrofitting with non-integral (*i.e.* without shear connectors between the infill wall and the frame members) masonry infills was an effective and economical method for improving strength and reducing drift of LRC frames.

2. Substantial strengthening of LRC frames was achieved, but the relatively strong masonry infills used in these tests resulted in catastrophic failures of the tension columns.

3. By proper selection of the infill masonry strength, along with prevention of its premature separation from the columns, a more desirable failure mode may be achieved, with yield hinges at the top and bottom of the columns and crushing of the masonry infills.

4. Anchorage of the masonry infills to the bounding frame members may be a critical factor in determining the overall performance. With proper anchorage, it could be possible to force failure in the masonry and prevent a premature shear/flexure column failure.

3.1.2 Cyclic loading and harmonic excitation

In this section, a brief literature review of selected experimental investigations of infilled frames tested under cyclic loading or under harmonic excitation is presented. Cyclic loading and harmonic excitation experiments allow the determination of strength and stiffness evolution upon load-reversal. Esteva [21] conducted the first cyclic loading tests on infilled frames in 1966. He subjected unreinforced masonry panels framed by reinforced concrete members to alternating diagonal compression loads. There is an extensive international literature on cyclic loading experiments conducted on reduced scale as well as full scale frames of different material and infilled with variety of walls [46] [23] [15] [19] [38] [36] [40] [14] [35] [39] [56] [79] [80] [81] [76] [66] [53] [4].

Liauw and Kwan [42] conducted experimental studies on cyclically loaded small-scale models of four-story infilled frames. They applied harmonic load at the top of the frames. Three categories of models were tested, namely, **non-integral** (*i.e.* no connectors at the interface), **partially integral** (*i.e.* connectors along the infill/beam interface only) and **integral** (*i.e.* connectors along all infill/frame interfaces). They evaluated the hysteretic characteristics, energy dissipation capacities and degradation properties under cyclic loading. They concluded that the integral infilled frames are structurally superior because of the following:

1. They are stiffer and stronger.
2. They are more ductile and more reliable since they maintain a gradual and fairly slow degradation rate.
3. Their energy dissipation capacities are much larger than those of the other types of construction.

Dawe *et al.* (1989) [18] tested 10 portal steel frames with and without infills of solid clay bricks to evaluate the dynamic stiffness and strength of the structure, the effect of ground motion intensity on the wall degradation behavior, the role of the enclosing frame stiffness and column-to-roof rotational rigidity. They subjected their specimens to a sinusoidal ground motion. They compared their experimental results with those obtained from a simple single-degree-of-freedom model and a braced frame model. They concluded that the linear response of infilled frames can be predicted by the single-degree-of-freedom model whereas the linear and the initial stages of the nonlinear response of these frames may be predicted using the braced frame model.

Several loading techniques for reduced scale models of two-story reinforced concrete frames infilled with solid clay bricks were investigated by Manos *et al.* [49]. These loading techniques included static tilt, low level impulse loading either on the first or the second story level, sweep (*i.e.* controlled sinusoidal motions of fixed amplitude with a frequency varying within a certain range) and simulated earthquake excitations. They observed that the placement of asymmetric masonry infills on the ground floor caused detrimental effects to the structure. They also observed that wide door openings in the second story have only little influence on the seismic behavior of the model for low to medium simulated earthquake excitations.

Valiasis and Stylianidis [73] tested 24 specimens of 1/3-scale single-bay, single-story infilled reinforced concrete ductile frame models under cyclic horizontal loading. The infills were unreinforced brick masonry walls which were not connected to the bounding frames. Later, Manos *et al.* [50] tested similar structures to those of Valiasis and Stylianidis [73] but with 1/9-scale rather than 1/3-scale. Manos *et al.* subjected their small-scale models to similar cyclic loading pattern as the one used for the larger scale models of Valiasis and Stylianidis [73]. The general conclusions indicated that despite some discrepancies, the overall cyclic behavior of masonry infilled reinforced concrete frames was satisfactorily simulated using small scale models.

Mander *et al.* [48] conducted experimental study on three infilled frame subassemblages. Bolted steel frames and clay brick masonry were used. Their specimens were tested in-plane under cyclic loading. The first specimen had undamaged infills whereas the last two specimens had retrofitted damaged walls using two different techniques of ferrocement[3] coating: (a) 0.5 inch coating and (b) 2 layers of ferrocement with diagonal rebars in one

[3]Ferrocement is a special type of reinforced concrete characterized by a small thickness and reinforced with small scale welded wire mesh.

layer and horizontal rebars in the other. Their major conclusions are summarized in the following:

1. If fallout of infill is not a problem, unreinforced clay brick masonry infills can act as a *ductile* lateral load resisting elements in multi-story frames.

2. The enhanced ferrocement layer (*i.e.* technique (b)) provided an improved ductility capacity and distributed cracking along the diagonals. Also the diagonal rebars prevented out-of-plane buckling of the ferrocement layer at the center of the panel.

3. The presence of infills greatly stiffened and strengthened the structural system compared with the bare frame. The infilled specimens were about 20 times stiffer and 5 times stronger at an inter-story drift up to 1.5%.

Mehrabi *et al.* [52] tested 14 half-scale reinforced concrete frames infilled with concrete block masonry. Their objectives were to evaluate the influence of the relative strength and stiffness of an infill with respect to those of the bounding frame, the lateral load history, the panel aspect ratio, the magnitude and distribution of vertical loads and the adjacent infilled bays on the performance of these frames. The general conclusions of Mehrabi *et al.* [52] are:

1. Infill panels can significantly enhance the load resistance capacities of reinforced concrete frames. Strong panels provided a better energy-dissipation capability, particularly for strong frames.

2. Three different modes of failure have been observed.
   - For weak panels, *slip along the bed joints of the panels and plastic hinges in the frame.*
   - For weak frame and strong panels, the interaction between the infill and the frame resulted in a *brittle shear failure of the columns.*
   - For strong frame and strong panels, the lateral strength was governed by *crushing of the infills.*

3. Specimens subjected to cyclic loading showed lower resistance and faster strength degradation than those subjected to monotonic loading.

4. Increasing the total vertical load resulted in a higher resistance but the influence of the distribution of the vertical load between the columns and the beams was insignificant.

5. The panel aspect ratio (height/length) in the range of 0.48 to 0.67 had only a small effect on the lateral stiffness and resistance.

6. Regarding the ultimate lateral load, the two-bay infilled frames were about 1.7 to 1.85 times stronger than similar one-bay infilled frames.

TABLE 3-I Experimental program.

Test	Openings	f_b [psi]	f_{cyl} [psi]	f_b/f_{cyl}	f_p [psi]	E_p [ksi]
Q11SSB	None	1900	1450	1.31	1800	800
Q21SSA	None	1900	2150	0.88	2000	820
Q21SSB	None	2800	1700	1.65	2400	880
Q21AOB	Asymmetric	2800	1700	1.65	2400	880
Q21SOC	Symmetric	4000	3100	1.29	3300	1500
P22SOC	Symmetric	4000	3100	1.29	3300	1500

$\star$ window and door • windows † in the 2^{nd} story only

□ block compressive strength based on net area

△ mortar cylinder compressive strength

◇ masonry prism strength (f_p) and stiffness (E_p) based on the face shell areas

It should be noted that, in addition to the references mentioned above, several important contributions in the filed of infilled frames can be found in the international literature. A complete review of research activities on infilled frames through 1987 has been reported by Moghaddam and Dowling [54].

3.2 Description of Experiments

In the present study, several experiments have been carried out to investigate the performance of reduced-scale infilled GLD frames under earthquake type loading. The parameters varied in these experiments included:

1. Relative strength between the concrete blocks and the mortar joints.
2. Number of bays and stories of the tested frames.
3. Opening configurations (door versus window and symmetric versus asymmetric arrangements) in the infills.

The characteristics of the tested specimens are summarized in Table 3-I. All specimens consisted of SRCS frames infilled with URM non-integral walls. The specimen names used in Table 3-I were selected according to the notations shown in the example of Figure 3-1. The two-story infilled frame was tested pseudo-dynamically as discussed in the second report of this series.

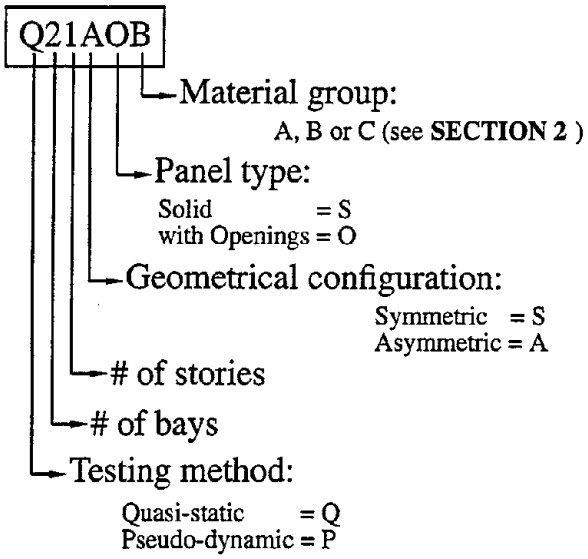

FIGURE 3-1 Naming technique of the tested specimens.

3.2.1 Loading system

The single-story specimens were subjected to quasi-static lateral displacements of increasing amplitude. The load application point was selected in such a way to preserve symmetry in the loading. Therefore, for the two-bay specimens, the load was applied at the top of the central column whereas for the single-bay specimen, the load was applied at the midpoint of the top beam [82]. The corresponding lateral loads simulated the effects of in-plane shear caused by lateral inertial forces at the floor level produced by earthquake loading.

A displacement feedback servo-hydraulic actuator of 55 kips capacity and a stroke of ± 3 inches was used. A closed-loop MTS servo control system, shown schematically in Figure 3-2, was used to control the actuator displacement. The LVDT located in the MTS actuator provided the necessary displacement feedback to the MTS controller. The displacement at the loaded point of the structure and the corresponding load were monitored and displayed using the graphical interface of the control software. The end of the actuator attached to the tested specimen allowed *in-plane free rotation* of the actuator axis with respect to the specimen. Therefore, shear forces were the only applied external action to the specimen (*i.e.* there was no action applied due to rotational restraint from the actuator assembly).

3.2.2 Load history protocol

To investigate the effect of repeated load on strength and stiffness degradation, three cycles of the same displacement amplitude were applied. The applied displacement patterns consisted of two sets of displacement histories as illustrated in Figure 3-3(a) for the specimens with panels of symmetrical geometric configuration (Q21SSB and Q21SOC), and Figure 3-

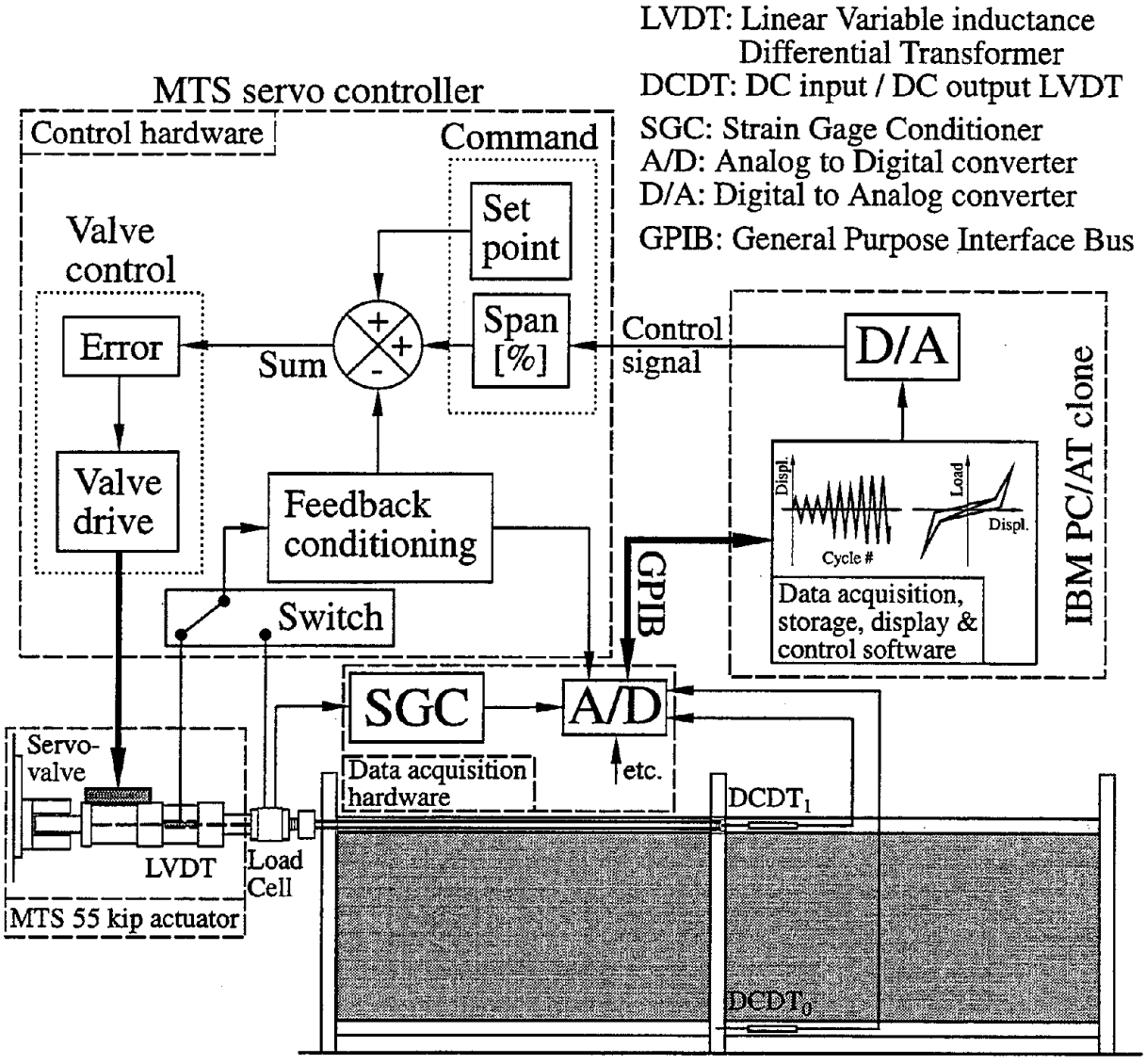

FIGURE 3-2 Schematic illustration of the quasi-static control and data acquisition system.

3(b) for the specimens with panels of asymmetrical geometric configuration (Q21AOB). The loading pattern of specimens Q11SSB and Q21SSA included only set (A) of displacement cycles as reported in references [25] and [82]. The second set of displacement cycles (set (B)) was used to study the performance of the structure with previously cracked walls. This situation was not possible in specimens Q11SSB and Q21SSA because the infill walls in these experiments failed by corner crushing.

Displacements were applied in small increments (0.006 inch) as long as the corresponding load changes were relatively large ($\geq$ 300 lb). These increments were increased to 0.012 inch and sometimes 0.018 inch when load changes were relatively small ($<$ 100 lb). The application of the small displacement increments was very important for Set (A) where small changes of applied displacement led to large changes of load, *i.e.* stiff behavior. Another objective of this *dual* control[4] technique was to accurately capture the abrupt changes of behavior produced by the opening and closing of frame/wall interface gaps and wall cracks without the need to apply an excessive number of small displacement increments when such small values were not needed.

3.2.3 Design and construction

The experimental layouts including loading system and dimensions of the specimen for the three experiments designated Q21SSB, Q21SOC and Q21AOB (see Table (3-I)) are shown in Figures 3-4(a), 3-4(b) and 3-4(c), respectively. The frame members were designed and constructed according to the specifications of the American Institute of Steel Construction (AISC) [1] and connected using bolted framed beam connections. These connections are those designated as "Type 2" according to Allowable Stress Design (ASD) or as "Type PR" (for Partial Restrained) according to Load & Resistance Factor Design (LRFD) [65]. An excellent review of LRFD of these connections is given by Thornton [72]. Two *clip angles* L2 $\times$ $1\frac{3}{16}$ $\times$ $\frac{1}{8}$ with clearance setback of $\frac{3}{16}$ inch were used as shown in Figure 3-5. All specimens were *pinned jointed* to the support structure which consisted of a heavy steel beam supported by the floor anchors.

The out-of-plane instability was prevented by supports perpendicular to the plane of loading using steel channel sections. These supports enclosed layers of grease at the interface between the column and the channel so as to mitigate any in-plane friction and allow free lateral displacements of the specimen. The out-of-plane movements of the tested structures were found to be minimal.

After the complete erection of the steel frame, the infill walls were constructed by an experienced mason using the miniature concrete blocks and the model mortar types described in the previous section. The construction of the masonry infill walls followed common practice of ungrouted masonry where mortar on only the face shell of the block was used (*i.e.* face

[4]The duality is attributed to the monitoring of both the applied load and displacement and consequently making the necessary adjustments.

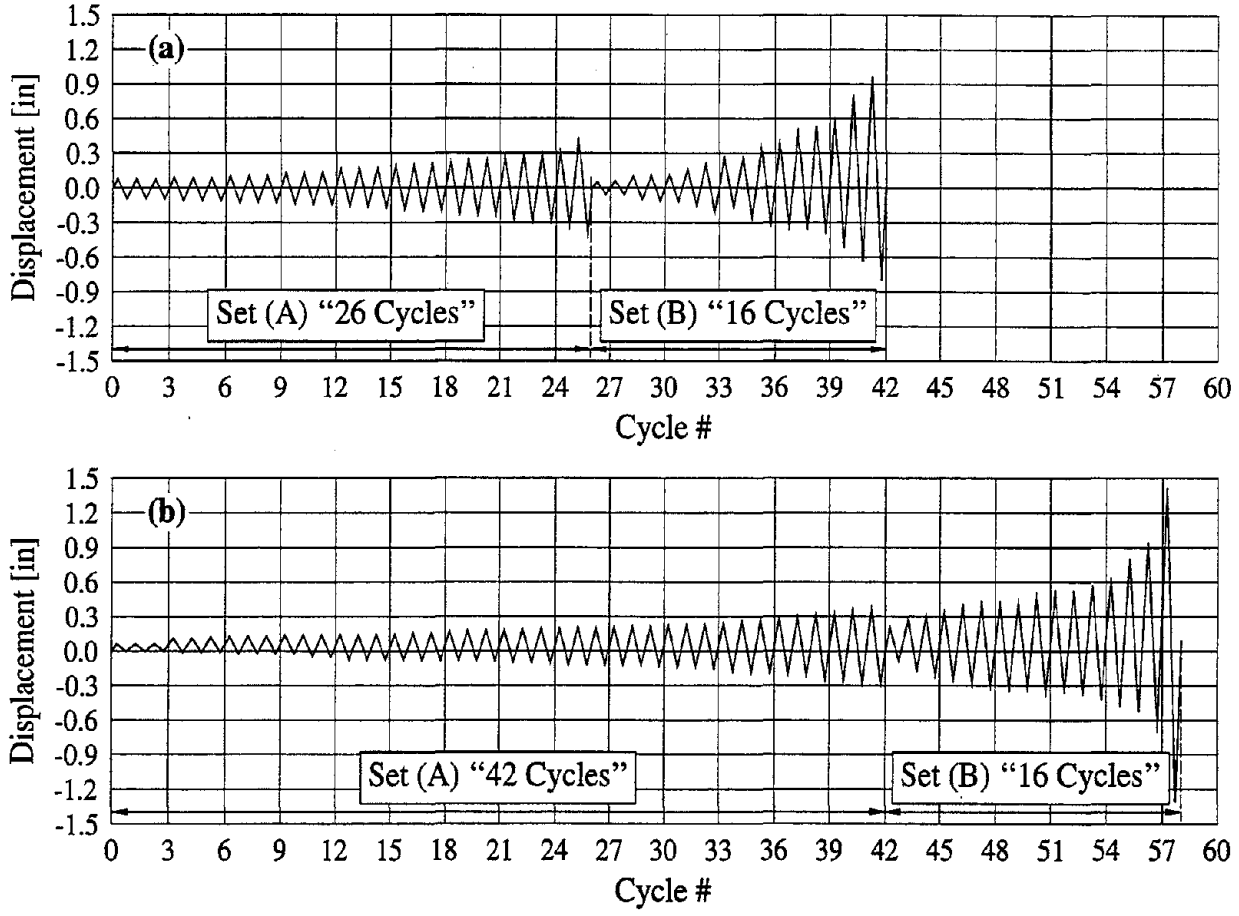

FIGURE 3-3 Displacement patterns applied quasi-statically; (a) Pattern for specimens Q21SSB and Q21SOC; (b) Pattern for specimen Q21AOB.

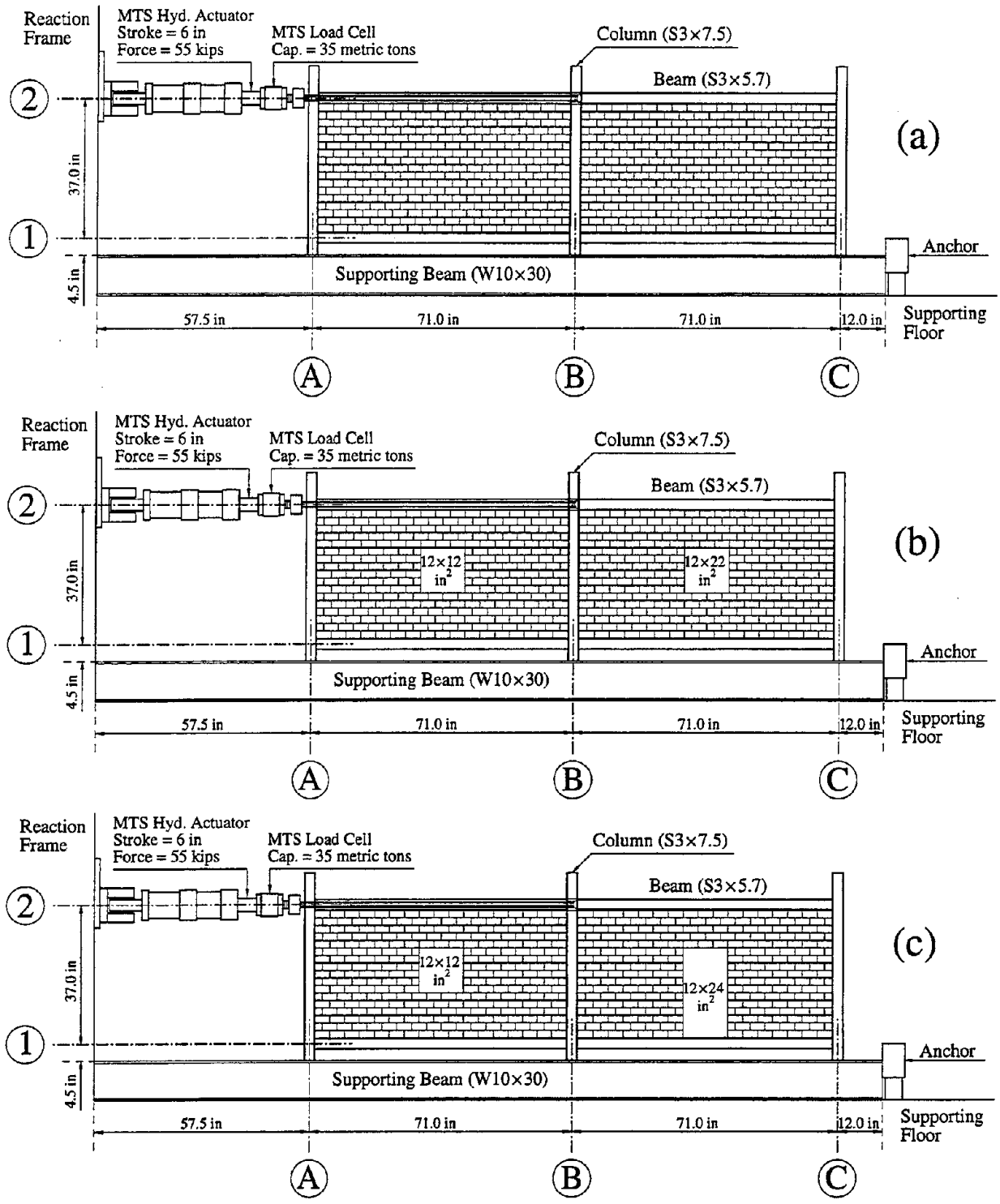

FIGURE 3-4 Experimental setup of quasi-static experiments; (a) Specimen Q21SSB; (b) Specimen Q21SOC; (c) Specimen Q21AOB.

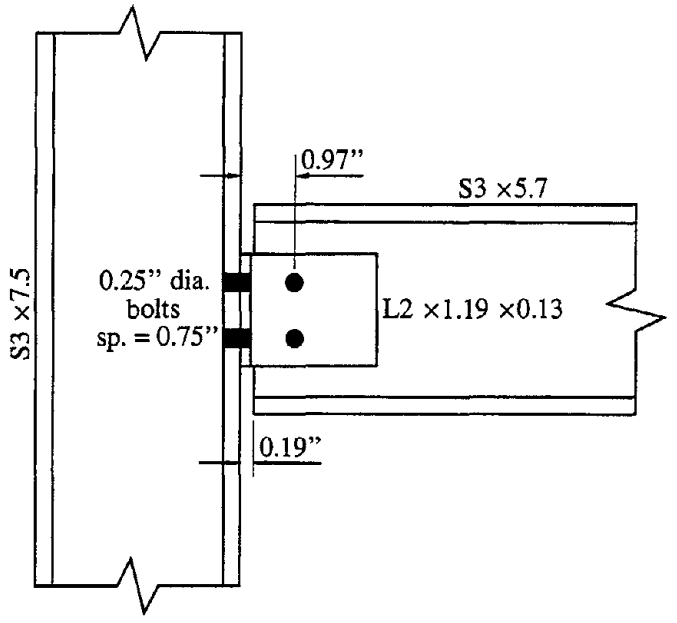

FIGURE 3-5 Detail of ASD-Type 2 (LRFD-Type PR) connection.

shell bedding). No shear connectors were used between the walls and the surrounding frame members (*i.e.* non-integral walls). The concrete block masonry cells around the openings were grouted. Bond beams on top of the openings were reinforced using 2 threaded rods of $\frac{1}{4}$ inch diameter and 20 threads per inch. The width of the supports of these bond beams was about 4 inches (*i.e.* one block).

3.2.4 Instrumentation

The specimens were instrumented to provide key quantities to characterize the structural response of the frame, the infill walls and the frame/wall interface. These key quantities included:

- The hysteresis loops and the corresponding strength deterioration and stiffness degradation.
- The straining actions (bending moment, shearing force and normal force) at different sections of the frame members.
- The principal strain directions in the infill wall panels.
- Deformation of the panels along the diagonals and off-diagonal struts as idealized by the compression-only six strut model of Chrysostomou [16].
- The deformation (distortion) of the openings in the infill walls.

- The frame/wall interface conditions in the form of gap opening and closing and wall sliding along the interface.
- Crack initiation and propagation upon the increase of loading.
- Crack opening and closing upon load reversals.

Strain gages at different sections of the frame members were used to determine the straining actions at these sections. At each section, three gages were bonded to the web. Two gages designated as 1 and 2 (one close to each flange) measured the strains along the axial direction of the member (ϵ_1, ϵ_2). From these gages, the curvature (Ψ) and the average strain ($\bar{\epsilon}$) at that section are as follows:

$$\Psi = (\epsilon_1 - \epsilon_2)/d \qquad \& \qquad \bar{\epsilon} = (\epsilon_1 + \epsilon_2)/2 \tag{3.1}$$

where d is the distance between the strain gages. The chosen sign convention implies that positive curvature means tension in the fibers close to gage 1 and positive $\bar{\epsilon}$ implies axial tensile strains. The strains and the corresponding stresses in the frame members for all the conducted experiments remained below the *elastic* limit. Therefore, the bending moment (M) and axial force (N) at any section are *linearly proportional* to the curvature (Ψ) and average strain ($\bar{\epsilon}$) at that section, respectively. From Eqs. (3.1), one can write

$$M = E_s I \Psi \qquad \& \qquad N = E_s A \bar{\epsilon} \tag{3.2}$$

where E_s is Young's modulus for the steel and I and A are the moment of inertia and the area of the considered section, respectively.

The third gage (designated as gage 3) is bonded at the Center Line (CL) of the web and oriented at 45^o from the axial direction of the member to measure the strain ϵ_3. Therefore, shear stress (τ) and consequently shearing force (Q) can be calculated as follows [57]

$$\tau = \frac{E}{2(1+\nu_s)}[2\epsilon_3 - (1-\nu_s)\bar{\epsilon}] \qquad \& \qquad Q \approx t_w d_w \tau \tag{3.3}$$

where ν_s is Poisson's ratio for the steel and t_w and d_w are the web thickness and depth, respectively.

The locations of the strain gages are shown in Figure 3-6 together with the locations of the displacement transducers used to measure the relative displacement along or orthogonal to the frame/wall interface and the absolute lateral displacement of the right column of the frame. It should be noted that the absolute displacements also included the deformation of the top and bottom ends of the central column measured using $DCDT_0$ and $DCDT_1$ as indicated in Figure 3-2. Although Figure 3-6 shows a specimen with solid panels, the shown instruments were used for all the quasi-static experiments of the two-bay, single-story infilled frames.

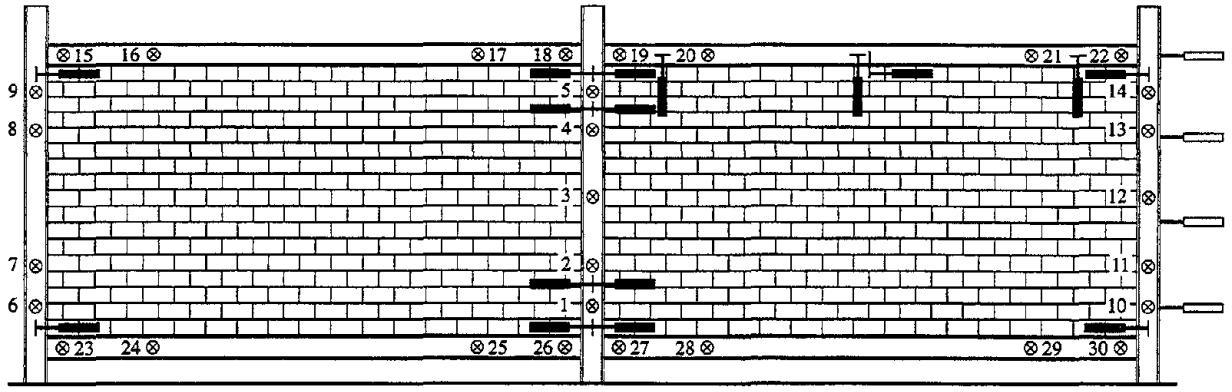

⊗ 3 Strain gages on the web [one close to each flange and the third at 45° at the CL]

DCDT for relative displacement measurements

DCDT for absolute displacement measurements

FIGURE 3-6 Common instruments to all quasi-static experiments.

Special instrumentation was used for each individual test depending on the geometrical configuration of the infill walls. For specimens Q11SSB, Q21SSA and Q21SSB, displacements along the wall diagonals and off-diagonals were measured to verify the compression-only six strut model [16] for solid infills. Also, rectangular rosettes [57] of strain gages and individual gages were bonded at the center of the panels and at the corners along the main diagonals of the walls. These strain measurements were intended to determine the direction of the principal strains of the infills and to investigate the concentration of strains at the wall corners. Typical locations of the displacement transducers and strain gages in specimens with solid walls are shown in Figure 3-7. For specimen Q21SSB, another set of displacement instruments were used to determine complete displacement fields of the panels for the purpose of parameter estimation of the material properties of the masonry infills. These measurements as well as the parameter estimation technique will be discussed in the third report of this series.

For the specimens with openings (*i.e.* Q21AOB and Q21SOC), special measurements were taken to quantify the distortion of the openings. Figure 3-8 shows the typical displacement instrumentation for infill walls with openings.

Most of the previously discussed displacement and strain measurements of the infill panels were found to be useful only before the infill walls experienced corner crushing as in specimens Q11SSB and Q21SSA, or cracking as in specimens Q21SSB, Q21AOB and Q21SOC. Therefore, after cracking, a new set of displacement transducers was aligned along and normal to the crack direction. These new measurements facilitated the determination of crack opening and closing upon load reversal. Useful information such as mortar joint dilatancy was also obtained from the new measurements. Typical locations of such transducers along and normal to the mortar cracks are shown in Figure 3-9. The switch from the general instruments described in the previous paragraphs to the new ones placed after

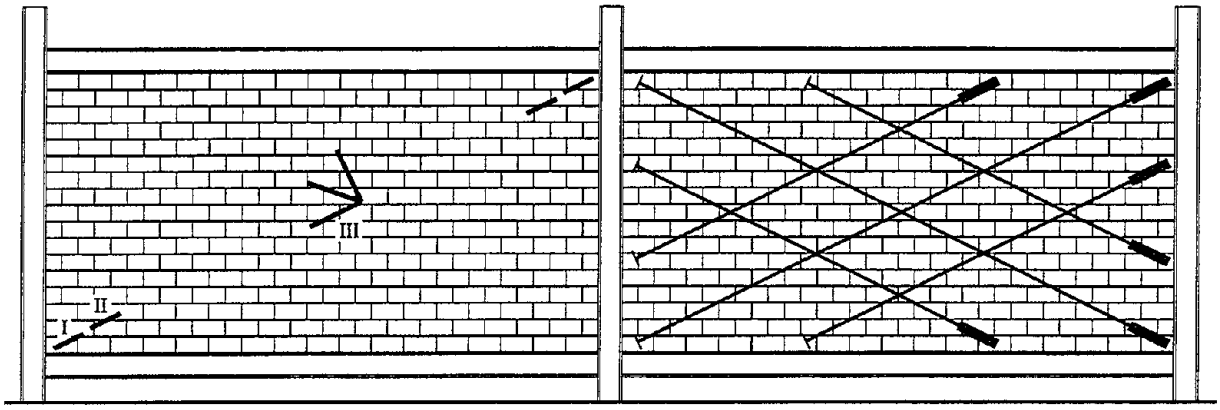

Strain gages along the diagonal (Typical)

DCDT's along the diagonals and off-diagonals (Typical)

FIGURE 3-7 Instruments for quasi-static experiments with solid infills.

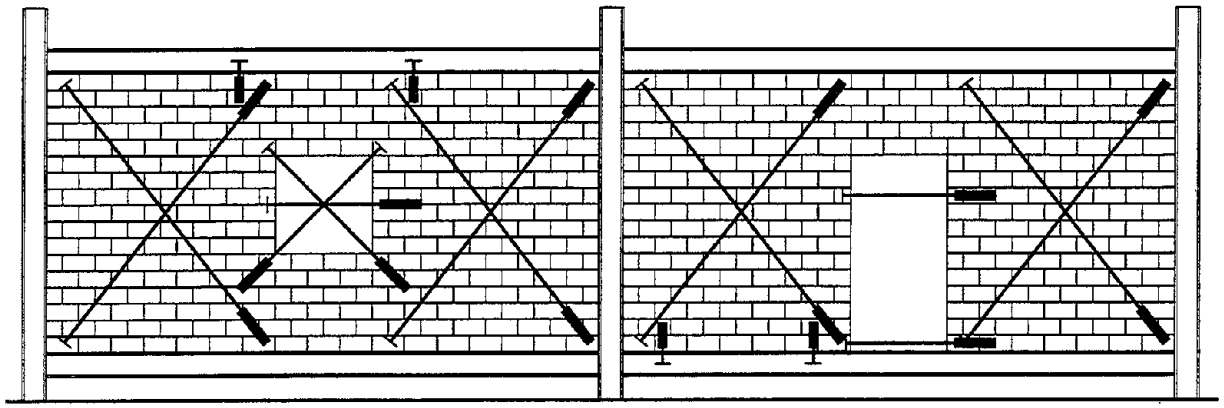

Typical instrumentation of infill panel with window opening

Typical instrumentation of infill panel with door opening

FIGURE 3-8 Instruments for quasi-static experiments with infills including openings.

cracking coincide with the switch from set (A) to set (B) of the loading protocols shown in Figures 3-3(a) and 3-3(b).

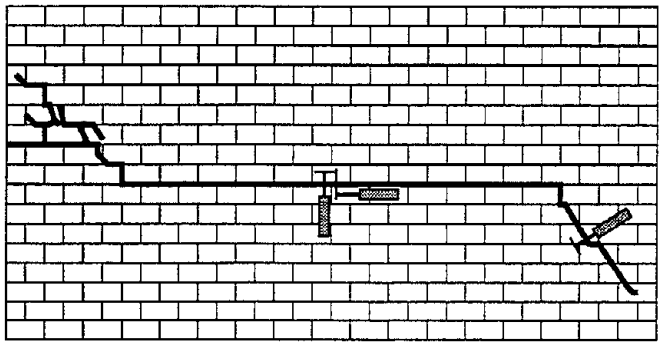

FIGURE 3-9 Typical instruments for quasi-static experiments of cracked infills.

3.3 Summary

The quasi-static experimentation technique was the focus of this section. First, review of literature of static experiments on infilled frames was given. Selected references of direct relevance to the present study were discussed in detail and the major conclusions were pointed out. The features of the conducted experimental program were presented and the main parameters of this experimental program were identified. Aspects related to the tested specimens such as loading, design, construction and instrumentation were described.

SECTION 4

RESULTS AND MODELING OF INFILLED FRAMES

In the present section, results from the quasi-static experiments will be presented and discussed. A modeling technique for SRCS frames infilled with URM walls will be formulated and calibrated using the results of some of the quasi-static experiments.

The global performance measures obtained from the quasi-static experiments are presented first. These measures include the hysteretic load-displacement relations and their corresponding envelopes and the crack patterns associated with different levels of the applied lateral displacements. Based on the experimental results of the global response, several key parameters are identified and calibrated. These parameters provide the physical meaning of a hysteretic force-displacement model for the infilled frames.

The second set of quasi-static results focuses on the local performance of infilled frames. The considered local measures include the straining actions at different locations of the frame members and the infill walls and the frame/wall interface conditions. For the sake of brevity, selected representative results from the measurements shown in Figures 3-6, 3-7, 3-8 and 3-9 are presented and discussed in the following sections.

4.1 Global Response

The load-displacement relations obtained from the quasi-static experiments of the three specimens designated Q21SSB, Q21SOC and Q21AOB are compared in Figures 4-1 and 4-2 for sets (A) and (B) of the displacement cycles, respectively. From the relations in Figure 4-1, the following three distinctive zones can be observed:

1. **Zone of non-active walls** represents the behavior of the frame without the interaction of the infills. Its extent is defined by the pre-existing gaps between the frame members and the walls. Based on the shrinkage strains of mortar and blocks which are reported by Grimm [27], the calculated shortening of the infill wall due to shrinkage is almost equivalent to the initial gap size between the wall and the bounding frame.

2. **Zone of walls with non-degrading strength** where walls interact with the bounding frame showing some stiffness degradation and small energy dissipation due to hysteresis.

3. **Zone of walls with degrading strength** initiates immediately after wall cracking when the response starts to show degradation of both stiffness and strength with

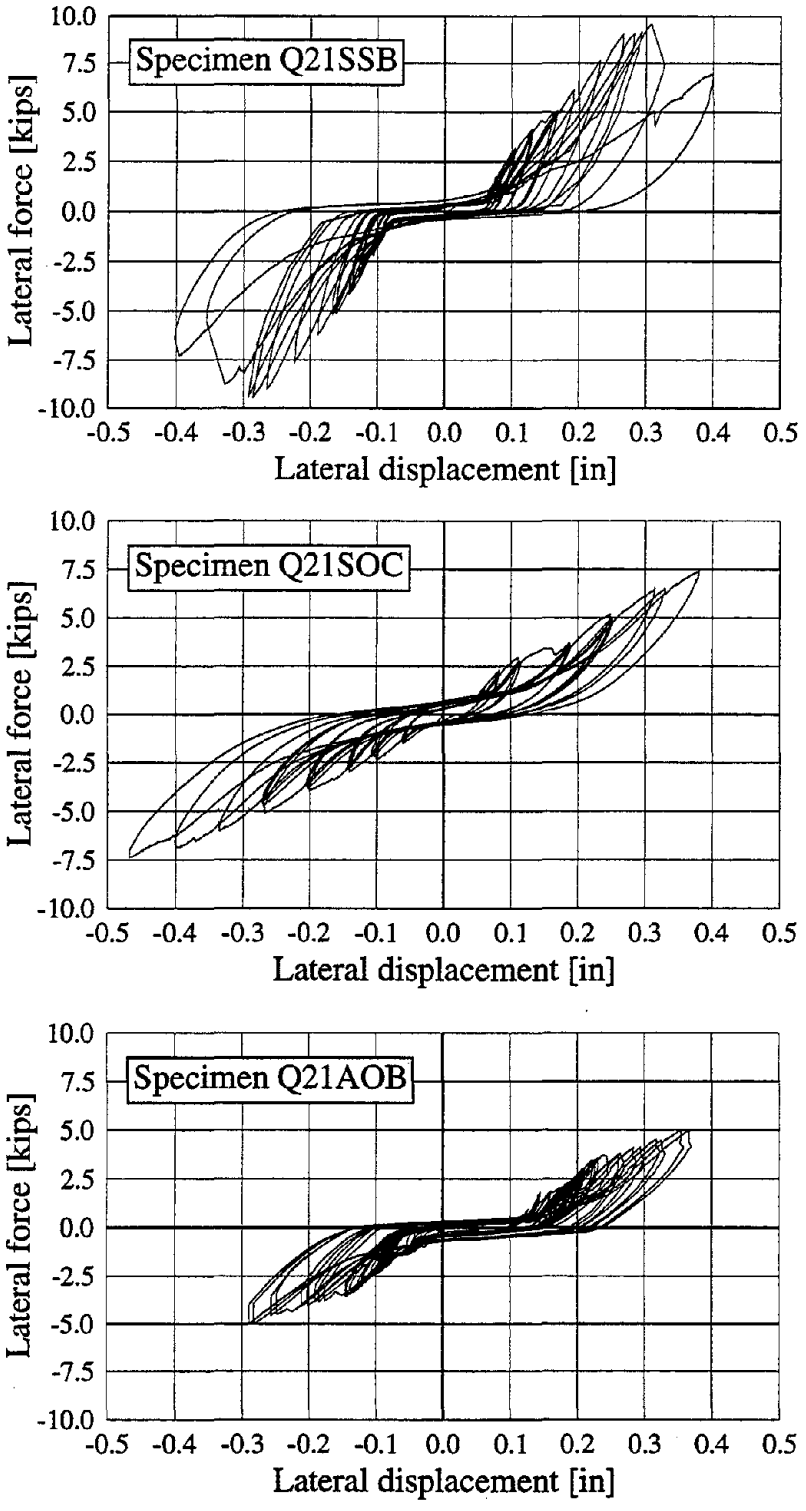

FIGURE 4-1 Load-displacement relations obtained from set (A).

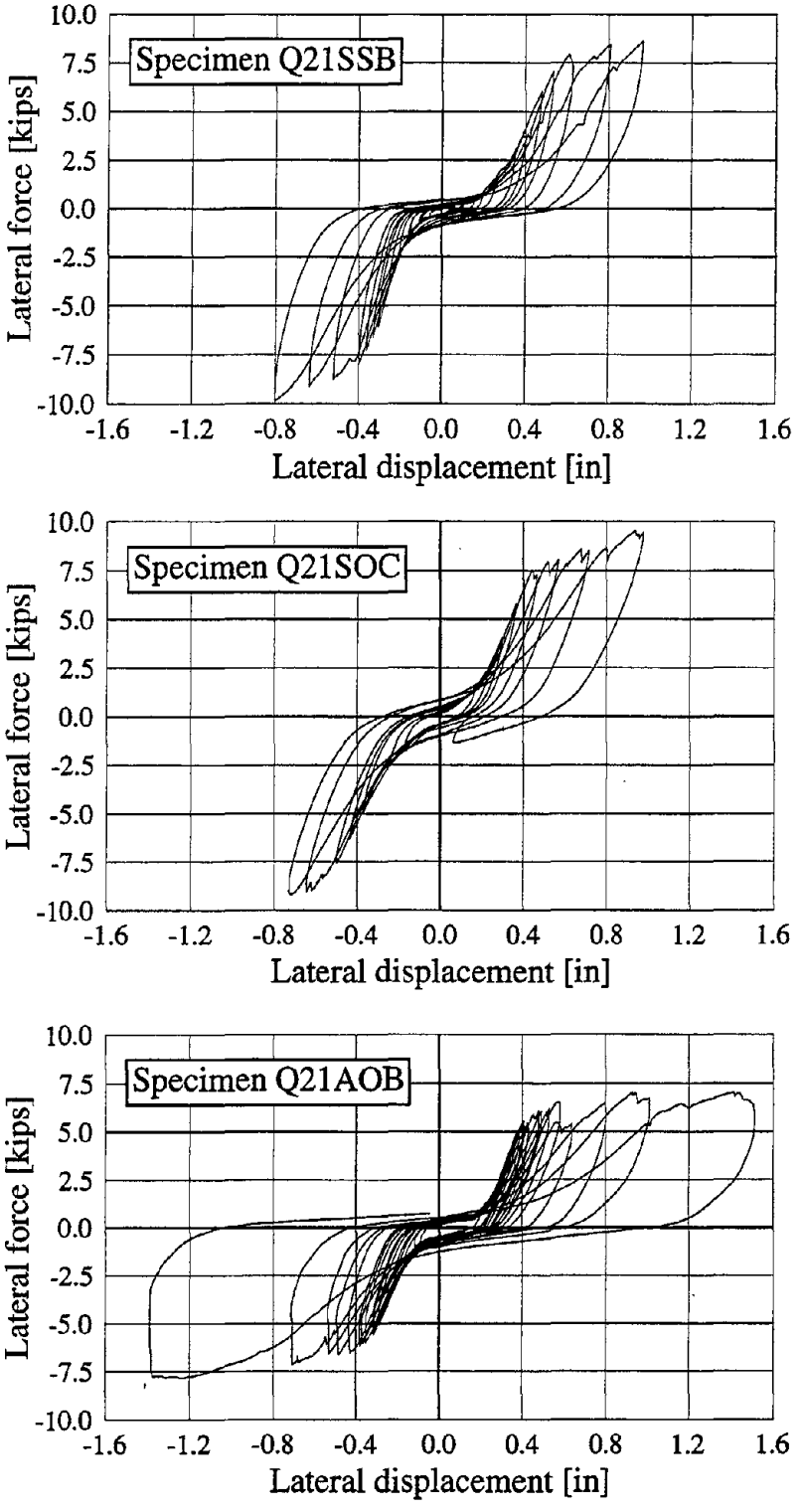

FIGURE 4-2 Load-displacement relations obtained from set (B).

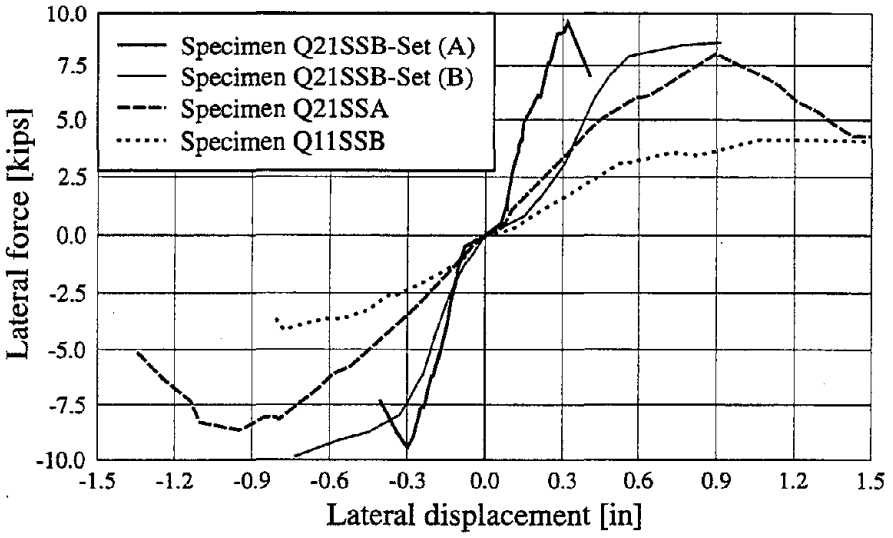

FIGURE 4-3 Effect of number of bays and material group on the hysteresis envelopes.

large energy dissipation through hysteresis.

For set (B) of the imposed displacement pattern, similar zones to those of set (A) can also be identified in Figure 4-2. In this case, however, the first zone is larger due to sliding along the pre-existing cracks especially those along the mortar bed joints. As initial cracking of the walls (due to set (A)) was stable, the second and third zones showed large stiffness degradation without further strength deterioration.

4.1.1 Effect of number of bays and material group

In Figure 4-3, the hysteresis envelope obtained from the single-bay specimen Q11SSB is compared with those of the two-bay specimens Q21SSA and Q21SSB (sets (A) and (B)) to show the effect of number of bays and the effect of infill wall material group. It should be noted that the deformation reported for specimens Q11SSB and Q21SSA were obtained from the LVDT inside the actuator without correction of possible deformation of the loading mechanism[1] and possible lateral motion of the supporting beam. This situation was rectified in specimen Q21SSB and all other specimens by reporting the deformation as the difference between the measurements of $DCDT_1$ and $DCDT_0$ shown in Figure 3-2. Therefore, it is speculated that the hysteretic envelopes of specimens Q11SSB and Q21SSA underestimate the lateral stiffnesses of the infilled frames because the relatively small deformation of the load transfer mechanism and the possible slight motion of the supporting

[1]The loading mechanism in all the experiments consisted of two channel sections C4 × 5.4 which connected the loaded point(s) on the specimen to the actuator(s).

TABLE 4-I Effect of number of bays and material group on stiffness and strength of infilled frames (dimensions in kips and inches).

Specimen	P_u^+	P_u^-	Δ_u^+	Δ_u^-	$K_{0.5P_u}$	K_{P_u}	Mode of failure
Q21SSB	9.6	9.5	0.32	0.30	51.0	30.8	Mortar cracking
Q21SSB	8.6	9.9	0.92	0.73	24.5	11.2	Joint slip & crushing
Q21SSA	8.1	8.7	0.90	0.95	10.9	9.1	Corner crushing
Q11SSB	4.1	4.1	1.07	0.78	6.4	4.4	Corner crushing

• From set (A) of the displacement cycles.
† From set (B) of the displacement cycles.

beam were included in the displacement measurements. Table 4-I summarizes key values for stiffness and strength parameters of these specimens and their corresponding modes of failure. In this table the superscripts + and − refer to the positive and negative excursions, respectively, P_u and Δ_u are the ultimate lateral force and the corresponding lateral displacement. The secant stiffnesses at $0.5P_u$ (*i.e.* $K_{0.5P_u}$) and at P_u (*i.e.* K_{P_u}) are given by Eqs. (4.1) and (4.2), respectively.

$$K_{0.5P_u} = \frac{1}{2}\left[\frac{0.5P_u^+}{\Delta_{0.5P_u}^+ - g^+} + \frac{0.5P_u^-}{\Delta_{0.5P_u}^- - g^-}\right] \tag{4.1}$$

where g^+ and g^- are the initial gap values at the positive and negative excursions, respectively.

$$K_{P_u} = \frac{P_u^+ + P_u^-}{\Delta_u^+ + \Delta_u^-} \tag{4.2}$$

All terms in Eqs. (4.1) and (4.2) are positive values. The modes of failure listed in Table 4-I are illustrated in Figures 4-4(a) and 4-4(b).

From the results shown in Figures 4-3 and 4-4 and Table 4-I, the following conclusions may be drawn:

1. The relative strength between the mortar joints and the concrete blocks comprising the infill walls has a significant influence on determining the mode of failure of infill panels. Weak blocks and moderate mortar joints (*i.e.* group B) lead to mortar cracking whereas weak blocks and strong mortar joints (*i.e.* group A) lead to corner crushing.

2. The capacity of the infilled frames is *slightly* dependent on the mode of failure. Ultimate load is only about 10% higher for mortar cracking mode of failure (specimen Q21SSB) than for corner crushing mode of failure (specimen Q21SSA) for similar specimens.

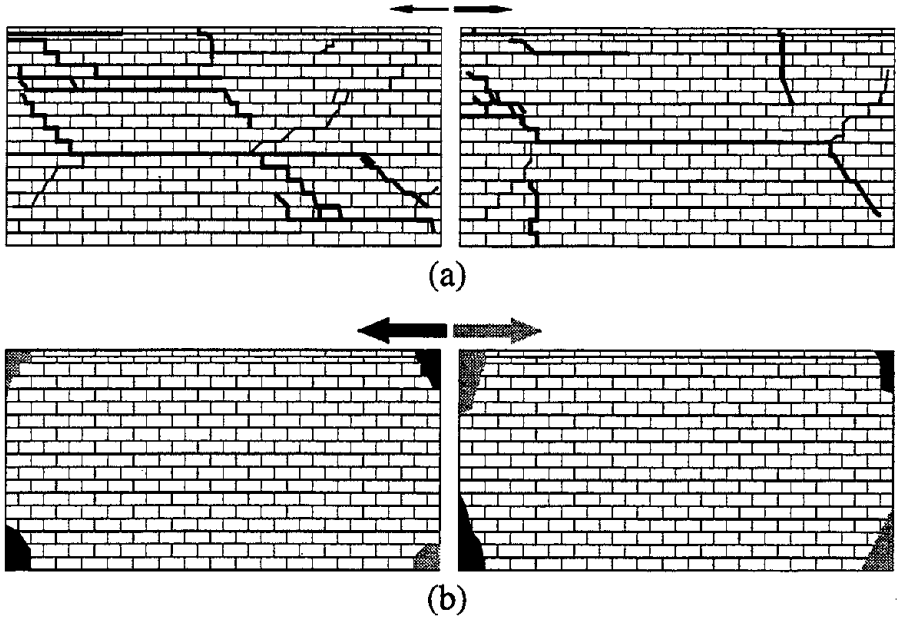

FIGURE 4-4 Modes of failure for infill walls; (a) Mortar cracking and joint slip for specimen Q21SSB; (b) Corner crushing for specimen Q21SSA.

3. Although the capacity (ultimate load) for the two bay specimen is about double the capacity of the single bay specimen, the stiffness is only 1.7 times higher (refer to specimens Q21SSA and Q11SSB).

4. From sets (A) and (B) of specimen Q21SSB, the *initial* stiffness (approximated by $K_{0.5P_u}$) of an infilled frame is reduced by about 50% after wall cracking.

4.1.2 Effect of openings on strength and ductility

The hysteresis envelopes shown in Figures 4-5 and 4-6 illustrate the effect of openings on the global performance of two-bay, single-story infilled frames for the two sets of applied displacement cycles (A) and (B), respectively. Two dimensionless parameters (H_u and D_u) are defined in Table 4-II to give a representation of the post-cracking force and deformation ratios, respectively. It should be noted that the cracking load and the associated deformation correspond to the point at which the load suddenly drops, specimen Q21SSB, or the point at which a major (*e.g.* complete diagonal) crack in the infill wall occurs as in specimens Q21AOB and Q21SOC. From Figures 4-5 and 4-6 and Table 4-II and for the considered opening types, one may conclude the following:

1. Solid infills cause the behavior of infilled frames to be brittle (*i.e.* sudden drop of load upon crack initiation).

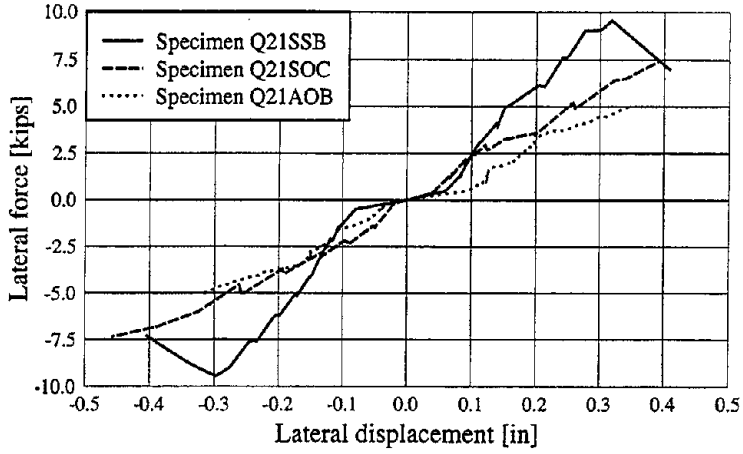

FIGURE 4-5 Effect of openings for set (A).

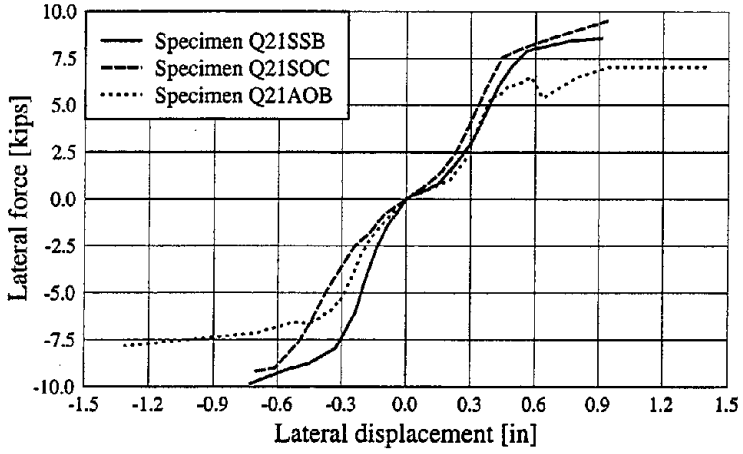

FIGURE 4-6 Effect of openings for set (B).

TABLE 4-II Effect of openings on post-cracking force and deformation ratios (dimensions in kips and inches).

Specimen	P_{cr}	Δ_{cr}	P_u	Δ_u	H_u	D_u
Q21SSB	9.6	0.26	9.9	0.69	1.03	2.65
Q21SOC	6.6	0.30	9.5	0.94	1.44	3.13
Q21AOB	4.5	0.22	7.8	1.21	1.73	5.50

∘ Excluding initial gaps.

• Excluding sliding along pre-existing cracks.

† Post-cracking force ratio ($H_u = \frac{P_u}{P_{cr}}$).

‡ Post-cracking deformation ratio ($D_u = \frac{\Delta_u}{\Delta_{cr}}$).

2. Openings in infill walls lead to a more ductile behavior and larger post-cracking force ratio (*i.e.* ultimate load becomes significantly higher than cracking load).

3. The larger the opening size, even for asymmetric arrangement of openings, the larger the post-cracking force and deformation ratios.

4. The ultimate load corresponding to set (A) of applied displacement cycles decreases with the increase of the opening size.

5. The application of a second set of displacement cycles resembling the effect of a second earthquake on a previously cracked infilled frames showed more flexible and ductile behavior with large energy dissipation for all the tested infilled frames.

4.1.3 Effect of openings on mode of failure

Close to the end of displacement cycles of set (A), all the two-bay, single-story specimens of material groups B and C experienced several cracks along the mortar bed and head joints. The sequences of crack initiation, propagation and closure upon load reversal for specimens QS21SSB, Q21SOC and Q21AOB are shown in Figures 4-7, 4-8 and 4-9, respectively. In all these figures the loading increases from left to right and from top to bottom. Therefore, empty spots indicate stages of unrecorded patterns where no significant changes occurred. In the figures, thick lines indicate fully open cracks while thinner lines indicate pre-existing closed cracks.

Cracks in masonry infill walls tend to *dilate*, *i.e.* cracks widen due to shear along crack surfaces. This phenomenon is illustrated in Figure 4-10, where shearing in the X-direction along the mortar bed joint crack, marked H, causes the crack to widen in the Y-direction. Therefore, the wall tends to swell and push towards the frame beams leading to contact in the middle region of the beam and loss of contact at the side regions. This frame/wall interaction leads to the formation of the vertical cracks, marked V in Figure 4-10. This observation explains the tight fit of the infill wall inside the frame after the completion of set (A). On the contrary, in specimens Q11SSB and Q21SSA, because of the absence of mortar cracking, after set (A), the wall became loose and set (B) could not be applied.

Horizontal cracks appeared first in the center of the solid infill walls, subsequently, propagating diagonally towards the loaded corners as shown in Figure 4-7. The crack patterns were affected by the presence of openings, whether door or window. Openings forced the cracks to initiate at their corners and subsequently, these cracks propagated towards the loaded corners, as shown in Figures 4-8 and 4-9.

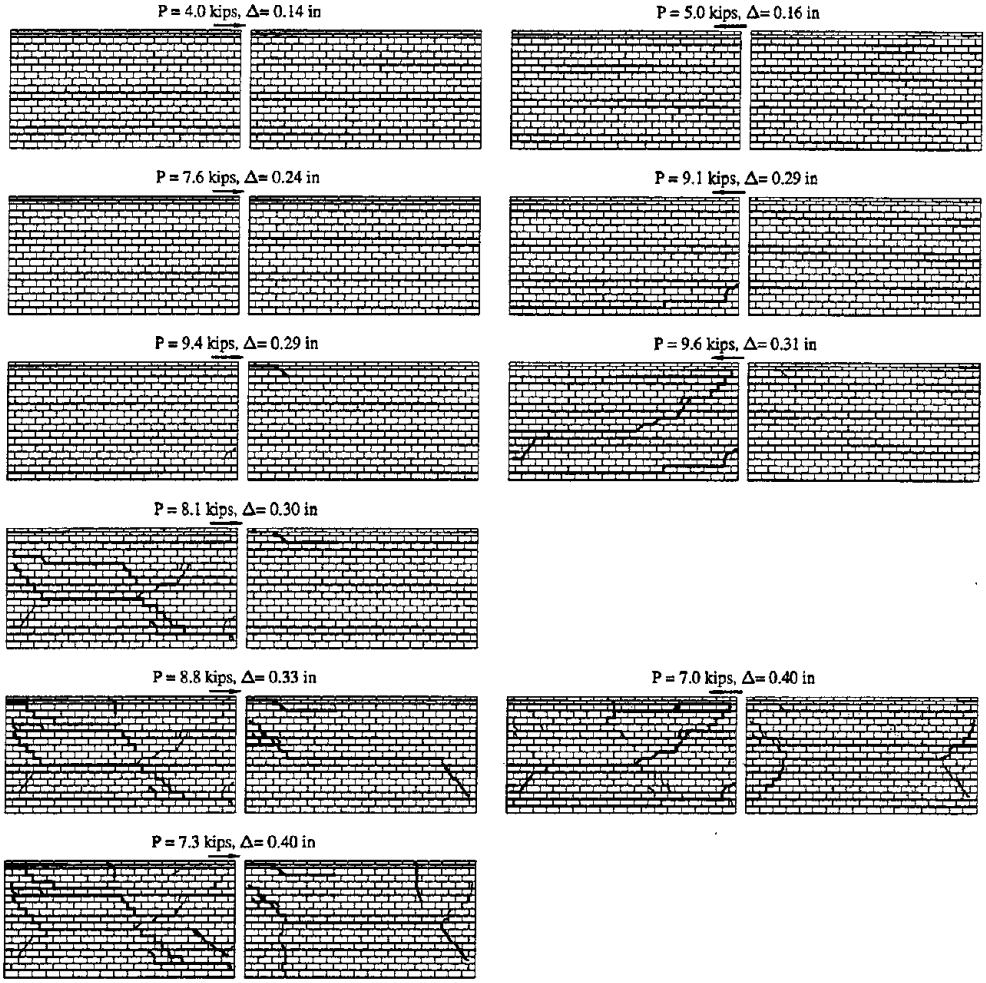

FIGURE 4-7 Sequence of crack patterns for specimen Q21SSB.

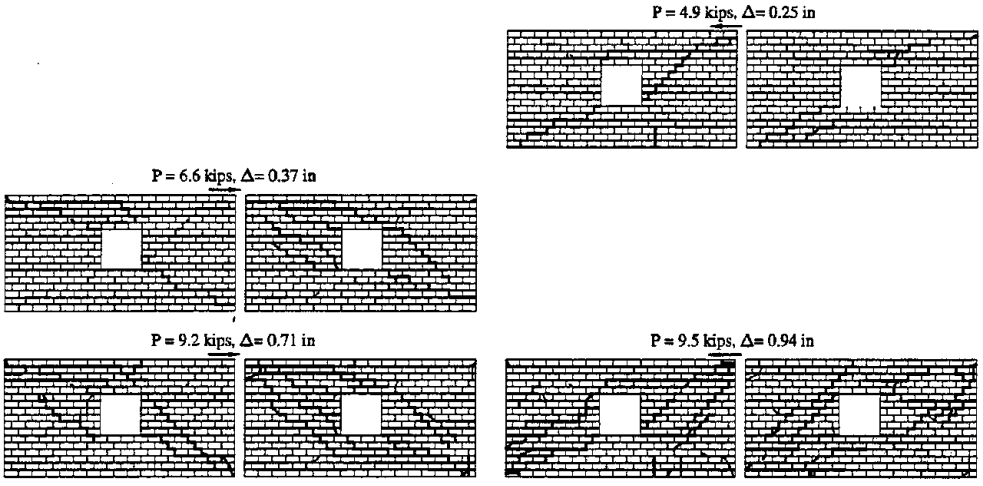

FIGURE 4-8 Sequence of crack patterns for specimen Q21SOC.

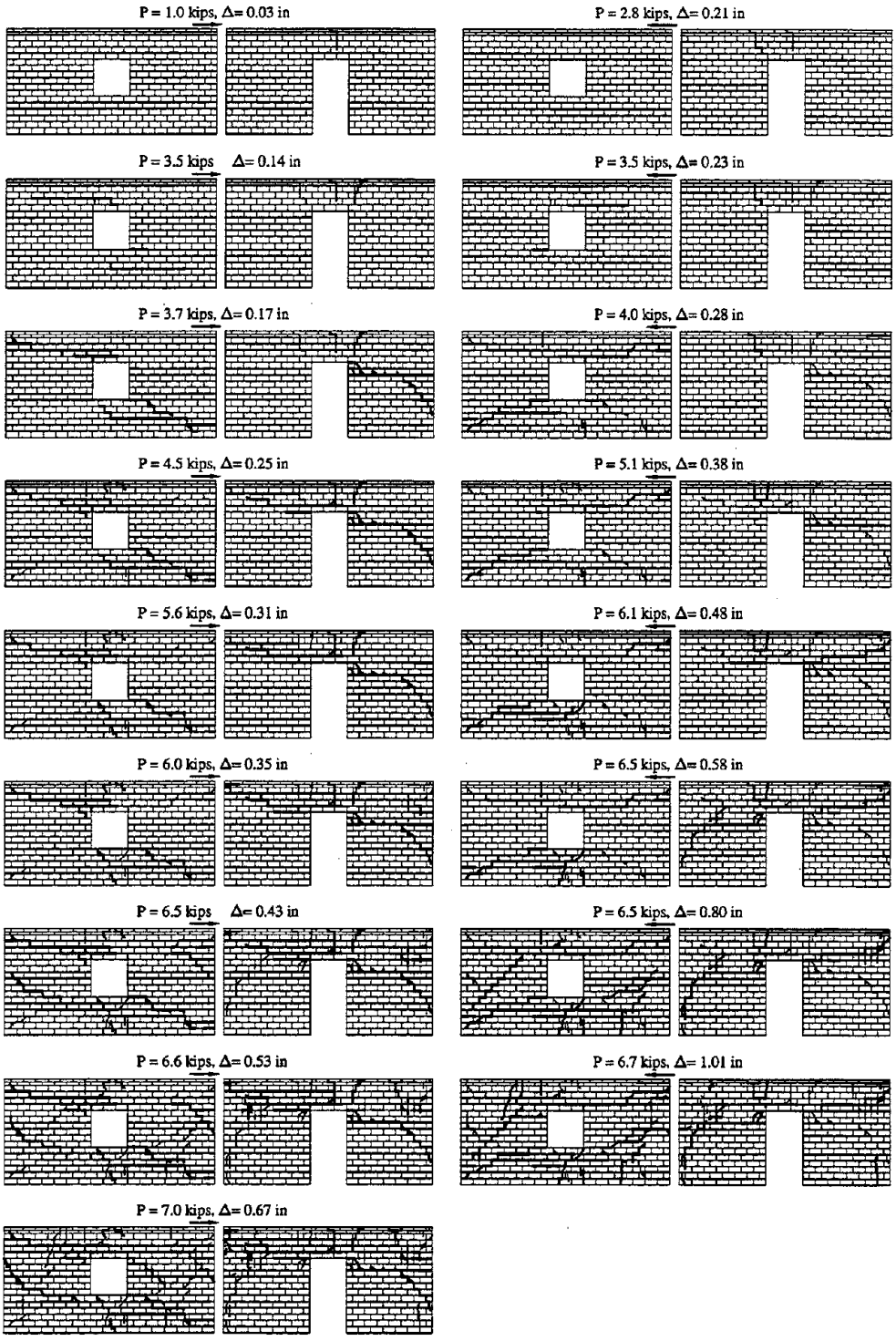

FIGURE 4-9 Sequence of crack patterns for specimen Q21AOB.

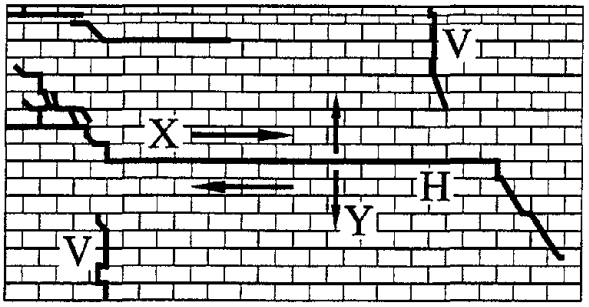

FIGURE 4-10 Dilation of cracks in masonry infill walls.

4.1.4 Identification of load-deformation parameters

From the hysteretic relations shown in Figures 4-1 and 4-2, a generic hysteresis loop for an infilled frame may be depicted as shown in Figure 4-11. The coordinates of the loop are normalized such that the loop ends are the points (1, 1) and (-1, -1). Considering the inter-story drift D_s and the story shear S_s, normalized equivalent quantities are given by

$$\rho = \frac{S_s}{S_s^{max}} \qquad \& \qquad \phi = \frac{D_s}{D_s^{max}} \tag{4.3}$$

where superscript (max) implies that the quantity is the maximum during a particular loop. To fully describe the loop, five physical quantities may be identified in Figure 4-11, namely,

1. The maximum slope of the unloading curve (K_+).
2. The maximum slope of the reloading curve (K_-).
3. The slope at zero displacement (K_0).
4. The residual story shear force at zero displacement (ρ_0).
5. The area of the loop (A).

All these parameters are defined in the normalized plane of the loop.

The experimental data obtained from specimen Q21SSB with sets (A) and (B) of applied displacement cycles are used, as an example, to study the behavior of the five parameters governing the shape of the loop. Also, the experimental data is used to obtain the envelopes of the hysteretic loops. These envelopes are necessary to characterize the evolution of the shape of the hysteretic loops under general loading history, *e.g.* earthquake excitation.

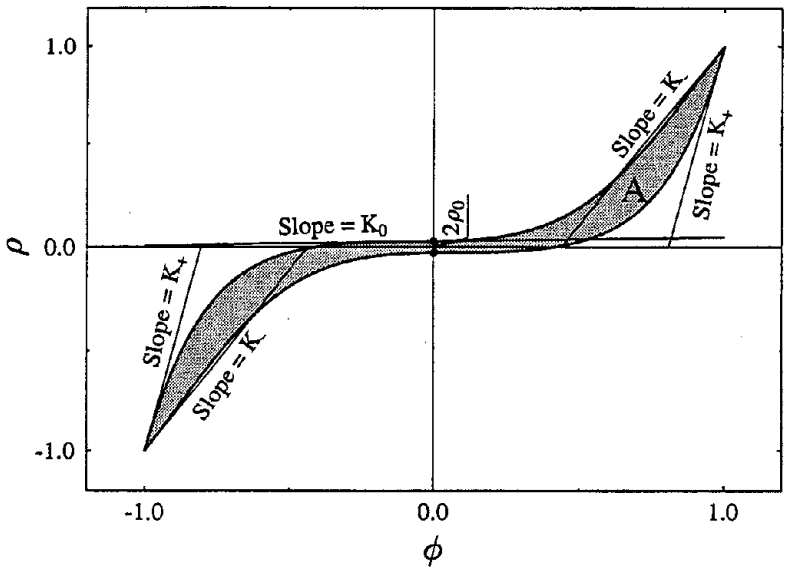

FIGURE 4-11 A generic hysteresis loop and its physical parameters.

The hysteresis envelopes are normalized with respect to the ultimate story shear and the corresponding inter-story drift (S_s^{ult}, D_s^{ult}) as shown in Figure 4-12. In the same figure the response of the bare frame is also plotted. The axes in this figure are given by

$$S_r = \frac{S_s}{S_s^{ult}} \qquad \& \qquad D_r = \frac{D_s}{D_s^{ult}} \tag{4.4}$$

The first four parameters (K_+, K_-, K_0, and ρ_0) are reasonably correlated with the maximum inter-story drift D_s^{max} applied for each loop through *simple polynomial functions.* This maximum applied inter-story drift is normalized with respect to the inter-story drift corresponding to the ultimate story shear, *i.e.*

$$DR_s^{max} = \frac{D_s^{max}}{D_s^{ult}} \tag{4.5}$$

Figures 4-13, 4-14, 4-15 and 4-16 show these relations.

The fifth parameter namely the area of the hysteresis loop (A) is *indirectly* related to the amount of input energy (E_I). This indirect relation, shown in Figure 4-17, is established between the accumulated amounts of energy dissipated (E_h) and E_I. These quantities are defined for the n^{th} loop as follows,

$$E_h|_n = \sum_{i=1}^{n} \left(A^i \; DR_s^{max}|_i \; SR_s^{max}|_i \right) \tag{4.6}$$

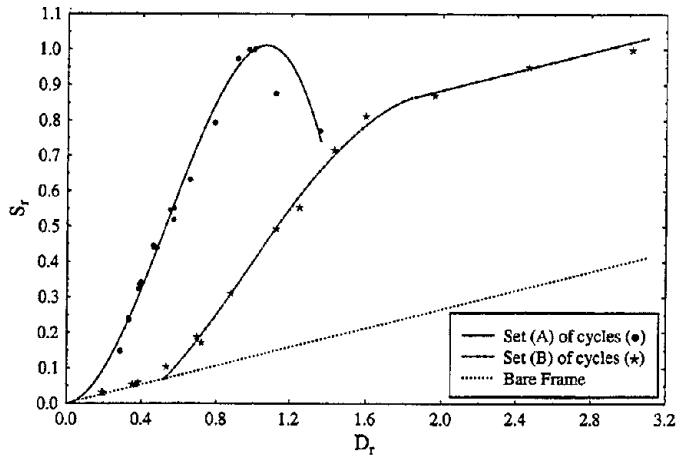

FIGURE 4-12 Normalized envelopes of the hysteresis loops.

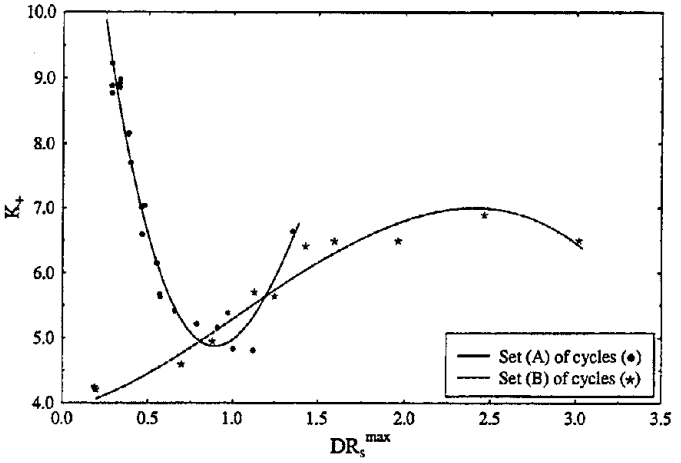

FIGURE 4-13 Relations for the maximum slope of the unloading curve (K_+).

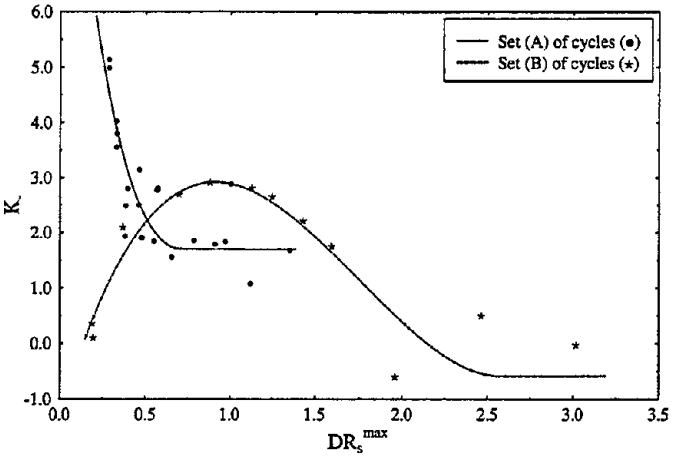

FIGURE 4-14 Relations for the maximum slope of the reloading curve (K_-).

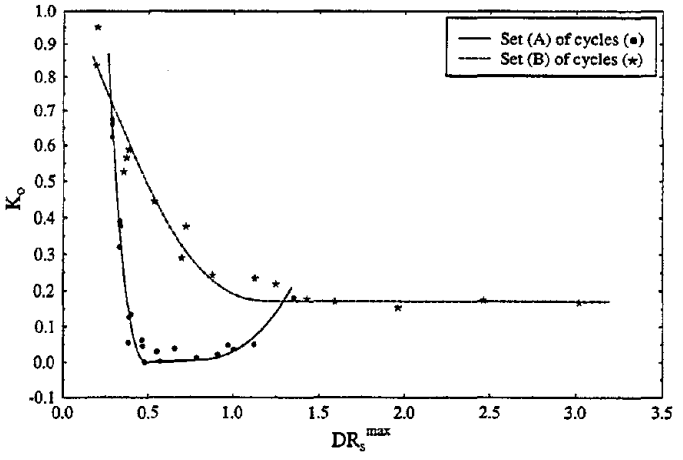

FIGURE 4-15 Relations for the slope at zero displacement (K_0).

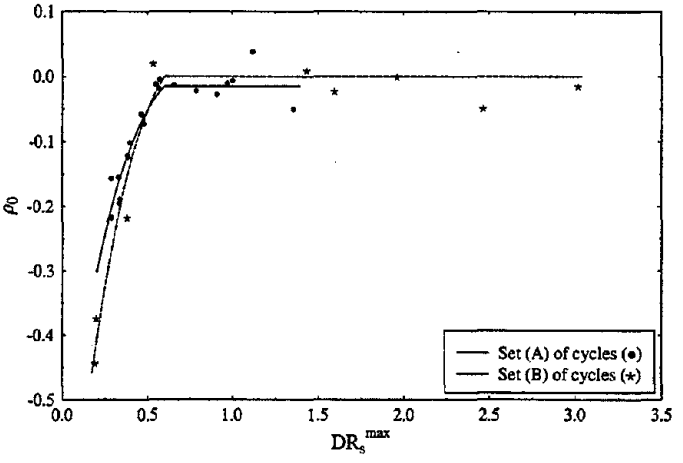

FIGURE 4-16 Relations for the residual story shear force (ρ_0).

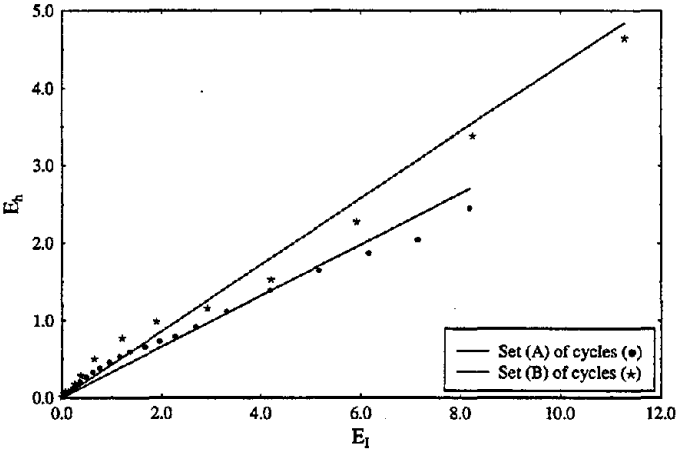

FIGURE 4-17 Relations for the accumulated hysteretic energy (E_h).

$$E_I|_n = \sum_{i=1}^{n} (DR_s^{max}|_i \, SR_s^{max}|_i) \tag{4.7}$$

where:

$$SR_s^{max} = \frac{S_{max}}{S_{ult}} \tag{4.8}$$

It should be noted that the obtained *linear* relations between E_h and E_I, shown in Figure 4-17, allow for a simple estimation of *damage* as a function of E_h for higher values of E_I.

4.2 Local Response

The structural responses of specific sections and components of the infilled frames are presented in the current section. These responses are in the form of deformed shapes, straining actions, interface conditions and opening distortions.

4.2.1 Deformed shapes and straining actions of an exterior column

From the measurements discussed in the previous section, the variations of lateral deformation along the height of the exterior column of the infilled frames are obtained. From the measurements of specimen Q21SSB, Figure 4-18 is obtained. In this figure, plots for the load-deformation hysteresis loops given at 4 different locations along the height of the right exterior column are shown. Before any visible damage of the infills, the deformed shapes along the height of the right exterior column of specimen Q21SSB are shown in Figure 4-19 where the shape corresponding to each loading direction at the same load level is indicated. It should be noted that because of the orientation of the DCDT's in Figure 3-6, negative displacement measurements in Figure 4-18 correspond to positive displacements in Figure 4-19. Based on the equivalent strut analogy, arrows indicating the directions of forces transmitted from the infill walls to the column are indicated in Figure 4-19. It is obvious that the locations of these forces coincide with the locations where an increase of the curvatures occur.

The variations of the bending moment with the applied lateral load obtained at locations 10, 12 and 14 shown in Figure 3-6 are plotted in Figure 4-20. In this figure, positive bending moment implies tension in the outer fibers of the section and positive load correspond to positive displacement in Figure 4-19. From Figures 4-19 and 4-20, the following points may be concluded:

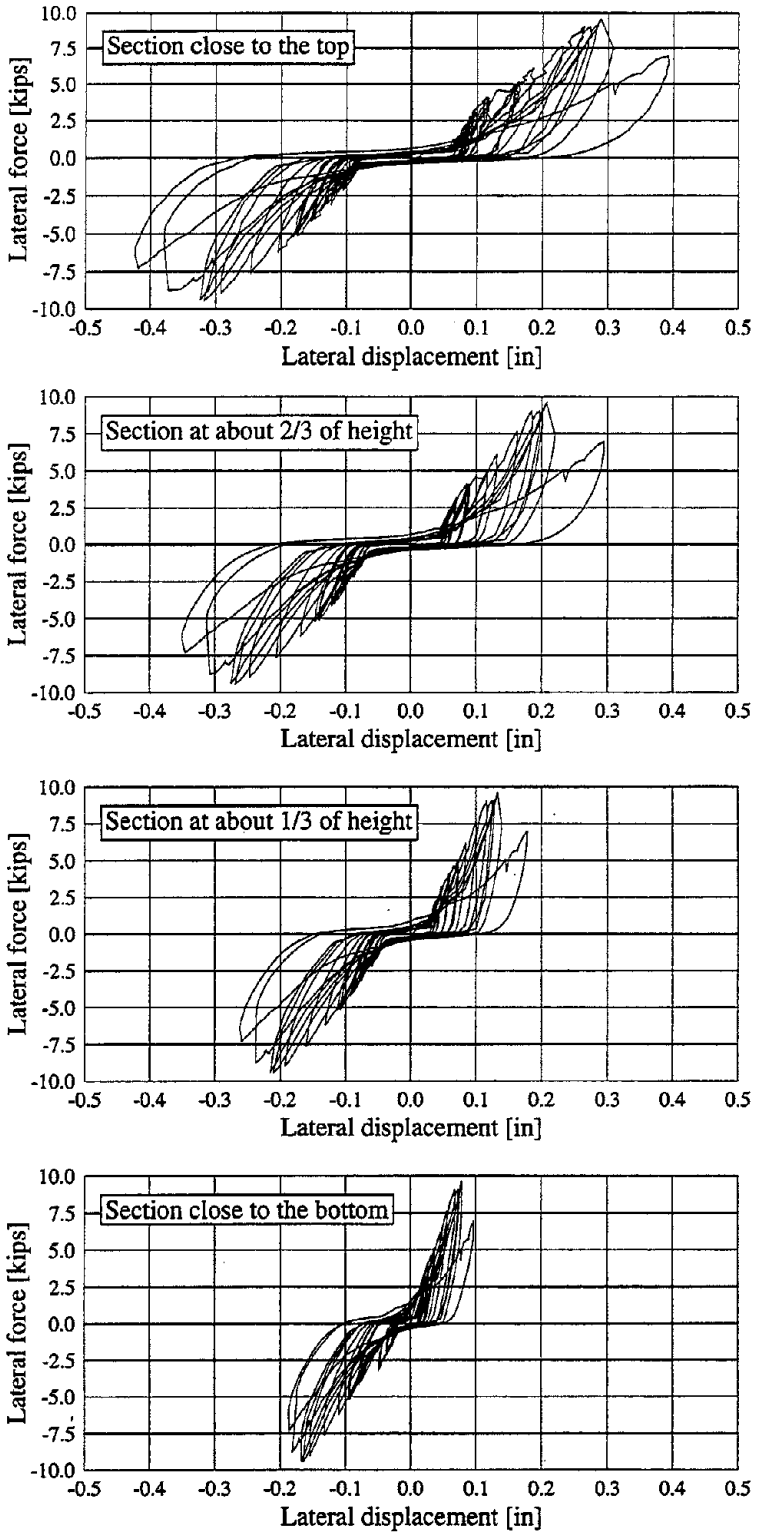

FIGURE 4-18 Load-displacement relations along the height of the right column of specimen Q21SSB obtained from set (A).

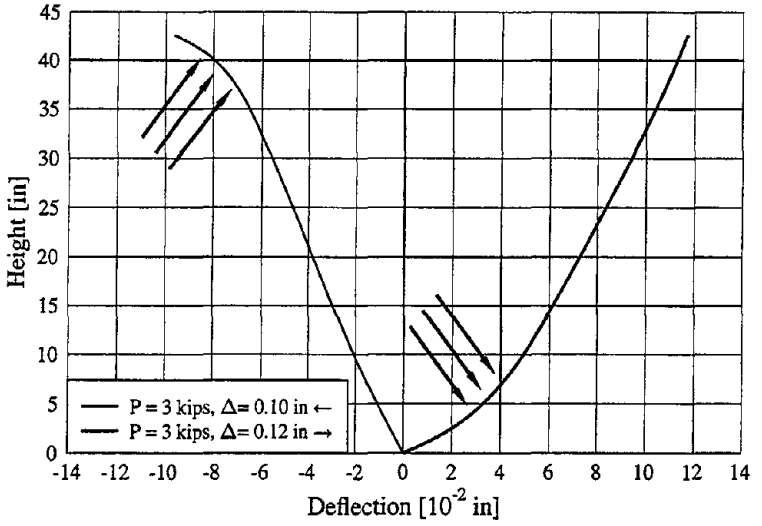

FIGURE 4-19 Deflected shapes of the right column of specimen Q21SSB.

1. For both loading directions, all sections of the right column are always under positive bending moment. This agrees with the observed *single curvature* of this column as shown in Figure 4-19.

2. Larger bending moment occurs at the bottom location of the column while loading in the positive direction whereas larger bending moment occurs at the top location of the column while loading in the negative direction. This observation is in agreement with the increase of curvatures at these locations due to the *compression-only* strut actions provided by the infill walls in both loading directions.

3. In general, the variation of bending moment in the infilled frame members with applied lateral loading is *highly* nonlinear because of the continuous variation of the contact length between the frame members and the infills. This nonlinearity becomes more severe when wall cracks causing the distribution of forces between the frame and the wall to become highly indeterminate.

4.2.2 Straining actions in the central column

Figures 4-21 and 4-22 illustrate the variation of the normal force and the bending moment at different locations of the central column with the variation of the applied lateral displacement at the top of the central column. In these figures, the direction of the positive lateral displacement (Δ) is indicated in the insert of each figure. The positive normal force indicates tension whereas the positive bending moment indicates tension in the left fibers of the section. From Figures 4-21 and 4-22, the following points may be concluded:

1. The normal force in the central column is always tension indicating a significant effect of the infill walls, particularly in the case of reinforced concrete frames where tension

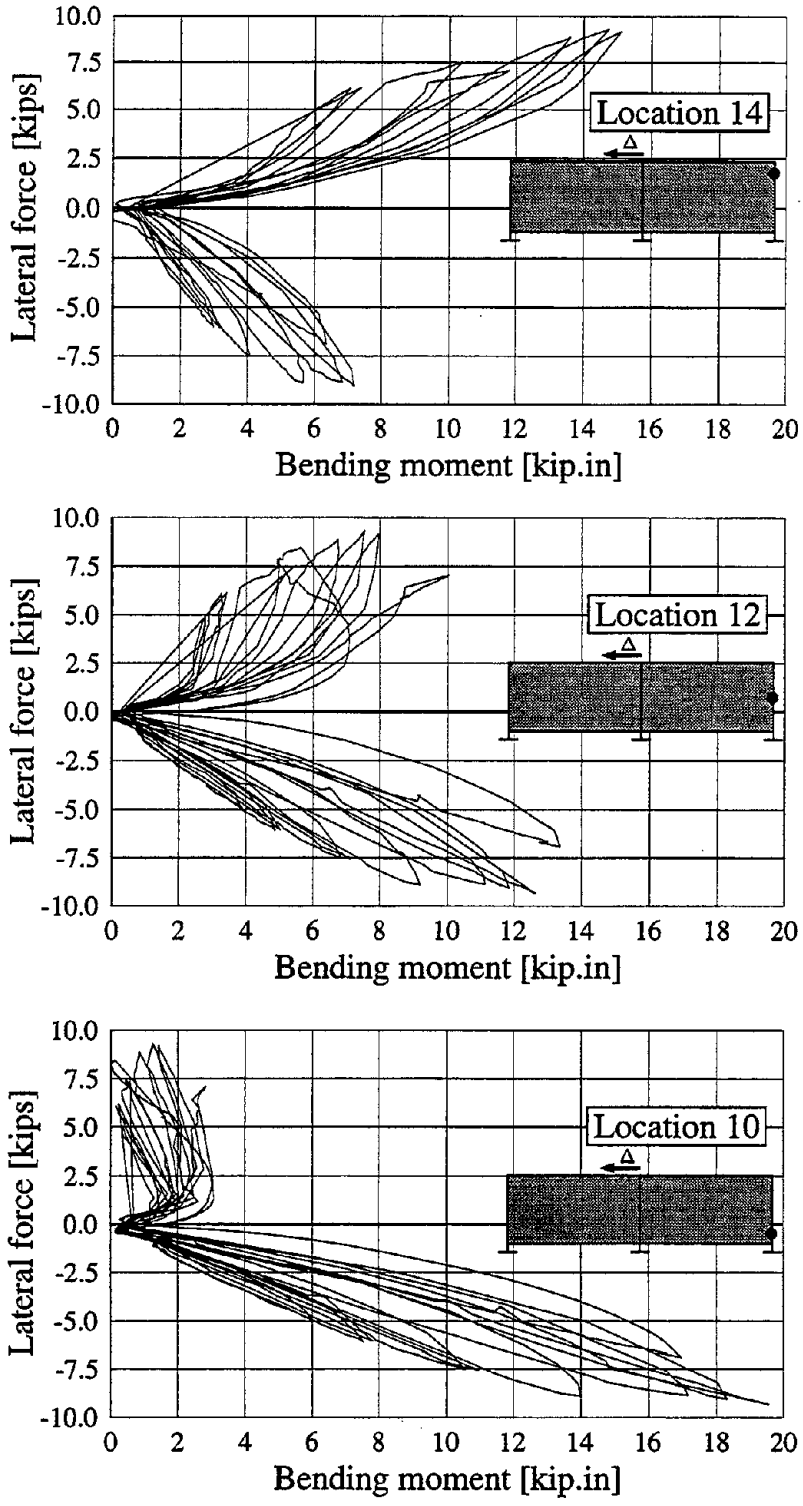

FIGURE 4-20 Variation of bending moment with applied lateral load at different locations of the right column of specimen Q21SSB obtained from set (A).

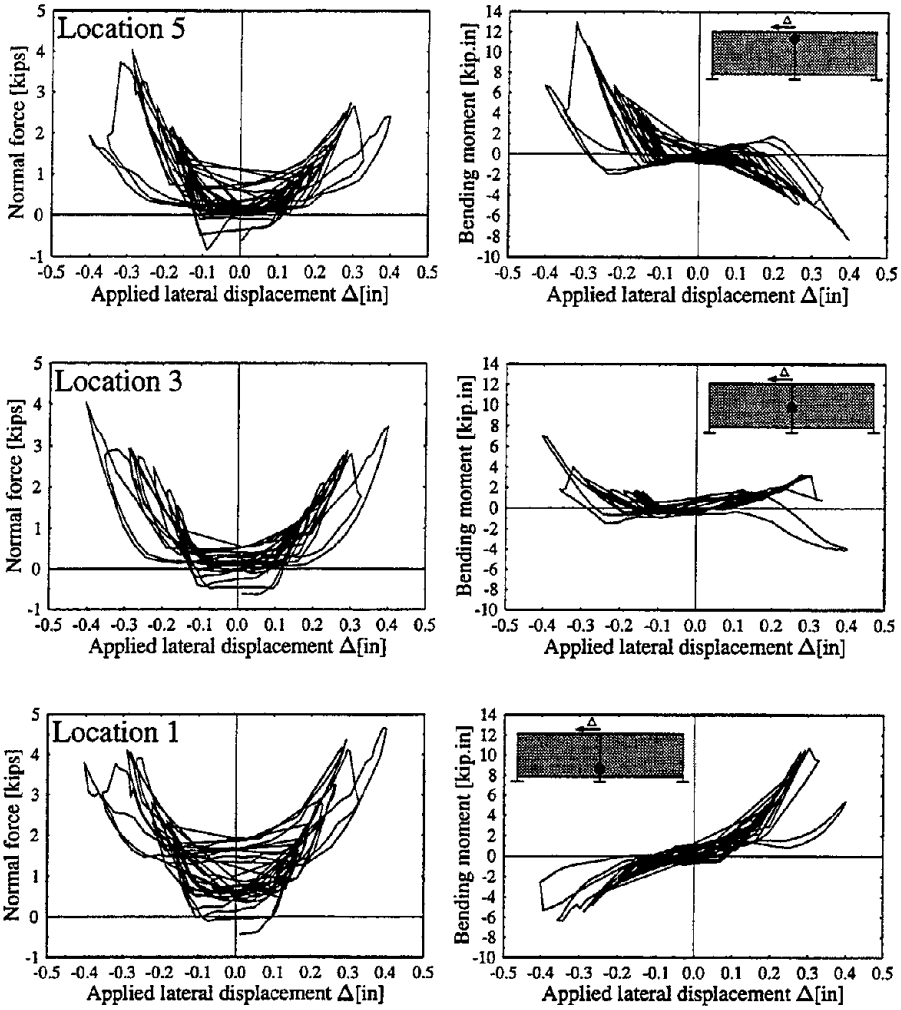

FIGURE 4-21 Variation of straining actions with applied lateral displacement at different locations of the central column of specimen Q21SSB obtained from set (A).

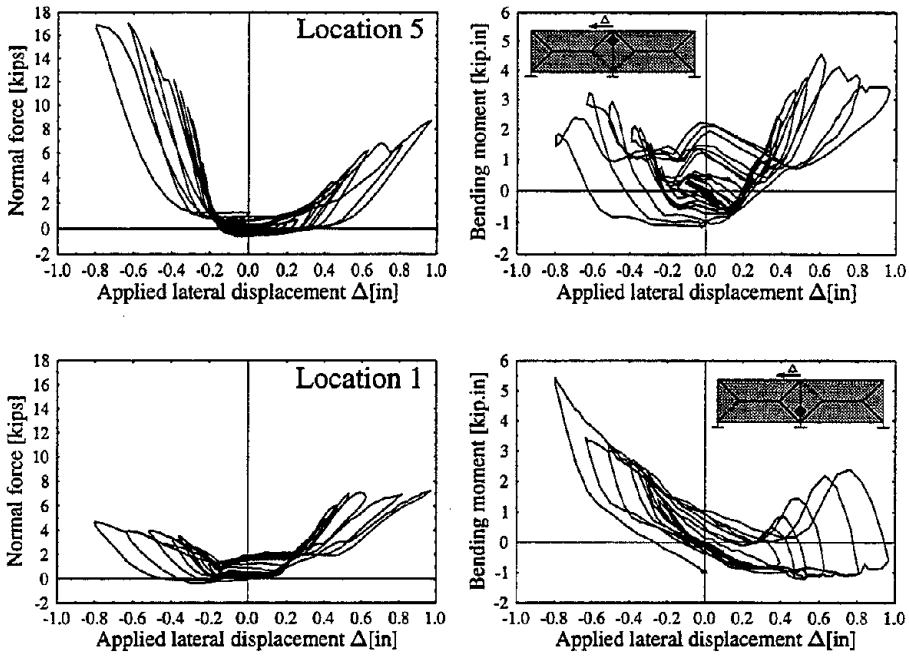

FIGURE 4-22 Variation of straining actions with applied lateral displacement at different locations of the central column of specimen Q21SSB obtained from set (B).

failure due to concrete cracking may lead to a catastrophic mode of failure.

2. The normal force in the central column significantly varies along the height of the column upon cracking of the infill walls.

3. Contrary to the single curvature of the exterior column, the central (interior) column experiences *double curvature* as evident by the reversed signs of the bending moments between locations 1 and 5.

4. Upon load reversal, the bending moment changes in sign indicating the reversed curvature which again is not the case for the exterior column.

5. Cracking in the infills significantly complicates the determination of the bending moment in the frame members because of the highly random distribution of cracks leading to difficulty in determining the contact length and contact pressure between the wall and the frame members.

4.2.3 Strains of the solid infills

The variations of the strain measurements at different locations on the diagonal of one of the infill walls of specimen Q21SSB with the applied lateral load for set (A) are illustrated in Figure 4-23. The positive value of the applied lateral load implies compression along

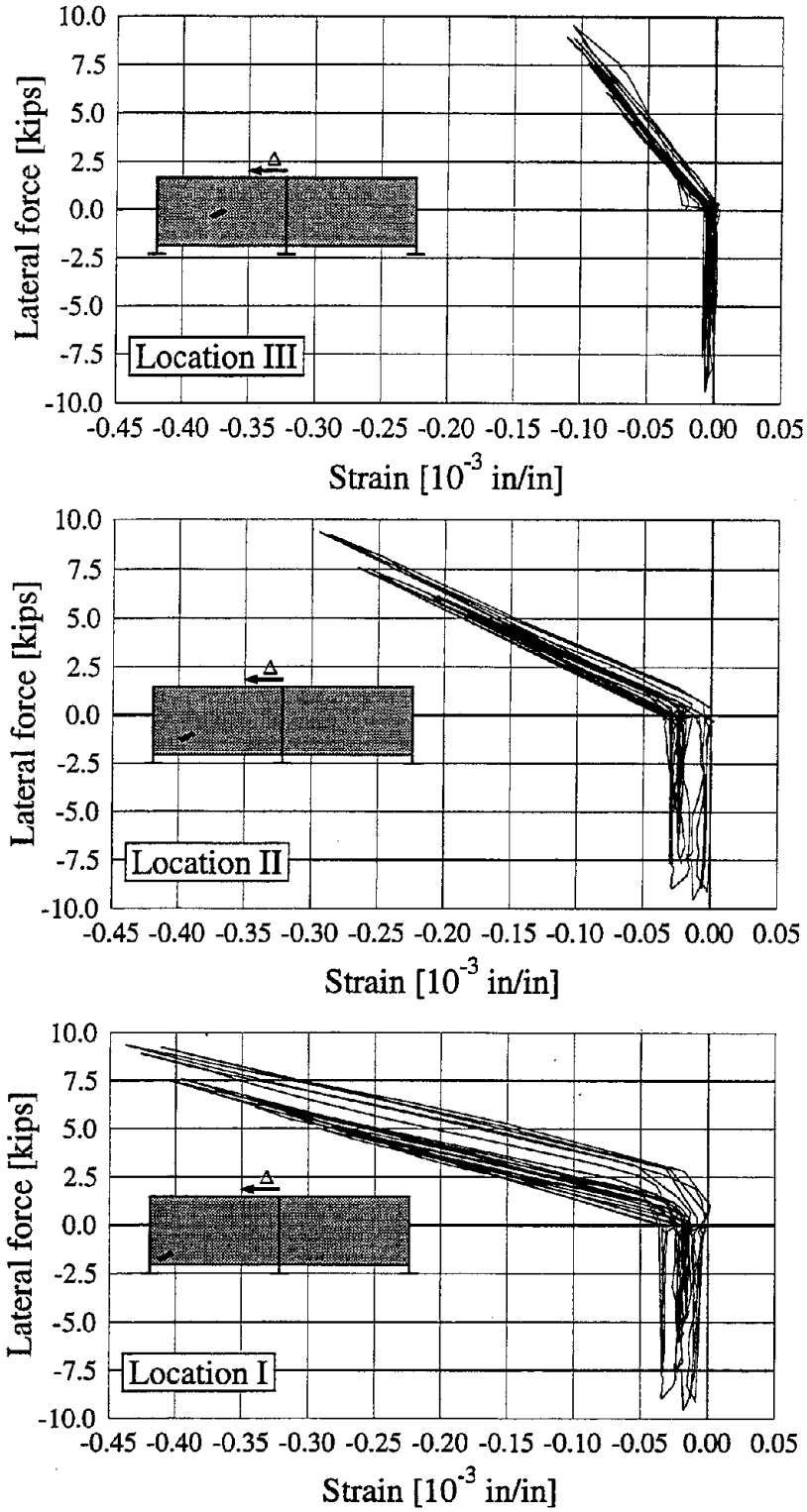

FIGURE 4-23 Variation of strains along the diagonal of an infill wall with applied lateral load of specimen Q21SSB obtained from set (A).

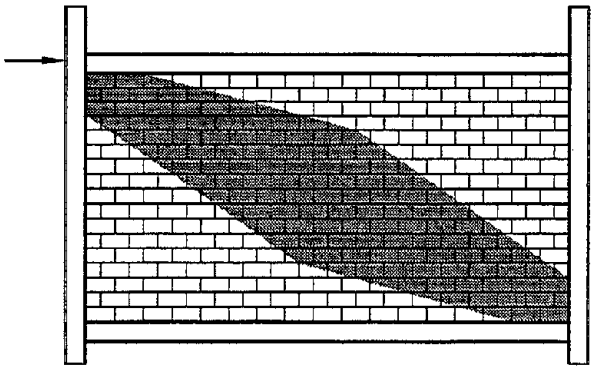

FIGURE 4-24 Possible variation of the cross-sectional area of the equivalent strut model in infilled frames.

the diagonal and negative value of the strain implies compression. Accordingly, the results given by Figure 4-23 can be interpreted as follows:

1. Only compressive stresses are transmitted along the diagonals (*i.e.* infills may be idealized using compression-only struts).
2. Strains and consequently stresses are highly concentrated at the compressed corners of the infill walls. These strains and stresses decay rapidly towards the center of the infill panel.
3. Up to the cracking load of the infill walls, the relation between the strains along the diagonals of the infill walls and the applied stresses are *almost linear* indicating the validity of the equivalent strut analogy for that stage of loading.

From the previous list one may conclude that an equivalent strut acting in compression only can be used to represent the effect of the infill wall on the bounding frame members. This strut tends to be wider towards the center of the infill wall as shown in Figure 4-24. With this *gradual increase* of the cross sectional area, the concentration of strains and stresses at the corners may be captured.

4.2.4 Infill wall deformations

The relative displacement measurements between two points in the infilled frames will be discussed in this section. These measurements give indications of the deformation field of the infill walls at locations of displacement discontinuities due to change of material (*e.g.* frame/wall interface), absence of material (*e.g.* openings) or cracking.

Deformations along the diagonals and off-diagonals of the solid infill walls were measured as indicated in Figure 3-7. Results from these measurements were reported in references

[82], [25] and [55] and will not be repeated here. In general, these results verified the compression-only six strut model for an infill wall [16].

The variation of the applied lateral load with the lateral displacement at the top of the central column shown in Figure 4-25(c) is compared with the variation of this load with the gap opening and closing at the top of the central column with respect to the right infill wall (Figure 4-25(a)) and the sliding of the right infill wall with respect to the center of the top beam (Figure 4-25(b)). The following points may be inferred from these relations:

1. Full contact without elastic deformation is obtained in the direction of gap closure.
2. Sliding response between the center of the top beam and the infill wall is almost symmetric.
3. The flat region in the gap response (Figure 4-25(a)) corresponds to one side of the flat region in the load-displacement relation of Figure 4-25(c).
4. In the gap opening direction, the sliding is about twice the gap opening indicating the equal distribution of the gap formation for both the infill/central column and the infill/exterior column.

The deformations along the two diagonals of the window opening in specimen Q12AOB for set (B) are illustrated in Figure 4-26. These two diagonals are designated (1) and (2) in the insert of Figure 4-26(a). The deformation along these diagonals are mainly due to crack opening and closing which explains the asymmetric variation of the displacement with the loading in Figures 4-26(b) and (c). From such measurements monitoring of crack opening and closing was achieved.

The mortar joint dilatancy was determined by special instruments (DCDT's) mounted on the walls after crack initiated. These instruments were depicted in Figure 3-9. A sample of the obtained measurements is illustrated in Figure 4-27 for a crack along the bed joint at the center of the right infill wall of specimen Q21SSB obtained for loading set (B). Defining the angle of dilatancy ψ as follows

$$\psi = \tan^{-1}\left(\frac{v}{u}\right) \tag{4.9}$$

where v and u are the displacements normal to and tangential along the bed joint crack, respectively. From Figure 4-27, at the maximum applied displacement, a small angle of dilatancy may be obtained. This angle ranges from 10^o to 30^o which is much lower than the angle of internal friction ϕ which may be obtained from Figure 2-13 ($\phi = \tan^{-1}(1.3) = 52^o$).

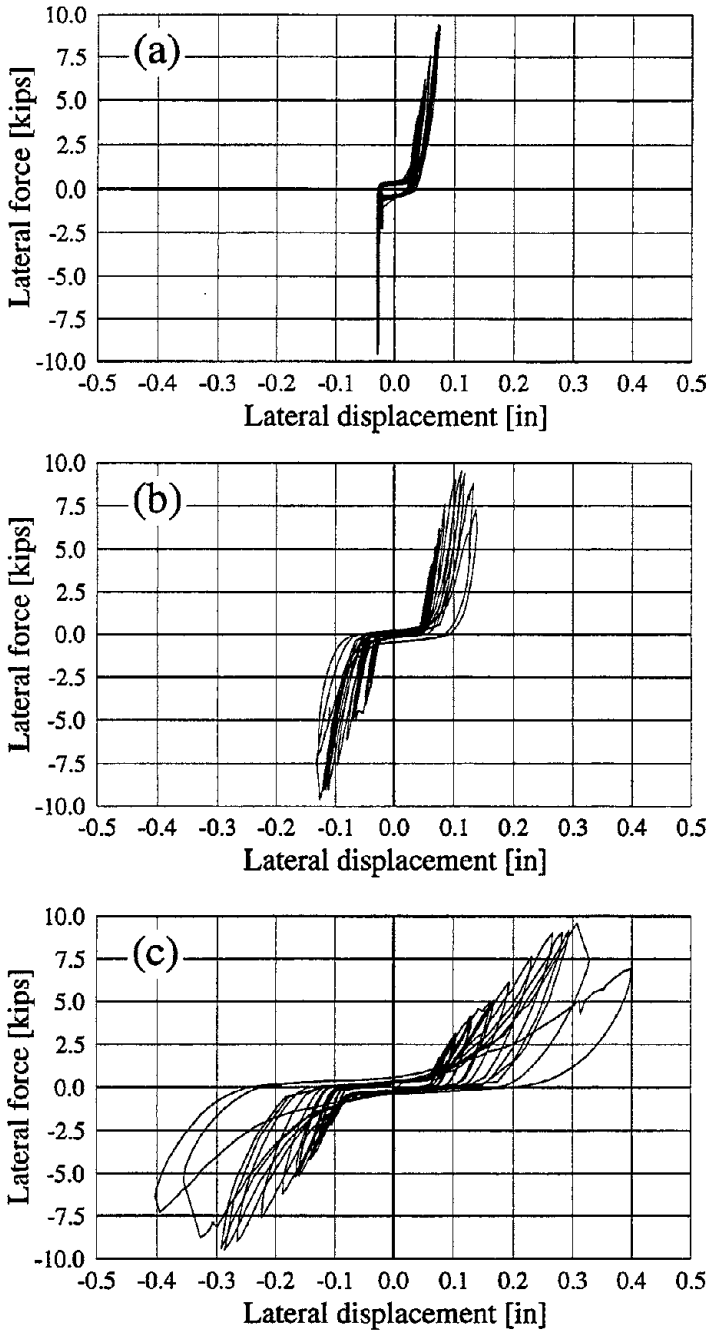

FIGURE 4-25 Variation of the applied lateral load with different displacements of specimen Q21SSB obtained from set (A); (a) Opening of gap at the top of the central column with the right panel; (b) Sliding of the right panel with respect to the center of the top beam; (c) Applied lateral displacement at the top of the central column.

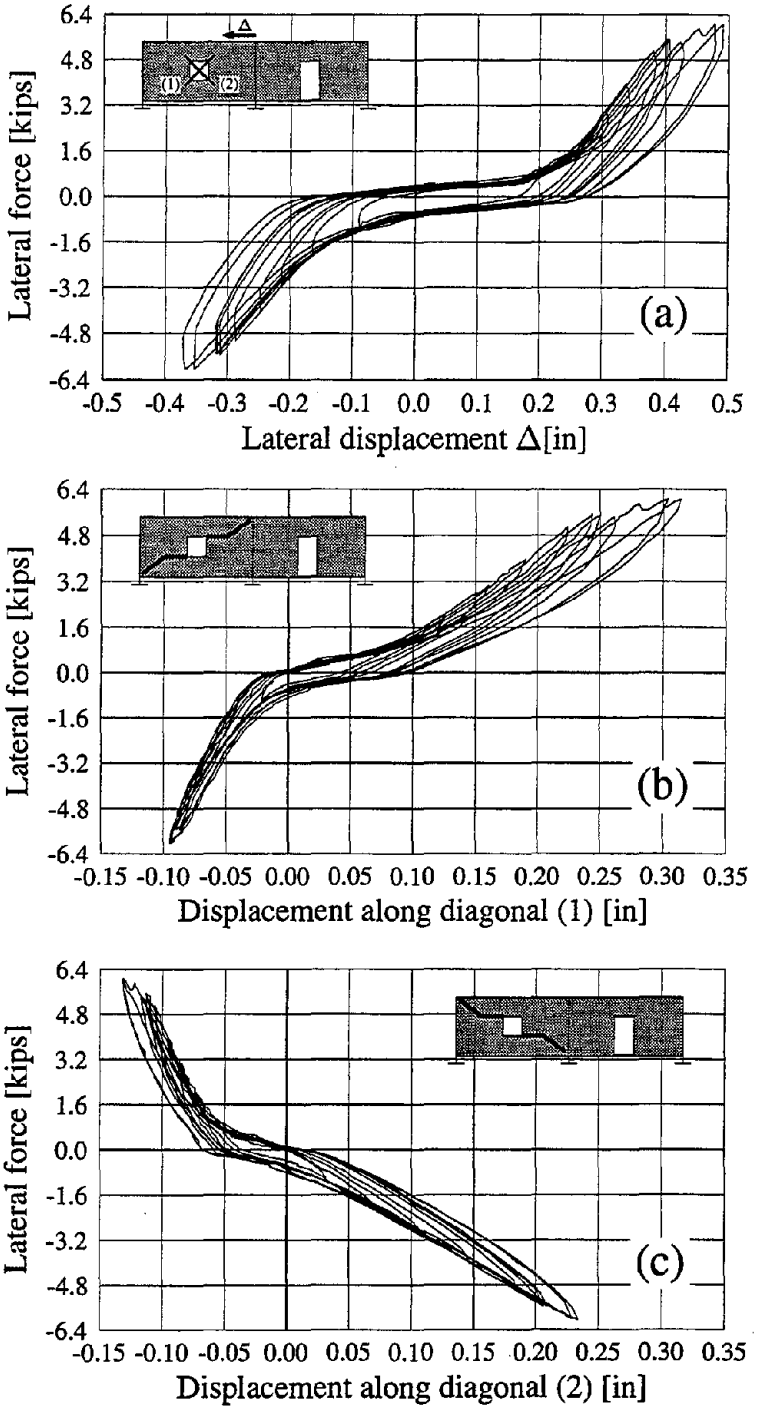

FIGURE 4-26 Results obtained from specimen Q21AOB for set (B); (a) Applied lateral displacement-load relation; (b) Deformation along diagonal (1); (c) Deformation along diagonal (2).

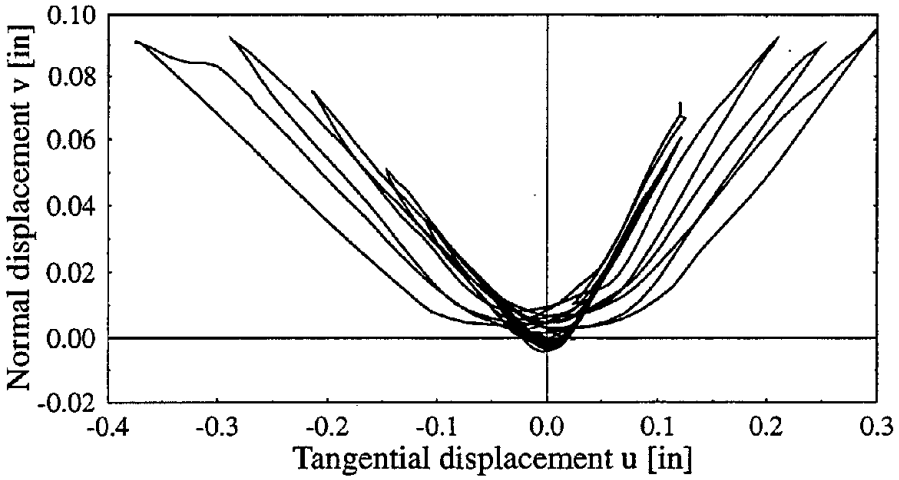

FIGURE 4-27 Bed joint dilatancy for a crack at the center of the right panel of specimen Q21SSB obtained from set (B).

4.3 Basis of Hysteresis Model Formulation

To represent the force-displacement response of infilled frames, the upper (upper sign) and lower (lower sign) curves of any hysteresis loop (see Figure 4-11) may be represented by

$$\rho = \mp a_0 + a_1\phi \mp a_2\phi^2 + a_3\phi^3 \mp a_4\phi^4 + a_5\phi^5 \mp a_6\phi^6 \tag{4.10}$$

where the coefficients $a_0, \ldots, a_6$ can be reduced to five by enforcing the conditions,

$$\rho|_{\phi=\pm 1.0} = \pm 1.0 \tag{4.11}$$

Accordingly,

$$a_6 = -(a_0 + a_2 + a_4) \qquad \& \qquad a_5 = 1 - (a_1 + a_3) \tag{4.12}$$

The resulting independent coefficients can be related to the previously discussed five physical quantities, defined in Figure 4-11, as follows:

$$\rho_0 = \rho|_{\phi=0.0} = \mp a_0 \tag{4.13}$$

$$K_0 = \left.\frac{\partial \rho}{\partial \phi}\right|_{\phi=0.0} = a_1 \tag{4.14}$$

The slopes at the ends of the lower curve of any loop (K_+ and K_-) are given by,

$$K_+ = \left.\frac{\partial \rho}{\partial \phi}\right|_{\phi=+1.0} = 5 - 6a_0 - 4a_1 - 4a_2 - 2a_3 - 2a_4 \tag{4.15}$$

$$K_- = \left.\frac{\partial \rho}{\partial \phi}\right|_{\phi=-1.0} = 5 + 6a_0 - 4a_1 + 4a_2 - 2a_3 + 2a_4 \tag{4.16}$$

From Eq. (4.10), the area of the hysteresis loop (representing the amount of energy dissipated during a cycle) can be calculated by subtracting the integral of the upper curve of the loop from that corresponding to the lower curve. Therefore, the area of the loop (A) is given by,

$$A = 2\int_{-1}^{+1} \rho \, d\phi = -\left(\frac{24}{7}a_0 + \frac{16}{21}a_2 + \frac{8}{35}a_4\right) \tag{4.17}$$

Eqs. (4.13), (4.14), (4.15), (4.16) and (4.17) can be simultaneously solved to give,

$$\begin{Bmatrix} a_0 \\ a_1 \\ a_2 \\ a_3 \\ a_4 \end{Bmatrix} = \frac{1}{32}\begin{Bmatrix} 00 \\ 00 \\ 00 \\ 80 \\ 00 \end{Bmatrix} + \frac{1}{32}\begin{bmatrix} 032 & 00 & 00 & 00 & 000 \\ 000 & 32 & 00 & 00 & 000 \\ -288 & 00 & 06 & -06 & -105 \\ 000 & -64 & -08 & -08 & 000 \\ 576 & 00 & -20 & 20 & 210 \end{bmatrix}\begin{Bmatrix} \rho_0 \\ K_0 \\ K_+ \\ K_- \\ A \end{Bmatrix} \tag{4.18}$$

Estimating the physical quantities ρ_0, K_0, K_+, K_-, and A through experimentation, Eq. (4.18) directly allow for the determination of the coefficients of Eq. 4.10. Having the envelopes of the hysteresis loops shown in Figure 4-12 and the hysteresis curves shown in Figure 4-11, it is possible to simulate the force-displacement relationship of an infilled frame for a given displacement protocol.

4.4 Summary

The results of the quasi-static experiments were presented in this section. These results reflected important points regarding the global as well as the local responses of the tested infilled frames. The effects of the number of bays, material group and openings on the hysteresis curves and the mode of failure were investigated. The hysteresis relations were investigated and key parameters were identified which were used at the end of this section to formulate a model for the hysteresis loop where all its parameters are physically meaningful. Deformation and straining actions of the exterior and the interior columns were presented. Also, the strains and deformations of the infill walls were illustrated and some conclusions regarding the equivalent strut model were drawn.

SECTION 5

CONCLUDING REMARKS

Unreinforced masonry infill walls can play an important role in the strength and ductility of framed structures, and should be considered in both analysis and design. Accounting for masonry infill walls in the design process mandates knowledge of complicated interaction mechanisms and failure modes. The nature of the problem requires experimental data which are easy to interpret and utilize, such as those obtained from quasi-static experiments.

This report started with the identification of the composite nature of masonry through static experimentation of basic specimens of masonry and its constituents. The results of this identification task led to a set of parameters for the geometrical, physical and mechanical properties of the materials.

The study proceeded through the adoption of quasi-static experimentation methodology where information regarding the structural capacity of infilled frames under cyclic loading was assessed. Major parameters were the material group, the number of bays and the openings. Effect of these parameters on the deformation and the load capacities and on the mode of failure were established. Observations on the local level of behavior indicated that infill walls significantly alter the distribution of the straining actions in the frame members.

The obtained experimental results provide the necessary data base to develop improved simple models for infilled frames such as the equivalent strut models. Although these models were explored in the present study, further refinements are still needed. Such models can be used for the evaluation of existing infilled structures and the design of new ones.

SECTION 6

REFERENCES

[1] American Institute of Steel Construction (AISC), *Manual of Steel Construction, Allowable Stress Design* (ASD), 9th edition, Chicago, Illinois (1989).

[2] American Society for Testing and Materials, *ASTM standards on masonry*, 1st edition, Philadelphia, Pennsylvania (1990).

[3] K. A. Amos, 'The shear strength of masonry infilled steel frames', *M.Sc. Thesis*, University of New Brunswick, Canada (1985).

[4] R. Angel, D. Abrams, D. Shapiro, J. Uzarski and M. Webster, 'Behavior of reinforced concrete frames with masonry infills', *Civil Engrg. Studies, Structural Research Series No. 589, UILU-ENG-94-2005*, Dept. of Civil Engrg., University of Illinois at Urbana-Champaign (1994).

[5] Applied Technology Council, 'Guidelines for cyclic seismic testing of components of steel structures', *Publication ATC-24*, Redwood City, California (1992).

[6] R. H. Atkinson, B. P. Amadei, S. Saeb and S. Sture, 'Response of masonry bed joints in direct shear', *J. Struct. Engrg.*, ASCE, **115**, 9, 2276-2296 (1989).

[7] G. R. Ballouz, 'Nonlinear behavior of infilled lightly reinforced concrete frames (LRCF's) under in-plane monotonic loading', *M.Sc. Thesis*, Drexel University, Philadelphia, Pennsylvania (1994).

[8] H. K. Barua and S. K. Mallick, 'Behaviour of mortar infilled steel frames under lateral load', *Building and Environment*, **12**, 3, 263-272 (1977).

[9] I. J. Becica and H. G. Harris, 'Evaluation of techniques in the direct modeling of concrete masonry structures', *Structural Models Laboratory Report No. M77-1*, Department of Civil Engineering, Drexel University, Philadelphia, Pennsylvania (1977).

[10] J. R. Benjamin and H. A. Williams, 'The behavior of one-storey reinforced concrete shear walls', *J. Struct. Div.*, ASCE, Proc. Paper 1254, **83**, ST3, 1-35 (1957).

[11] J. R. Benjamin and H. A. Williams, 'The behavior of one-storey brick shear walls', *J. Struct. Div.*, ASCE, Proc. Paper 1723, **84**, ST4 (1958).

[12] J. R. Benjamin and H. A. Williams, 'Behavior of one-storey walls containing opening', *J. Amer. Concrete Inst.*, **30**, 5, 605-618 (1958).

[13] B. A. Bolt, 'Chapter 1: The nature of earthquake ground motion', *The seismic design handbook*, F. Naeim (ed.), Van Nostrand Reinhold, New York, 1-31 (1989).

[14] S. T. Brokken and V. V. Bertero, 'Studies on effects of infills in seismic resistant R/C construction', *Report No. UCB/EERC-81/12*, Earthquake Engrg. Res. Ctr., Univ. of California, Berkeley (1981).

[15] A. R. Chandrasekaran and B. Chandra, 'Experimental study of infilled frames', *Proc. 4th Symposium on Earthquake Engrg.*, Roorkee U. P., India, 75-80 (1970).

[16] C. Z. Chrysostomou, 'Effects of degrading infill walls on the nonlinear seismic response of two-dimensional steel frames', *Ph.D. Dissertation*, Cornell University, Ithaca, New York (1991).

[17] J. L. Dawe and C. K. Seah, 'Behavior of masonry infill steel frames', *Canadian J. of Civil Engrg.*, **16**, 865-876 (1989).

[18] J. L. Dawe A. B. Schriver and C. Sofocleous, 'Masonry infilled steel frames subjected to dynamic load', *Canadian J. of Civil Engrg.*, **16**, 877-885 (1989).

[19] R. V. Dawson, 'An analytical and experimental study of the lateral load response of framed structures before and after the inclusion of infill walls', *Ph.D. Dissertation*, The university of Calgary, Canada (1972).

[20] R. G. Drysdale, A. A. Hamid and L. R. Baker, *Masonry structures: behavior and design*, Prentice-Hall, Inc., Englewood Cliffs, New Jersy (1994).

[21] L. Esteva, 'Behavior under alternating loads of masonry diaphragms framed by reinforced concrete members', *Proc. Int. Symposium on the Effects of Repeated Loading of Materials and Structures (RILEM)*, Mexico City, **V** (1966).

[22] S. G. Fattal and L. E. Cattaneo, 'Evaluation of structural properties of masonry in existing buildings', NBSIR 74-520, National Bureau of Standards, Washington, D.C., July (1974).

[23] A. E. Fiorato, M. A. Sozen and W. L. Gamble, 'Behavior of five-storey reinforced concrete frames with filler walls', *Interim report to the department of defense office of secretary of the army, Office of civil defense*, Urbana, Illinois (1970).

[24] C. C. Fishburn, 'Effect of mortar properties on strength of masonry', NBS Monograph 36, *National Bureau of Standards*, Washington, D.C., November (1961).

[25] P. Gergely, R. N. White, D. Zawilinski and K. M. Mosalam, 'The interaction of masonry infill and steel or concrete frames', *Proc. 1993 National Earthquake Conf.*, Memphis, Tennessee, **II**, 183-192 (1993).

[26] G. M. M. Ghanem, 'Behavioral characteristics of partially reinforced loadbearing masonry wall structures', *Ph.D. Dissertation*, Helwan University, Cairo, Egypt (1992).

[27] C. T. Grimm, 'Masonry cracks: a review of the literature', *Masonry: materials, design, construction, & maintenance*, H. A. Harris, editor, ASTM, **STP 992**, 257-280 (1988).

[28] P. Guo, 'Investigation and modelling of the mechanical properties of masonry', *Ph.D. Dissertation*, McMaster University, Hamilton, Canada (1991).

[29] A. A. Hamid, 'Behavior characteristics of concrete masonry', *Ph.D. Dissertation*, McMaster University, Hamilton, Canada (1978).

[30] A. Hamid and B. Abboud, 'Direct modeling of ungrouted and grouted block masonry under in-plane loading', *Report No. MS84-1*, Department of Civil Engineering, Drexel University, Philadelphia, Pennsylvania (1984).

[31] H. G. Harris, G. R. Ballouz and K. W. Kopatz, 'Preliminary studies in seismic retrofitting of lightly reinforced concrete frames using masonry infills', *Proc. 6th North American Masonry Conf.*, Philadelphia, Pennsylvania, **1**, 383-395 (1993).

[32] M. Holmes, 'Steel frames with brick work and concrete infilling', *Proc. Instn. of Civ. Engrs.*, **19**, 473-478 (1961).

[33] M. Holmes, 'Combined loading on infilled frames', *Proc. Instn. of Civ. Engrs.*, **25**, 31-38 (1963).

[34] F. B. Johnson and J. N. Thompson, 'Development of diametral testing procedures to provide a measure of strength characteristics of masonry assemblages', *Designing engineering and construction with masonry products*, F. B. Johnson (ed.), Gulf Publishing Co., Houstone, Texas, 51-57 (1969).

[35] L. F. Kahn and R. D. Hanson, 'Infilled walls for earthquake strengthening', *J. Struct. Div.*, ASCE, **105**, ST2, 283-296 (1979).

[36] R. E. Klingner and V. V. Bertero, 'Infilled frames in earthquake-resistant construction', *Report No. EERC 76-32*, Earthquake Engrg. Res. Ctr., Univ. of California, Berkeley (1976).

[37] H. Krawinkler, 'Cyclic loading histories for seismic experimentation on structural components', *Earthquake SPECTRA*, **12**, 1, 1-12 (1996).

[38] J. M. Leuchars and J. C. Scrivener, 'Masonry infill panels subjected to cyclic in-plane loading', *Proc. South Pacific Regional Conf. of the NNSEE*, Wellington, New Zealand (1975).

[39] W. Lian, W. Qiyun, T. Jiahua and D. Groying, 'Inelastic earthquake response analysis of brick infilled frames', *Proc. 7th World Conf. on Earthquake Engrg.*, 307-314 (1980).

[40] T. C. Liauw, 'Tests on multistorey infilled frames subjected to dynamic lateral loading', *ACI Journal*, **97**, 4, 551-563 (1979).

[41] T. C. Liauw and K. H. Kwan, 'Plastic theory of infilled frames with finite interface shear strength', *Proc. Instn. of Civ. Engrs.*, Part 2, **75**, 3, 707-723 (1983).

[42] T. C. Liauw and K. H. Kwan, 'Static and cyclic behaviours of multistory infilled frames with different interface conditions', *Journal of Sounds and Vibrations*, **99**, 2, 275-283 (1985).

[43] T. C. Liauw and C. Q. Lo, 'On multibay infilled frames', *Proc. Instn. of Civ. Engrs.*, Part 2, **85**, 469-483 (1988).

[44] R. J. Mainstone, 'On the stiffnesses and strengths of infilled frames', *Proc. Instn. of Civ. Engrs.*, London, England, Paper 7360 S, 57-90 (1971).

[45] D. V. Mallick and R. T. Severn, 'The behavior of infilled frames under static loading', *Proc. Instn. of Civ. Engrs.*, London, England, **38**, 639-656 (1967).

[46] D. V. Mallick and R. T. Severn, 'Dynamic characteristics of infilled frames', *Proc. Instn. of Civ. Engrs.*, London, England, **39**, 261-287 (1968).

[47] D. V. Mallick and R. P. Garg, 'Effect of openings on the lateral stiffness of infilled frames', *Proc. Instn. of Civ. Engrs.*, London, England, **49**, 193-209 (1971).

[48] J. B. Mander, B. Nair, K. Wojtkowski and J. Ma, 'An experimental study on the seismic performance of brick-infilled steel frames with and without retrofit', *Technical Report NCEER-93-0001*, State University of New York at Buffalo (1993).

[49] G. C. Manos, D. Mpoufidis, M. Demosthenous and M. Triamataki, 'Influence of masonry infill panels on the response of R. C. structures subjected to lateral loads', *Proc. 5th North American Masonry Conf.*, University of Illinois at Urbana-Champaign, **I**, 93-104 (1990).

[50] G. C. Manos, B. Yasin and T. Valiasis, 'Small scale model simulation of the cyclic behavior of infill brick panels', *Proc. 6th North American Masonry Conf.*, Philadelphia, Pennsylvania, **1**, 359-370 (1993).

[51] R. T. McBride, 'The behavior of masonry infilled steel frames subjected to racking', *M. Sc. Thesis*, University of New Brunswick, Canada (1984).

[52] A. B. Mehrabi, P. B. Shing, M. P. Schuller and J. L Noland, 'Performance of masonry-infilled R/C frames under in-plane lateral loads', *Report CU/SR-94/6 Struct. Engrg. and Struct. Mech. Research Series*, Dept. of Civil, Environ. and Arch. Engrg., University of Colorado at Boulder (1994).

[53] O. R. Mestas, 'Nonlinear finite element analysis or confined masonry walls', *Individual Studies by Participants at the Int. Institute of Seismology and Earthquake Engrg.*, **30**, Tsukuba, Japan, 293-308 (1994).

[54] H. A. Moghaddam and P. J. Dowling, 'The state of the art in infilled frames', *ESEE Research Report No. 87-2*, Imperial College of Science and Technology, Civil Engrg. Dept., London (1987).

[55] K. M. Mosalam, P. Gergely, R. N. White and D. Zawilinski, 'The behavior of frames with concrete block infill walls', *Proc. 1st Egyptian Conf. on Earthquake Engrg.*, Hurghada, Egypt, 283-292 (1993).

[56] A. Parducci and M. Mezzi, 'Repeated horizontal displacements of infilled frames having different stiffness and connection systems - Experimental analysis', *Proc. 7th World Conf. on Earthquake Engrg.*, Istanbul, **V**, 193-196 (1980).

[57] C. C. Perry and H. R. Lissner, *The strain gage primer*, 2nd edition, McGraw-Hill Book Company, New York (1962).

[58] S. V. Polyakov, 'On the interaction between masonry filler walls and enclosing frame when loaded in the plane of the wall', *Transaction in Earthquake Engrg., EERI*, San Francisco, California, 36-42 (1967).

[59] L. L. Pook and J. L. Dawe, 'Effects of interface conditions between a masonry shear panel and surrounding steel frame', *Proc. 4th Conc. Masonry Symp.*, Fredericton, NB, Canada, 910-921 (1986).

[60] J. Richardson, 'The influence of initial gaps on infilled frame behavior', *M.Sc. Thesis*, University of New Brunswick, Canada (1986).

[61] J. R. Riddington, 'The influence of initial gaps on infilled frame behaviour', *Proc. Instn. of Civ. Engrs.*, Part 2, **77**, 295-310 (1984).

[62] G. M. Sabnis, H. G. Harris, R. N. White and M. S. Mirza, *Structural modeling and experimental techniques*, Prentice-Hall, Inc., New Jersy (1983).

[63] S. Sachanski, 'Analysis of the earthquake resistance of frame buildings taking into consideration the carrying capacity of the filling masonry', *Proc. 2nd World Conf. on Earthquake Engrg.*, Tokyo, **3**, 2127-2141 (1960).

[64] S. Sahlin, *Structural masonry*, Prentice-Hall, Inc., New Jersy (1971).

[65] C. G. Salmon and J. E. Johnson, *Steel structures: design and behavior emphasizing load and resistance factor design*, Harper & Row, Publishers, New York (1990).

[66] T. Schmidt, 'Experiments on the nonlinear behaviour of masonry infilled reinforced concrete frames', *Darmstadt Concrete, Annual J. on Concrete Structures*, Darmstadt, Germany, 4, 185-194 (1989).

[67] B. S. Stafford-Smith, 'Lateral stiffness of infilled frames', *J. Struct. Div.*, ASCE, **88**, ST6, 183-199 (1962).

[68] B. S. Stafford-Smith, 'Behavior of square infilled frames', *J. Struct. Div.*, ASCE, **91**, ST1, 381-403 (1966).

[69] B. S. Stafford-Smith, 'Model test results of vertical and horizontal loading of infilled frames', *ACI Journal*, Title No. 65-44, 618-625 (1968).

[70] S. Stockl and P. Hofman, 'Tests on the shear bond behavior in the bed joints of masonry', *Masonry International*, **9**, December (1986).

[71] F. C. Thomas, 'The strength of brickwork', *The Structural Engineer*, **33**, 2, 35-46 (1952).

[72] W. A. Thornton, 'Load and resistance factor design of connections', *Proc. National Engrg. Conf., solutions in steel*, American Institute of Steel Construction, Chicago, Illinois, 33-1 to 33-22 (1986).

[73] T. Valiasis and K. Stylianidis, 'Masonry infilled R/C frames under horizontal loading. Experimental results', *European Earthquake Engrg.*, **3**, 10-20 (1989).

[74] R. N. White, 'Seismic rehabilitation of non-ductile reinforced concrete frames - A summary of issues, methods, and needs', *NIST Workshop on Retrofitting of Lightly Reinforced Concrete Frames*, May (1995).

[75] R. H. Wood, 'Stability of tall buildings', *Proc. Instn. of Civ. Engrs.*, **11**, 69-102 (1985).

[76] B. Yanev and H. D. McNiven, 'An experimental program for studying the dynamic response of a steel frame with a variety of infill partitions', *Report No. UCB/EERC-85/16*, Earthquake Engrg. Res. Ctr., Univ. of California, Berkeley (1985).

[77] T. C. Yong, 'Shear strength of masonry infilled panels in steel frames', *M.Sc. Thesis*, University of New Brunswick, Canada (1984).

[78] M. Yorulmaz and M. A. Sozen, 'Behavior of single-storey reinforced concrete frames with filler walls', *University of Illinois at Urbana-Champaign, Civil Engrg. Studies, Structural Research Series No. 337*, Urbana (1968).

[79] R. Žarnić and M. Tomaževič, 'Study of the behaviour of masonry infilled reinforced concrete frames subjected to seismic loading - Part one', *Report ZRMK/IKPI-84/04*, Institute for Testing and Research in Materials and Structures, Ljubljana, Yugoslavia (1984).

[80] R. Žarnić and M. Tomaževič, 'Study of the behaviour of masonry infilled reinforced concrete frames subjected to seismic loading - Part two', *Report ZRMK/IKPI-85/02*, Institute for Testing and Research in Materials and Structures, Ljubljana, Yugoslavia (1985).

[81] R. Žarnić and M. Tomaževič, 'An experimentally obtained method for evaluation of the behaviour of masonry infilled R/C frames', *Proc. 9th World Conf. on Earthquake Engrg.*, Tokyo-Kyoto, Japan, **VI**, 162-168 (1988).

[82] D. J. Zawilinski, 'Experimental investigation of infilled frames under lateral loading', *M.Sc. Thesis*, Cornell University, Ithaca, New York (1994).

NATIONAL CENTER FOR EARTHQUAKE ENGINEERING RESEARCH
LIST OF TECHNICAL REPORTS

The National Center for Earthquake Engineering Research (NCEER) publishes technical reports on a variety of subjects related to earthquake engineering written by authors funded through NCEER. These reports are available from both NCEER Publications and the National Technical Information Service (NTIS). Requests for reports should be directed to NCEER Publications, National Center for Earthquake Engineering Research, State University of New York at Buffalo, Red Jacket Quadrangle, Buffalo, New York 14261. Reports can also be requested through NTIS, 5285 Port Royal Road, Springfield, Virginia 22161. NTIS accession numbers are shown in parenthesis, if available.

NCEER-87-0001 "First-Year Program in Research, Education and Technology Transfer," 3/5/87, (PB88-134275, A04, MF-A01).

NCEER-87-0002 "Experimental Evaluation of Instantaneous Optimal Algorithms for Structural Control," by R.C. Lin, T.T. Soong and A.M. Reinhorn, 4/20/87, (PB88-134341, A04, MF-A01).

NCEER-87-0003 "Experimentation Using the Earthquake Simulation Facilities at University at Buffalo," by A.M. Reinhorn and R.L. Ketter, to be published.

NCEER-87-0004 "The System Characteristics and Performance of a Shaking Table," by J.S. Hwang, K.C. Chang and G.C. Lee, 6/1/87, (PB88-134259, A03, MF-A01). This report is available only through NTIS (see address given above).

NCEER-87-0005 "A Finite Element Formulation for Nonlinear Viscoplastic Material Using a Q Model," by O. Gyebi and G. Dasgupta, 11/2/87, (PB88-213764, A08, MF-A01).

NCEER-87-0006 "Symbolic Manipulation Program (SMP) - Algebraic Codes for Two and Three Dimensional Finite Element Formulations," by X. Lee and G. Dasgupta, 11/9/87, (PB88-218522, A05, MF-A01).

NCEER-87-0007 "Instantaneous Optimal Control Laws for Tall Buildings Under Seismic Excitations," by J.N. Yang, A. Akbarpour and P. Ghaemmaghami, 6/10/87, (PB88-134333, A06, MF-A01). This report is only available through NTIS (see address given above).

NCEER-87-0008 "IDARC: Inelastic Damage Analysis of Reinforced Concrete Frame - Shear-Wall Structures," by Y.J. Park, A.M. Reinhorn and S.K. Kunnath, 7/20/87, (PB88-134325, A09, MF-A01). This report is only available through NTIS (see address given above).

NCEER-87-0009 "Liquefaction Potential for New York State: A Preliminary Report on Sites in Manhattan and Buffalo," by M. Budhu, V. Vijayakumar, R.F. Giese and L. Baumgras, 8/31/87, (PB88-163704, A03, MF-A01). This report is available only through NTIS (see address given above).

NCEER-87-0010 "Vertical and Torsional Vibration of Foundations in Inhomogeneous Media," by A.S. Veletsos and K.W. Dotson, 6/1/87, (PB88-134291, A03, MF-A01). This report is only available through NTIS (see address given above).

NCEER-87-0011 "Seismic Probabilistic Risk Assessment and Seismic Margins Studies for Nuclear Power Plants," by Howard H.M. Hwang, 6/15/87, (PB88-134267, A03, MF-A01). This report is only available through NTIS (see address given above).

NCEER-87-0012 "Parametric Studies of Frequency Response of Secondary Systems Under Ground-Acceleration Excitations," by Y. Yong and Y.K. Lin, 6/10/87, (PB88-134309, A03, MF-A01). This report is only available through NTIS (see address given above).

NCEER-87-0013 "Frequency Response of Secondary Systems Under Seismic Excitation," by J.A. HoLung, J. Cai and Y.K. Lin, 7/31/87, (PB88-134317, A05, MF-A01). This report is only available through NTIS (see address given above).

NCEER-87-0014 "Modelling Earthquake Ground Motions in Seismically Active Regions Using Parametric Time Series Methods," by G.W. Ellis and A.S. Cakmak, 8/25/87, (PB88-134283, A08, MF-A01). This report is only available through NTIS (see address given above).

NCEER-87-0015 "Detection and Assessment of Seismic Structural Damage," by E. DiPasquale and A.S. Cakmak, 8/25/87, (PB88-163712, A05, MF-A01). This report is only available through NTIS (see address given above).

NCEER-87-0016 "Pipeline Experiment at Parkfield, California," by J. Isenberg and E. Richardson, 9/15/87, (PB88-163720, A03, MF-A01). This report is available only through NTIS (see address given above).

NCEER-87-0017 "Digital Simulation of Seismic Ground Motion," by M. Shinozuka, G. Deodatis and T. Harada, 8/31/87, (PB88-155197, A04, MF-A01). This report is available only through NTIS (see address given above).

NCEER-87-0018 "Practical Considerations for Structural Control: System Uncertainty, System Time Delay and Truncation of Small Control Forces," J.N. Yang and A. Akbarpour, 8/10/87, (PB88-163738, A08, MF-A01). This report is only available through NTIS (see address given above).

NCEER-87-0019 "Modal Analysis of Nonclassically Damped Structural Systems Using Canonical Transformation," by J.N. Yang, S. Sarkani and F.X. Long, 9/27/87, (PB88-187851, A04, MF-A01).

NCEER-87-0020 "A Nonstationary Solution in Random Vibration Theory," by J.R. Red-Horse and P.D. Spanos, 11/3/87, (PB88-163746, A03, MF-A01).

NCEER-87-0021 "Horizontal Impedances for Radially Inhomogeneous Viscoelastic Soil Layers," by A.S. Veletsos and K.W. Dotson, 10/15/87, (PB88-150859, A04, MF-A01).

NCEER-87-0022 "Seismic Damage Assessment of Reinforced Concrete Members," by Y.S. Chung, C. Meyer and M. Shinozuka, 10/9/87, (PB88-150867, A05, MF-A01). This report is available only through NTIS (see address given above).

NCEER-87-0023 "Active Structural Control in Civil Engineering," by T.T. Soong, 11/11/87, (PB88-187778, A03, MF-A01).

NCEER-87-0024 "Vertical and Torsional Impedances for Radially Inhomogeneous Viscoelastic Soil Layers," by K.W. Dotson and A.S. Veletsos, 12/87, (PB88-187786, A03, MF-A01).

NCEER-87-0025 "Proceedings from the Symposium on Seismic Hazards, Ground Motions, Soil-Liquefaction and Engineering Practice in Eastern North America," October 20-22, 1987, edited by K.H. Jacob, 12/87, (PB88-188115, A23, MF-A01).

NCEER-87-0026 "Report on the Whittier-Narrows, California, Earthquake of October 1, 1987," by J. Pantelic and A. Reinhorn, 11/87, (PB88-187752, A03, MF-A01). This report is available only through NTIS (see address given above).

NCEER-87-0027 "Design of a Modular Program for Transient Nonlinear Analysis of Large 3-D Building Structures," by S. Srivastav and J.F. Abel, 12/30/87, (PB88-187950, A05, MF-A01). This report is only available through NTIS (see address given above).

NCEER-87-0028 "Second-Year Program in Research, Education and Technology Transfer," 3/8/88, (PB88-219480, A04, MF-A01).

NCEER-88-0001 "Workshop on Seismic Computer Analysis and Design of Buildings With Interactive Graphics," by W. McGuire, J.F. Abel and C.H. Conley, 1/18/88, (PB88-187760, A03, MF-A01). This report is only available through NTIS (see address given above).

NCEER-88-0002 "Optimal Control of Nonlinear Flexible Structures," by J.N. Yang, F.X. Long and D. Wong, 1/22/88, (PB88-213772, A06, MF-A01).

NCEER-88-0003 "Substructuring Techniques in the Time Domain for Primary-Secondary Structural Systems," by G.D. Manolis and G. Juhn, 2/10/88, (PB88-213780, A04, MF-A01).

NCEER-88-0004 "Iterative Seismic Analysis of Primary-Secondary Systems," by A. Singhal, L.D. Lutes and P.D. Spanos, 2/23/88, (PB88-213798, A04, MF-A01).

NCEER-88-0005 "Stochastic Finite Element Expansion for Random Media," by P.D. Spanos and R. Ghanem, 3/14/88, (PB88-213806, A03, MF-A01).

NCEER-88-0006 "Combining Structural Optimization and Structural Control," by F.Y. Cheng and C.P. Pantelides, 1/10/88, (PB88-213814, A05, MF-A01).

NCEER-88-0007 "Seismic Performance Assessment of Code-Designed Structures," by H.H-M. Hwang, J-W. Jaw and H-J. Shau, 3/20/88, (PB88-219423, A04, MF-A01). This report is only available through NTIS (see address given above).

NCEER-88-0008 "Reliability Analysis of Code-Designed Structures Under Natural Hazards," by H.H-M. Hwang, H. Ushiba and M. Shinozuka, 2/29/88, (PB88-229471, A07, MF-A01). This report is only available through NTIS (see address given above).

NCEER-88-0009 "Seismic Fragility Analysis of Shear Wall Structures," by J-W Jaw and H.H-M. Hwang, 4/30/88, (PB89-102867, A04, MF-A01).

NCEER-88-0010 "Base Isolation of a Multi-Story Building Under a Harmonic Ground Motion - A Comparison of Performances of Various Systems," by F-G Fan, G. Ahmadi and I.G. Tadjbakhsh, 5/18/88, (PB89-122238, A06, MF-A01). This report is only available through NTIS (see address given above).

NCEER-88-0011 "Seismic Floor Response Spectra for a Combined System by Green's Functions," by F.M. Lavelle, L.A. Bergman and P.D. Spanos, 5/1/88, (PB89-102875, A03, MF-A01).

NCEER-88-0012 "A New Solution Technique for Randomly Excited Hysteretic Structures," by G.Q. Cai and Y.K. Lin, 5/16/88, (PB89-102883, A03, MF-A01).

NCEER-88-0013 "A Study of Radiation Damping and Soil-Structure Interaction Effects in the Centrifuge," by K. Weissman, supervised by J.H. Prevost, 5/24/88, (PB89-144703, A06, MF-A01).

NCEER-88-0014 "Parameter Identification and Implementation of a Kinematic Plasticity Model for Frictional Soils," by J.H. Prevost and D.V. Griffiths, to be published.

NCEER-88-0015 "Two- and Three- Dimensional Dynamic Finite Element Analyses of the Long Valley Dam," by D.V. Griffiths and J.H. Prevost, 6/17/88, (PB89-144711, A04, MF-A01).

NCEER-88-0016 "Damage Assessment of Reinforced Concrete Structures in Eastern United States," by A.M. Reinhorn, M.J. Seidel, S.K. Kunnath and Y.J. Park, 6/15/88, (PB89-122220, A04, MF-A01). This report is only available through NTIS (see address given above).

NCEER-88-0017 "Dynamic Compliance of Vertically Loaded Strip Foundations in Multilayered Viscoelastic Soils," by S. Ahmad and A.S.M. Israil, 6/17/88, (PB89-102891, A04, MF-A01).

NCEER-88-0018 "An Experimental Study of Seismic Structural Response With Added Viscoelastic Dampers," by R.C. Lin, Z. Liang, T.T. Soong and R.H. Zhang, 6/30/88, (PB89-122212, A05, MF-A01). This report is available only through NTIS (see address given above).

NCEER-88-0019 "Experimental Investigation of Primary - Secondary System Interaction," by G.D. Manolis, G. Juhn and A.M. Reinhorn, 5/27/88, (PB89-122204, A04, MF-A01).

NCEER-88-0020 "A Response Spectrum Approach For Analysis of Nonclassically Damped Structures," by J.N. Yang, S. Sarkani and F.X. Long, 4/22/88, (PB89-102909, A04, MF-A01).

NCEER-88-0021 "Seismic Interaction of Structures and Soils: Stochastic Approach," by A.S. Veletsos and A.M. Prasad, 7/21/88, (PB89-122196, A04, MF-A01). This report is only available through NTIS (see address given above).

NCEER-88-0022 "Identification of the Serviceability Limit State and Detection of Seismic Structural Damage," by E. DiPasquale and A.S. Cakmak, 6/15/88, (PB89-122188, A05, MF-A01). This report is available only through NTIS (see address given above).

NCEER-88-0023 "Multi-Hazard Risk Analysis: Case of a Simple Offshore Structure," by B.K. Bhartia and E.H. Vanmarcke, 7/21/88, (PB89-145213, A05, MF-A01).

NCEER-88-0024 "Automated Seismic Design of Reinforced Concrete Buildings," by Y.S. Chung, C. Meyer and M. Shinozuka, 7/5/88, (PB89-122170, A06, MF-A01). This report is available only through NTIS (see address given above).

NCEER-88-0025 "Experimental Study of Active Control of MDOF Structures Under Seismic Excitations," by L.L. Chung, R.C. Lin, T.T. Soong and A.M. Reinhorn, 7/10/88, (PB89-122600, A04, MF-A01).

NCEER-88-0026 "Earthquake Simulation Tests of a Low-Rise Metal Structure," by J.S. Hwang, K.C. Chang, G.C. Lee and R.L. Ketter, 8/1/88, (PB89-102917, A04, MF-A01).

NCEER-88-0027 "Systems Study of Urban Response and Reconstruction Due to Catastrophic Earthquakes," by F. Kozin and H.K. Zhou, 9/22/88, (PB90-162348, A04, MF-A01).

NCEER-88-0028 "Seismic Fragility Analysis of Plane Frame Structures," by H.H-M. Hwang and Y.K. Low, 7/31/88, (PB89-131445, A06, MF-A01).

NCEER-88-0029 "Response Analysis of Stochastic Structures," by A. Kardara, C. Bucher and M. Shinozuka, 9/22/88, (PB89-174429, A04, MF-A01).

NCEER-88-0030 "Nonnormal Accelerations Due to Yielding in a Primary Structure," by D.C.K. Chen and L.D. Lutes, 9/19/88, (PB89-131437, A04, MF-A01).

NCEER-88-0031 "Design Approaches for Soil-Structure Interaction," by A.S. Veletsos, A.M. Prasad and Y. Tang, 12/30/88, (PB89-174437, A03, MF-A01). This report is available only through NTIS (see address given above).

NCEER-88-0032 "A Re-evaluation of Design Spectra for Seismic Damage Control," by C.J. Turkstra and A.G. Tallin, 11/7/88, (PB89-145221, A05, MF-A01).

NCEER-88-0033 "The Behavior and Design of Noncontact Lap Splices Subjected to Repeated Inelastic Tensile Loading," by V.E. Sagan, P. Gergely and R.N. White, 12/8/88, (PB89-163737, A08, MF-A01).

NCEER-88-0034 "Seismic Response of Pile Foundations," by S.M. Mamoon, P.K. Banerjee and S. Ahmad, 11/1/88, (PB89-145239, A04, MF-A01).

NCEER-88-0035 "Modeling of R/C Building Structures With Flexible Floor Diaphragms (IDARC2)," by A.M. Reinhorn, S.K. Kunnath and N. Panahshahi, 9/7/88, (PB89-207153, A07, MF-A01).

NCEER-88-0036 "Solution of the Dam-Reservoir Interaction Problem Using a Combination of FEM, BEM with Particular Integrals, Modal Analysis, and Substructuring," by C-S. Tsai, G.C. Lee and R.L. Ketter, 12/31/88, (PB89-207146, A04, MF-A01).

NCEER-88-0037 "Optimal Placement of Actuators for Structural Control," by F.Y. Cheng and C.P. Pantelides, 8/15/88, (PB89-162846, A05, MF-A01).

NCEER-88-0038 "Teflon Bearings in Aseismic Base Isolation: Experimental Studies and Mathematical Modeling," by A. Mokha, M.C. Constantinou and A.M. Reinhorn, 12/5/88, (PB89-218457, A10, MF-A01). This report is available only through NTIS (see address given above).

NCEER-88-0039 "Seismic Behavior of Flat Slab High-Rise Buildings in the New York City Area," by P. Weidlinger and M. Ettouney, 10/15/88, (PB90-145681, A04, MF-A01).

NCEER-88-0040 "Evaluation of the Earthquake Resistance of Existing Buildings in New York City," by P. Weidlinger and M. Ettouney, 10/15/88, to be published.

NCEER-88-0041 "Small-Scale Modeling Techniques for Reinforced Concrete Structures Subjected to Seismic Loads," by W. Kim, A. El-Attar and R.N. White, 11/22/88, (PB89-189625, A05, MF-A01).

NCEER-88-0042 "Modeling Strong Ground Motion from Multiple Event Earthquakes," by G.W. Ellis and A.S. Cakmak, 10/15/88, (PB89-174445, A03, MF-A01).

NCEER-88-0043 "Nonstationary Models of Seismic Ground Acceleration," by M. Grigoriu, S.E. Ruiz and E. Rosenblueth, 7/15/88, (PB89-189617, A04, MF-A01).

NCEER-88-0044 "SARCF User's Guide: Seismic Analysis of Reinforced Concrete Frames," by Y.S. Chung, C. Meyer and M. Shinozuka, 11/9/88, (PB89-174452, A08, MF-A01).

NCEER-88-0045 "First Expert Panel Meeting on Disaster Research and Planning," edited by J. Pantelic and J. Stoyle, 9/15/88, (PB89-174460, A05, MF-A01). This report is only available through NTIS (see address given above).

NCEER-88-0046 "Preliminary Studies of the Effect of Degrading Infill Walls on the Nonlinear Seismic Response of Steel Frames," by C.Z. Chrysostomou, P. Gergely and J.F. Abel, 12/19/88, (PB89-208383, A05, MF-A01).

NCEER-88-0047 "Reinforced Concrete Frame Component Testing Facility - Design, Construction, Instrumentation and Operation," by S.P. Pessiki, C. Conley, T. Bond, P. Gergely and R.N. White, 12/16/88, (PB89-174478, A04, MF-A01).

NCEER-89-0001 "Effects of Protective Cushion and Soil Compliancy on the Response of Equipment Within a Seismically Excited Building," by J.A. HoLung, 2/16/89, (PB89-207179, A04, MF-A01).

NCEER-89-0002 "Statistical Evaluation of Response Modification Factors for Reinforced Concrete Structures," by H.H-M. Hwang and J-W. Jaw, 2/17/89, (PB89-207187, A05, MF-A01).

NCEER-89-0003 "Hysteretic Columns Under Random Excitation," by G-Q. Cai and Y.K. Lin, 1/9/89, (PB89-196513, A03, MF-A01).

NCEER-89-0004 "Experimental Study of `Elephant Foot Bulge' Instability of Thin-Walled Metal Tanks," by Z-H. Jia and R.L. Ketter, 2/22/89, (PB89-207195, A03, MF-A01).

NCEER-89-0005 "Experiment on Performance of Buried Pipelines Across San Andreas Fault," by J. Isenberg, E. Richardson and T.D. O'Rourke, 3/10/89, (PB89-218440, A04, MF-A01). This report is available only through NTIS (see address given above).

NCEER-89-0006 "A Knowledge-Based Approach to Structural Design of Earthquake-Resistant Buildings," by M. Subramani, P. Gergely, C.H. Conley, J.F. Abel and A.H. Zaghw, 1/15/89, (PB89-218465, A06, MF-A01).

NCEER-89-0007 "Liquefaction Hazards and Their Effects on Buried Pipelines," by T.D. O'Rourke and P.A. Lane, 2/1/89, (PB89-218481, A09, MF-A01).

NCEER-89-0008 "Fundamentals of System Identification in Structural Dynamics," by H. Imai, C-B. Yun, O. Maruyama and M. Shinozuka, 1/26/89, (PB89-207211, A04, MF-A01).

NCEER-89-0009 "Effects of the 1985 Michoacan Earthquake on Water Systems and Other Buried Lifelines in Mexico," by A.G. Ayala and M.J. O'Rourke, 3/8/89, (PB89-207229, A06, MF-A01).

NCEER-89-R010 "NCEER Bibliography of Earthquake Education Materials," by K.E.K. Ross, Second Revision, 9/1/89, (PB90-125352, A05, MF-A01). This report is replaced by NCEER-92-0018.

NCEER-89-0011 "Inelastic Three-Dimensional Response Analysis of Reinforced Concrete Building Structures (IDARC-3D), Part I - Modeling," by S.K. Kunnath and A.M. Reinhorn, 4/17/89, (PB90-114612, A07, MF-A01).

NCEER-89-0012 "Recommended Modifications to ATC-14," by C.D. Poland and J.O. Malley, 4/12/89, (PB90-108648, A15, MF-A01).

NCEER-89-0013 "Repair and Strengthening of Beam-to-Column Connections Subjected to Earthquake Loading," by M. Corazao and A.J. Durrani, 2/28/89, (PB90-109885, A06, MF-A01).

NCEER-89-0014 "Program EXKAL2 for Identification of Structural Dynamic Systems," by O. Maruyama, C-B. Yun, M. Hoshiya and M. Shinozuka, 5/19/89, (PB90-109877, A09, MF-A01).

NCEER-89-0015 "Response of Frames With Bolted Semi-Rigid Connections, Part I - Experimental Study and Analytical Predictions," by P.J. DiCorso, A.M. Reinhorn, J.R. Dickerson, J.B. Radziminski and W.L. Harper, 6/1/89, to be published.

NCEER-89-0016 "ARMA Monte Carlo Simulation in Probabilistic Structural Analysis," by P.D. Spanos and M.P. Mignolet, 7/10/89, (PB90-109893, A03, MF-A01).

NCEER-89-P017 "Preliminary Proceedings from the Conference on Disaster Preparedness - The Place of Earthquake Education in Our Schools," Edited by K.E.K. Ross, 6/23/89, (PB90-108606, A03, MF-A01).

NCEER-89-0017 "Proceedings from the Conference on Disaster Preparedness - The Place of Earthquake Education in Our Schools," Edited by K.E.K. Ross, 12/31/89, (PB90-207895, A012, MF-A02). This report is available only through NTIS (see address given above).

NCEER-89-0018 "Multidimensional Models of Hysteretic Material Behavior for Vibration Analysis of Shape Memory Energy Absorbing Devices, by E.J. Graesser and F.A. Cozzarelli, 6/7/89, (PB90-164146, A04, MF-A01).

NCEER-89-0019 "Nonlinear Dynamic Analysis of Three-Dimensional Base Isolated Structures (3D-BASIS)," by S. Nagarajaiah, A.M. Reinhorn and M.C. Constantinou, 8/3/89, (PB90-161936, A06, MF-A01). This report has been replaced by NCEER-93-0011.

NCEER-89-0020 "Structural Control Considering Time-Rate of Control Forces and Control Rate Constraints," by F.Y. Cheng and C.P. Pantelides, 8/3/89, (PB90-120445, A04, MF-A01).

NCEER-89-0021 "Subsurface Conditions of Memphis and Shelby County," by K.W. Ng, T-S. Chang and H-H.M. Hwang, 7/26/89, (PB90-120437, A03, MF-A01).

NCEER-89-0022 "Seismic Wave Propagation Effects on Straight Jointed Buried Pipelines," by K. Elhmadi and M.J. O'Rourke, 8/24/89, (PB90-162322, A10, MF-A02).

NCEER-89-0023 "Workshop on Serviceability Analysis of Water Delivery Systems," edited by M. Grigoriu, 3/6/89, (PB90-127424, A03, MF-A01).

NCEER-89-0024 "Shaking Table Study of a 1/5 Scale Steel Frame Composed of Tapered Members," by K.C. Chang, J.S. Hwang and G.C. Lee, 9/18/89, (PB90-160169, A04, MF-A01).

NCEER-89-0025 "DYNA1D: A Computer Program for Nonlinear Seismic Site Response Analysis - Technical Documentation," by Jean H. Prevost, 9/14/89, (PB90-161944, A07, MF-A01). This report is available only through NTIS (see address given above).

NCEER-89-0026 "1:4 Scale Model Studies of Active Tendon Systems and Active Mass Dampers for Aseismic Protection," by A.M. Reinhorn, T.T. Soong, R.C. Lin, Y.P. Yang, Y. Fukao, H. Abe and M. Nakai, 9/15/89, (PB90-173246, A10, MF-A02).

NCEER-89-0027 "Scattering of Waves by Inclusions in a Nonhomogeneous Elastic Half Space Solved by Boundary Element Methods," by P.K. Hadley, A. Askar and A.S. Cakmak, 6/15/89, (PB90-145699, A07, MF-A01).

NCEER-89-0028 "Statistical Evaluation of Deflection Amplification Factors for Reinforced Concrete Structures," by H.H.M. Hwang, J-W. Jaw and A.L. Ch'ng, 8/31/89, (PB90-164633, A05, MF-A01).

NCEER-89-0029 "Bedrock Accelerations in Memphis Area Due to Large New Madrid Earthquakes," by H.H.M. Hwang, C.H.S. Chen and G. Yu, 11/7/89, (PB90-162330, A04, MF-A01).

NCEER-89-0030 "Seismic Behavior and Response Sensitivity of Secondary Structural Systems," by Y.Q. Chen and T.T. Soong, 10/23/89, (PB90-164658, A08, MF-A01).

NCEER-89-0031 "Random Vibration and Reliability Analysis of Primary-Secondary Structural Systems," by Y. Ibrahim, M. Grigoriu and T.T. Soong, 11/10/89, (PB90-161951, A04, MF-A01).

NCEER-89-0032 "Proceedings from the Second U.S. - Japan Workshop on Liquefaction, Large Ground Deformation and Their Effects on Lifelines, September 26-29, 1989," Edited by T.D. O'Rourke and M. Hamada, 12/1/89, (PB90-209388, A22, MF-A03).

NCEER-89-0033 "Deterministic Model for Seismic Damage Evaluation of Reinforced Concrete Structures," by J.M. Bracci, A.M. Reinhorn, J.B. Mander and S.K. Kunnath, 9/27/89, (PB91-108803, A06, MF-A01).

NCEER-89-0034 "On the Relation Between Local and Global Damage Indices," by E. DiPasquale and A.S. Cakmak, 8/15/89, (PB90-173865, A05, MF-A01).

NCEER-89-0035 "Cyclic Undrained Behavior of Nonplastic and Low Plasticity Silts," by A.J. Walker and H.E. Stewart, 7/26/89, (PB90-183518, A10, MF-A01).

NCEER-89-0036 "Liquefaction Potential of Surficial Deposits in the City of Buffalo, New York," by M. Budhu, R. Giese and L. Baumgrass, 1/17/89, (PB90-208455, A04, MF-A01).

NCEER-89-0037 "A Deterministic Assessment of Effects of Ground Motion Incoherence," by A.S. Veletsos and Y. Tang, 7/15/89, (PB90-164294, A03, MF-A01).

NCEER-89-0038 "Workshop on Ground Motion Parameters for Seismic Hazard Mapping," July 17-18, 1989, edited by R.V. Whitman, 12/1/89, (PB90-173923, A04, MF-A01).

NCEER-89-0039 "Seismic Effects on Elevated Transit Lines of the New York City Transit Authority," by C.J. Costantino, C.A. Miller and E. Heymsfield, 12/26/89, (PB90-207887, A06, MF-A01).

NCEER-89-0040 "Centrifugal Modeling of Dynamic Soil-Structure Interaction," by K. Weissman, Supervised by J.H. Prevost, 5/10/89, (PB90-207879, A07, MF-A01).

NCEER-89-0041 "Linearized Identification of Buildings With Cores for Seismic Vulnerability Assessment," by I-K. Ho and A.E. Aktan, 11/1/89, (PB90-251943, A07, MF-A01).

NCEER-90-0001 "Geotechnical and Lifeline Aspects of the October 17, 1989 Loma Prieta Earthquake in San Francisco," by T.D. O'Rourke, H.E. Stewart, F.T. Blackburn and T.S. Dickerman, 1/90, (PB90-208596, A05, MF-A01).

NCEER-90-0002 "Nonnormal Secondary Response Due to Yielding in a Primary Structure," by D.C.K. Chen and L.D. Lutes, 2/28/90, (PB90-251976, A07, MF-A01).

NCEER-90-0003 "Earthquake Education Materials for Grades K-12," by K.E.K. Ross, 4/16/90, (PB91-251984, A05, MF-A05). This report has been replaced by NCEER-92-0018.

NCEER-90-0004 "Catalog of Strong Motion Stations in Eastern North America," by R.W. Busby, 4/3/90, (PB90-251984, A05, MF-A01).

NCEER-90-0005 "NCEER Strong-Motion Data Base: A User Manual for the GeoBase Release (Version 1.0 for the Sun3)," by P. Friberg and K. Jacob, 3/31/90 (PB90-258062, A04, MF-A01).

NCEER-90-0006 "Seismic Hazard Along a Crude Oil Pipeline in the Event of an 1811-1812 Type New Madrid Earthquake," by H.H.M. Hwang and C-H.S. Chen, 4/16/90, (PB90-258054, A04, MF-A01).

NCEER-90-0007 "Site-Specific Response Spectra for Memphis Sheahan Pumping Station," by H.H.M. Hwang and C.S. Lee, 5/15/90, (PB91-108811, A05, MF-A01).

NCEER-90-0008 "Pilot Study on Seismic Vulnerability of Crude Oil Transmission Systems," by T. Ariman, R. Dobry, M. Grigoriu, F. Kozin, M. O'Rourke, T. O'Rourke and M. Shinozuka, 5/25/90, (PB91-108837, A06, MF-A01).

NCEER-90-0009 "A Program to Generate Site Dependent Time Histories: EQGEN," by G.W. Ellis, M. Srinivasan and A.S. Cakmak, 1/30/90, (PB91-108829, A04, MF-A01).

NCEER-90-0010 "Active Isolation for Seismic Protection of Operating Rooms," by M.E. Talbott, Supervised by M. Shinozuka, 6/8/9, (PB91-110205, A05, MF-A01).

NCEER-90-0011 "Program LINEARID for Identification of Linear Structural Dynamic Systems," by C-B. Yun and M. Shinozuka, 6/25/90, (PB91-110312, A08, MF-A01).

NCEER-90-0012 "Two-Dimensional Two-Phase Elasto-Plastic Seismic Response of Earth Dams," by A.N. Yiagos, Supervised by J.H. Prevost, 6/20/90, (PB91-110197, A13, MF-A02).

NCEER-90-0013 "Secondary Systems in Base-Isolated Structures: Experimental Investigation, Stochastic Response and Stochastic Sensitivity," by G.D. Manolis, G. Juhn, M.C. Constantinou and A.M. Reinhorn, 7/1/90, (PB91-110320, A08, MF-A01).

NCEER-90-0014 "Seismic Behavior of Lightly-Reinforced Concrete Column and Beam-Column Joint Details," by S.P. Pessiki, C.H. Conley, P. Gergely and R.N. White, 8/22/90, (PB91-108795, A11, MF-A02).

NCEER-90-0015 "Two Hybrid Control Systems for Building Structures Under Strong Earthquakes," by J.N. Yang and A. Danielians, 6/29/90, (PB91-125393, A04, MF-A01).

NCEER-90-0016 "Instantaneous Optimal Control with Acceleration and Velocity Feedback," by J.N. Yang and Z. Li, 6/29/90, (PB91-125401, A03, MF-A01).

NCEER-90-0017 "Reconnaissance Report on the Northern Iran Earthquake of June 21, 1990," by M. Mehrain, 10/4/90, (PB91-125377, A03, MF-A01).

NCEER-90-0018 "Evaluation of Liquefaction Potential in Memphis and Shelby County," by T.S. Chang, P.S. Tang, C.S. Lee and H. Hwang, 8/10/90, (PB91-125427, A09, MF-A01).

NCEER-90-0019 "Experimental and Analytical Study of a Combined Sliding Disc Bearing and Helical Steel Spring Isolation System," by M.C. Constantinou, A.S. Mokha and A.M. Reinhorn, 10/4/90, (PB91-125385, A06, MF-A01). This report is available only through NTIS (see address given above).

NCEER-90-0020 "Experimental Study and Analytical Prediction of Earthquake Response of a Sliding Isolation System with a Spherical Surface," by A.S. Mokha, M.C. Constantinou and A.M. Reinhorn, 10/11/90, (PB91-125419, A05, MF-A01).

NCEER-90-0021 "Dynamic Interaction Factors for Floating Pile Groups," by G. Gazetas, K. Fan, A. Kaynia and E. Kausel, 9/10/90, (PB91-170381, A05, MF-A01).

NCEER-90-0022 "Evaluation of Seismic Damage Indices for Reinforced Concrete Structures," by S. Rodriguez-Gomez and A.S. Cakmak, 9/30/90, PB91-171322, A06, MF-A01).

NCEER-90-0023 "Study of Site Response at a Selected Memphis Site," by H. Desai, S. Ahmad, E.S. Gazetas and M.R. Oh, 10/11/90, (PB91-196857, A03, MF-A01).

NCEER-90-0024 "A User's Guide to Strongmo: Version 1.0 of NCEER's Strong-Motion Data Access Tool for PCs and Terminals," by P.A. Friberg and C.A.T. Susch, 11/15/90, (PB91-171272, A03, MF-A01).

NCEER-90-0025 "A Three-Dimensional Analytical Study of Spatial Variability of Seismic Ground Motions," by L-L. Hong and A.H.-S. Ang, 10/30/90, (PB91-170399, A09, MF-A01).

NCEER-90-0026 "MUMOID User's Guide - A Program for the Identification of Modal Parameters," by S. Rodriguez-Gomez and E. DiPasquale, 9/30/90, (PB91-171298, A04, MF-A01).

NCEER-90-0027 "SARCF-II User's Guide - Seismic Analysis of Reinforced Concrete Frames," by S. Rodriguez-Gomez, Y.S. Chung and C. Meyer, 9/30/90, (PB91-171280, A05, MF-A01).

NCEER-90-0028 "Viscous Dampers: Testing, Modeling and Application in Vibration and Seismic Isolation," by N. Makris and M.C. Constantinou, 12/20/90 (PB91-190561, A06, MF-A01).

NCEER-90-0029 "Soil Effects on Earthquake Ground Motions in the Memphis Area," by H. Hwang, C.S. Lee, K.W. Ng and T.S. Chang, 8/2/90, (PB91-190751, A05, MF-A01).

NCEER-91-0001 "Proceedings from the Third Japan-U.S. Workshop on Earthquake Resistant Design of Lifeline Facilities and Countermeasures for Soil Liquefaction, December 17-19, 1990," edited by T.D. O'Rourke and M. Hamada, 2/1/91, (PB91-179259, A99, MF-A04).

NCEER-91-0002 "Physical Space Solutions of Non-Proportionally Damped Systems," by M. Tong, Z. Liang and G.C. Lee, 1/15/91, (PB91-179242, A04, MF-A01).

NCEER-91-0003 "Seismic Response of Single Piles and Pile Groups," by K. Fan and G. Gazetas, 1/10/91, (PB92-174994, A04, MF-A01).

NCEER-91-0004 "Damping of Structures: Part 1 - Theory of Complex Damping," by Z. Liang and G. Lee, 10/10/91, (PB92-197235, A12, MF-A03).

NCEER-91-0005 "3D-BASIS - Nonlinear Dynamic Analysis of Three Dimensional Base Isolated Structures: Part II," by S. Nagarajaiah, A.M. Reinhorn and M.C. Constantinou, 2/28/91, (PB91-190553, A07, MF-A01). This report has been replaced by NCEER-93-0011.

NCEER-91-0006 "A Multidimensional Hysteretic Model for Plasticity Deforming Metals in Energy Absorbing Devices," by E.J. Graesser and F.A. Cozzarelli, 4/9/91, (PB92-108364, A04, MF-A01).

NCEER-91-0007 "A Framework for Customizable Knowledge-Based Expert Systems with an Application to a KBES for Evaluating the Seismic Resistance of Existing Buildings," by E.G. Ibarra-Anaya and S.J. Fenves, 4/9/91, (PB91-210930, A08, MF-A01).

NCEER-91-0008 "Nonlinear Analysis of Steel Frames with Semi-Rigid Connections Using the Capacity Spectrum Method," by G.G. Deierlein, S-H. Hsieh, Y-J. Shen and J.F. Abel, 7/2/91, (PB92-113828, A05, MF-A01).

NCEER-91-0009 "Earthquake Education Materials for Grades K-12," by K.E.K. Ross, 4/30/91, (PB91-212142, A06, MF-A01). This report has been replaced by NCEER-92-0018.

NCEER-91-0010 "Phase Wave Velocities and Displacement Phase Differences in a Harmonically Oscillating Pile," by N. Makris and G. Gazetas, 7/8/91, (PB92-108356, A04, MF-A01).

NCEER-91-0011 "Dynamic Characteristics of a Full-Size Five-Story Steel Structure and a 2/5 Scale Model," by K.C. Chang, G.C. Yao, G.C. Lee, D.S. Hao and Y.C. Yeh," 7/2/91, (PB93-116648, A06, MF-A02).

NCEER-91-0012 "Seismic Response of a 2/5 Scale Steel Structure with Added Viscoelastic Dampers," by K.C. Chang, T.T. Soong, S-T. Oh and M.L. Lai, 5/17/91, (PB92-110816, A05, MF-A01).

NCEER-91-0013 "Earthquake Response of Retaining Walls; Full-Scale Testing and Computational Modeling," by S. Alampalli and A-W.M. Elgamal, 6/20/91, to be published.

NCEER-91-0014 "3D-BASIS-M: Nonlinear Dynamic Analysis of Multiple Building Base Isolated Structures," by P.C. Tsopelas, S. Nagarajaiah, M.C. Constantinou and A.M. Reinhorn, 5/28/91, (PB92-113885, A09, MF-A02).

NCEER-91-0015 "Evaluation of SEAOC Design Requirements for Sliding Isolated Structures," by D. Theodossiou and M.C. Constantinou, 6/10/91, (PB92-114602, A11, MF-A03).

NCEER-91-0016 "Closed-Loop Modal Testing of a 27-Story Reinforced Concrete Flat Plate-Core Building," by H.R. Somaprasad, T. Toksoy, H. Yoshiyuki and A.E. Aktan, 7/15/91, (PB92-129980, A07, MF-A02).

NCEER-91-0017 "Shake Table Test of a 1/6 Scale Two-Story Lightly Reinforced Concrete Building," by A.G. El-Attar, R.N. White and P. Gergely, 2/28/91, (PB92-222447, A06, MF-A02).

NCEER-91-0018 "Shake Table Test of a 1/8 Scale Three-Story Lightly Reinforced Concrete Building," by A.G. El-Attar, R.N. White and P. Gergely, 2/28/91, (PB93-116630, A08, MF-A02).

NCEER-91-0019 "Transfer Functions for Rigid Rectangular Foundations," by A.S. Veletsos, A.M. Prasad and W.H. Wu, 7/31/91, to be published.

NCEER-91-0020 "Hybrid Control of Seismic-Excited Nonlinear and Inelastic Structural Systems," by J.N. Yang, Z. Li and A. Danielians, 8/1/91, (PB92-143171, A06, MF-A02).

NCEER-91-0021 "The NCEER-91 Earthquake Catalog: Improved Intensity-Based Magnitudes and Recurrence Relations for U.S. Earthquakes East of New Madrid," by L. Seeber and J.G. Armbruster, 8/28/91, (PB92-176742, A06, MF-A02).

NCEER-91-0022 "Proceedings from the Implementation of Earthquake Planning and Education in Schools: The Need for Change - The Roles of the Changemakers," by K.E.K. Ross and F. Winslow, 7/23/91, (PB92-129998, A12, MF-A03).

NCEER-91-0023 "A Study of Reliability-Based Criteria for Seismic Design of Reinforced Concrete Frame Buildings," by H.H.M. Hwang and H-M. Hsu, 8/10/91, (PB92-140235, A09, MF-A02).

NCEER-91-0024 "Experimental Verification of a Number of Structural System Identification Algorithms," by R.G. Ghanem, H. Gavin and M. Shinozuka, 9/18/91, (PB92-176577, A18, MF-A04).

NCEER-91-0025 "Probabilistic Evaluation of Liquefaction Potential," by H.H.M. Hwang and C.S. Lee," 11/25/91, (PB92-143429, A05, MF-A01).

NCEER-91-0026 "Instantaneous Optimal Control for Linear, Nonlinear and Hysteretic Structures - Stable Controllers," by J.N. Yang and Z. Li, 11/15/91, (PB92-163807, A04, MF-A01).

NCEER-91-0027 "Experimental and Theoretical Study of a Sliding Isolation System for Bridges," by M.C. Constantinou, A. Kartoum, A.M. Reinhorn and P. Bradford, 11/15/91, (PB92-176973, A10, MF-A03).

NCEER-92-0001 "Case Studies of Liquefaction and Lifeline Performance During Past Earthquakes, Volume 1: Japanese Case Studies," Edited by M. Hamada and T. O'Rourke, 2/17/92, (PB92-197243, A18, MF-A04).

NCEER-92-0002 "Case Studies of Liquefaction and Lifeline Performance During Past Earthquakes, Volume 2: United States Case Studies," Edited by T. O'Rourke and M. Hamada, 2/17/92, (PB92-197250, A20, MF-A04).

NCEER-92-0003 "Issues in Earthquake Education," Edited by K. Ross, 2/3/92, (PB92-222389, A07, MF-A02).

NCEER-92-0004 "Proceedings from the First U.S. - Japan Workshop on Earthquake Protective Systems for Bridges," Edited by I.G. Buckle, 2/4/92, (PB94-142239, A99, MF-A06).

NCEER-92-0005 "Seismic Ground Motion from a Haskell-Type Source in a Multiple-Layered Half-Space," A.P. Theoharis, G. Deodatis and M. Shinozuka, 1/2/92, to be published.

NCEER-92-0006 "Proceedings from the Site Effects Workshop," Edited by R. Whitman, 2/29/92, (PB92-197201, A04, MF-A01).

NCEER-92-0007 "Engineering Evaluation of Permanent Ground Deformations Due to Seismically-Induced Liquefaction," by M.H. Baziar, R. Dobry and A-W.M. Elgamal, 3/24/92, (PB92-222421, A13, MF-A03).

NCEER-92-0008 "A Procedure for the Seismic Evaluation of Buildings in the Central and Eastern United States," by C.D. Poland and J.O. Malley, 4/2/92, (PB92-222439, A20, MF-A04).

NCEER-92-0009 "Experimental and Analytical Study of a Hybrid Isolation System Using Friction Controllable Sliding Bearings," by M.Q. Feng, S. Fujii and M. Shinozuka, 5/15/92, (PB93-150282, A06, MF-A02).

NCEER-92-0010 "Seismic Resistance of Slab-Column Connections in Existing Non-Ductile Flat-Plate Buildings," by A.J. Durrani and Y. Du, 5/18/92, (PB93-116812, A06, MF-A02).

NCEER-92-0011 "The Hysteretic and Dynamic Behavior of Brick Masonry Walls Upgraded by Ferrocement Coatings Under Cyclic Loading and Strong Simulated Ground Motion," by H. Lee and S.P. Prawel, 5/11/92, to be published.

NCEER-92-0012 "Study of Wire Rope Systems for Seismic Protection of Equipment in Buildings," by G.F. Demetriades, M.C. Constantinou and A.M. Reinhorn, 5/20/92, (PB93-116655, A08, MF-A02).

NCEER-92-0013 "Shape Memory Structural Dampers: Material Properties, Design and Seismic Testing," by P.R. Witting and F.A. Cozzarelli, 5/26/92, (PB93-116663, A05, MF-A01).

NCEER-92-0014 "Longitudinal Permanent Ground Deformation Effects on Buried Continuous Pipelines," by M.J. O'Rourke, and C. Nordberg, 6/15/92, (PB93-116671, A08, MF-A02).

NCEER-92-0015 "A Simulation Method for Stationary Gaussian Random Functions Based on the Sampling Theorem," by M. Grigoriu and S. Balopoulou, 6/11/92, (PB93-127496, A05, MF-A01).

NCEER-92-0016 "Gravity-Load-Designed Reinforced Concrete Buildings: Seismic Evaluation of Existing Construction and Detailing Strategies for Improved Seismic Resistance," by G.W. Hoffmann, S.K. Kunnath, A.M. Reinhorn and J.B. Mander, 7/15/92, (PB94-142007, A08, MF-A02).

NCEER-92-0017 "Observations on Water System and Pipeline Performance in the Limón Area of Costa Rica Due to the April 22, 1991 Earthquake," by M. O'Rourke and D. Ballantyne, 6/30/92, (PB93-126811, A06, MF-A02).

NCEER-92-0018 "Fourth Edition of Earthquake Education Materials for Grades K-12," Edited by K.E.K. Ross, 8/10/92, (PB93-114023, A07, MF-A02).

NCEER-92-0019 "Proceedings from the Fourth Japan-U.S. Workshop on Earthquake Resistant Design of Lifeline Facilities and Countermeasures for Soil Liquefaction," Edited by M. Hamada and T.D. O'Rourke, 8/12/92, (PB93-163939, A99, MF-E11).

NCEER-92-0020 "Active Bracing System: A Full Scale Implementation of Active Control," by A.M. Reinhorn, T.T. Soong, R.C. Lin, M.A. Riley, Y.P. Wang, S. Aizawa and M. Higashino, 8/14/92, (PB93-127512, A06, MF-A02).

NCEER-92-0021 "Empirical Analysis of Horizontal Ground Displacement Generated by Liquefaction-Induced Lateral Spreads," by S.F. Bartlett and T.L. Youd, 8/17/92, (PB93-188241, A06, MF-A02).

NCEER-92-0022 "IDARC Version 3.0: Inelastic Damage Analysis of Reinforced Concrete Structures," by S.K. Kunnath, A.M. Reinhorn and R.F. Lobo, 8/31/92, (PB93-227502, A07, MF-A02).

NCEER-92-0023 "A Semi-Empirical Analysis of Strong-Motion Peaks in Terms of Seismic Source, Propagation Path and Local Site Conditions, by M. Kamiyama, M.J. O'Rourke and R. Flores-Berrones, 9/9/92, (PB93-150266, A08, MF-A02).

NCEER-92-0024 "Seismic Behavior of Reinforced Concrete Frame Structures with Nonductile Details, Part I: Summary of Experimental Findings of Full Scale Beam-Column Joint Tests," by A. Beres, R.N. White and P. Gergely, 9/30/92, (PB93-227783, A05, MF-A01).

NCEER-92-0025 "Experimental Results of Repaired and Retrofitted Beam-Column Joint Tests in Lightly Reinforced Concrete Frame Buildings," by A. Beres, S. El-Borgi, R.N. White and P. Gergely, 10/29/92, (PB93-227791, A05, MF-A01).

NCEER-92-0026 "A Generalization of Optimal Control Theory: Linear and Nonlinear Structures," by J.N. Yang, Z. Li and S. Vongchavalitkul, 11/2/92, (PB93-188621, A05, MF-A01).

NCEER-92-0027 "Seismic Resistance of Reinforced Concrete Frame Structures Designed Only for Gravity Loads: Part I - Design and Properties of a One-Third Scale Model Structure," by J.M. Bracci, A.M. Reinhorn and J.B. Mander, 12/1/92, (PB94-104502, A08, MF-A02).

NCEER-92-0028 "Seismic Resistance of Reinforced Concrete Frame Structures Designed Only for Gravity Loads: Part II - Experimental Performance of Subassemblages," by L.E. Aycardi, J.B. Mander and A.M. Reinhorn, 12/1/92, (PB94-104510, A08, MF-A02).

NCEER-92-0029 "Seismic Resistance of Reinforced Concrete Frame Structures Designed Only for Gravity Loads: Part III - Experimental Performance and Analytical Study of a Structural Model," by J.M. Bracci, A.M. Reinhorn and J.B. Mander, 12/1/92, (PB93-227528, A09, MF-A01).

NCEER-92-0030 "Evaluation of Seismic Retrofit of Reinforced Concrete Frame Structures: Part I - Experimental Performance of Retrofitted Subassemblages," by D. Choudhuri, J.B. Mander and A.M. Reinhorn, 12/8/92, (PB93-198307, A07, MF-A02).

NCEER-92-0031 "Evaluation of Seismic Retrofit of Reinforced Concrete Frame Structures: Part II - Experimental Performance and Analytical Study of a Retrofitted Structural Model," by J.M. Bracci, A.M. Reinhorn and J.B. Mander, 12/8/92, (PB93-198315, A09, MF-A03).

NCEER-92-0032 "Experimental and Analytical Investigation of Seismic Response of Structures with Supplemental Fluid Viscous Dampers," by M.C. Constantinou and M.D. Symans, 12/21/92, (PB93-191435, A10, MF-A03).

NCEER-92-0033 "Reconnaissance Report on the Cairo, Egypt Earthquake of October 12, 1992," by M. Khater, 12/23/92, (PB93-188621, A03, MF-A01).

NCEER-92-0034 "Low-Level Dynamic Characteristics of Four Tall Flat-Plate Buildings in New York City," by H. Gavin, S. Yuan, J. Grossman, E. Pekelis and K. Jacob, 12/28/92, (PB93-188217, A07, MF-A02).

NCEER-93-0001 "An Experimental Study on the Seismic Performance of Brick-Infilled Steel Frames With and Without Retrofit," by J.B. Mander, B. Nair, K. Wojtkowski and J. Ma, 1/29/93, (PB93-227510, A07, MF-A02).

NCEER-93-0002 "Social Accounting for Disaster Preparedness and Recovery Planning," by S. Cole, E. Pantoja and V. Razak, 2/22/93, (PB94-142114, A12, MF-A03).

NCEER-93-0003 "Assessment of 1991 NEHRP Provisions for Nonstructural Components and Recommended Revisions," by T.T. Soong, G. Chen, Z. Wu, R-H. Zhang and M. Grigoriu, 3/1/93, (PB93-188639, A06, MF-A02).

NCEER-93-0004 "Evaluation of Static and Response Spectrum Analysis Procedures of SEAOC/UBC for Seismic Isolated Structures," by C.W. Winters and M.C. Constantinou, 3/23/93, (PB93-198299, A10, MF-A03).

NCEER-93-0005 "Earthquakes in the Northeast - Are We Ignoring the Hazard? A Workshop on Earthquake Science and Safety for Educators," edited by K.E.K. Ross, 4/2/93, (PB94-103066, A09, MF-A02).

NCEER-93-0006 "Inelastic Response of Reinforced Concrete Structures with Viscoelastic Braces," by R.F. Lobo, J.M. Bracci, K.L. Shen, A.M. Reinhorn and T.T. Soong, 4/5/93, (PB93-227486, A05, MF-A02).

NCEER-93-0007 "Seismic Testing of Installation Methods for Computers and Data Processing Equipment," by K. Kosar, T.T. Soong, K.L. Shen, J.A. HoLung and Y.K. Lin, 4/12/93, (PB93-198299, A07, MF-A02).

NCEER-93-0008 "Retrofit of Reinforced Concrete Frames Using Added Dampers," by A. Reinhorn, M. Constantinou and C. Li, to be published.

NCEER-93-0009 "Seismic Behavior and Design Guidelines for Steel Frame Structures with Added Viscoelastic Dampers," by K.C. Chang, M.L. Lai, T.T. Soong, D.S. Hao and Y.C. Yeh, 5/1/93, (PB94-141959, A07, MF-A02).

NCEER-93-0010 "Seismic Performance of Shear-Critical Reinforced Concrete Bridge Piers," by J.B. Mander, S.M. Waheed, M.T.A. Chaudhary and S.S. Chen, 5/12/93, (PB93-227494, A08, MF-A02).

NCEER-93-0011 "3D-BASIS-TABS: Computer Program for Nonlinear Dynamic Analysis of Three Dimensional Base Isolated Structures," by S. Nagarajaiah, C. Li, A.M. Reinhorn and M.C. Constantinou, 8/2/93, (PB94-141819, A09, MF-A02).

NCEER-93-0012 "Effects of Hydrocarbon Spills from an Oil Pipeline Break on Ground Water," by O.J. Helweg and H.H.M. Hwang, 8/3/93, (PB94-141942, A06, MF-A02).

NCEER-93-0013 "Simplified Procedures for Seismic Design of Nonstructural Components and Assessment of Current Code Provisions," by M.P. Singh, L.E. Suarez, E.E. Matheu and G.O. Maldonado, 8/4/93, (PB94-141827, A09, MF-A02).

NCEER-93-0014 "An Energy Approach to Seismic Analysis and Design of Secondary Systems," by G. Chen and T.T. Soong, 8/6/93, (PB94-142767, A11, MF-A03).

NCEER-93-0015 "Proceedings from School Sites: Becoming Prepared for Earthquakes - Commemorating the Third Anniversary of the Loma Prieta Earthquake," Edited by F.E. Winslow and K.E.K. Ross, 8/16/93, (PB94-154275, A16, MF-A02).

NCEER-93-0016 "Reconnaissance Report of Damage to Historic Monuments in Cairo, Egypt Following the October 12, 1992 Dahshur Earthquake," by D. Sykora, D. Look, G. Croci, E. Karaesmen and E. Karaesmen, 8/19/93, (PB94-142221, A08, MF-A02).

NCEER-93-0017 "The Island of Guam Earthquake of August 8, 1993," by S.W. Swan and S.K. Harris, 9/30/93, (PB94-141843, A04, MF-A01).

NCEER-93-0018 "Engineering Aspects of the October 12, 1992 Egyptian Earthquake," by A.W. Elgamal, M. Amer, K. Adalier and A. Abul-Fadl, 10/7/93, (PB94-141983, A05, MF-A01).

NCEER-93-0019 "Development of an Earthquake Motion Simulator and its Application in Dynamic Centrifuge Testing," by I. Krstelj, Supervised by J.H. Prevost, 10/23/93, (PB94-181773, A-10, MF-A03).

NCEER-93-0020 "NCEER-Taisei Corporation Research Program on Sliding Seismic Isolation Systems for Bridges: Experimental and Analytical Study of a Friction Pendulum System (FPS)," by M.C. Constantinou, P. Tsopelas, Y-S. Kim and S. Okamoto, 11/1/93, (PB94-142775, A08, MF-A02).

NCEER-93-0021 "Finite Element Modeling of Elastomeric Seismic Isolation Bearings," by L.J. Billings, Supervised by R. Shepherd, 11/8/93, to be published.

NCEER-93-0022 "Seismic Vulnerability of Equipment in Critical Facilities: Life-Safety and Operational Consequences," by K. Porter, G.S. Johnson, M.M. Zadeh, C. Scawthorn and S. Eder, 11/24/93, (PB94-181765, A16, MF-A03).

NCEER-93-0023 "Hokkaido Nansei-oki, Japan Earthquake of July 12, 1993, by P.I. Yanev and C.R. Scawthorn, 12/23/93, (PB94-181500, A07, MF-A01).

NCEER-94-0001 "An Evaluation of Seismic Serviceability of Water Supply Networks with Application to the San Francisco Auxiliary Water Supply System," by I. Markov, Supervised by M. Grigoriu and T. O'Rourke, 1/21/94, (PB94-204013, A07, MF-A02).

NCEER-94-0002 "NCEER-Taisei Corporation Research Program on Sliding Seismic Isolation Systems for Bridges: Experimental and Analytical Study of Systems Consisting of Sliding Bearings, Rubber Restoring Force Devices and Fluid Dampers," Volumes I and II, by P. Tsopelas, S. Okamoto, M.C. Constantinou, D. Ozaki and S. Fujii, 2/4/94, (PB94-181740, A09, MF-A02 and PB94-181757, A12, MF-A03).

NCEER-94-0003 "A Markov Model for Local and Global Damage Indices in Seismic Analysis," by S. Rahman and M. Grigoriu, 2/18/94, (PB94-206000, A12, MF-A03).

NCEER-94-0004 "Proceedings from the NCEER Workshop on Seismic Response of Masonry Infills," edited by D.P. Abrams, 3/1/94, (PB94-180783, A07, MF-A02).

NCEER-94-0005 "The Northridge, California Earthquake of January 17, 1994: General Reconnaissance Report," edited by J.D. Goltz, 3/11/94, (PB193943, A10, MF-A03).

NCEER-94-0006 "Seismic Energy Based Fatigue Damage Analysis of Bridge Columns: Part I - Evaluation of Seismic Capacity," by G.A. Chang and J.B. Mander, 3/14/94, (PB94-219185, A11, MF-A03).

NCEER-94-0007 "Seismic Isolation of Multi-Story Frame Structures Using Spherical Sliding Isolation Systems," by T.M. Al-Hussaini, V.A. Zayas and M.C. Constantinou, 3/17/94, (PB193745, A09, MF-A02).

NCEER-94-0008 "The Northridge, California Earthquake of January 17, 1994: Performance of Highway Bridges," edited by I.G. Buckle, 3/24/94, (PB94-193851, A06, MF-A02).

NCEER-94-0009 "Proceedings of the Third U.S.-Japan Workshop on Earthquake Protective Systems for Bridges," edited by I.G. Buckle and I. Friedland, 3/31/94, (PB94-195815, A99, MF-A06).

NCEER-94-0010 "3D-BASIS-ME: Computer Program for Nonlinear Dynamic Analysis of Seismically Isolated Single and Multiple Structures and Liquid Storage Tanks," by P.C. Tsopelas, M.C. Constantinou and A.M. Reinhorn, 4/12/94, (PB94-204922, A09, MF-A02).

NCEER-94-0011 "The Northridge, California Earthquake of January 17, 1994: Performance of Gas Transmission Pipelines," by T.D. O'Rourke and M.C. Palmer, 5/16/94, (PB94-204989, A05, MF-A01).

NCEER-94-0012 "Feasibility Study of Replacement Procedures and Earthquake Performance Related to Gas Transmission Pipelines," by T.D. O'Rourke and M.C. Palmer, 5/25/94, (PB94-206638, A09, MF-A02).

NCEER-94-0013 "Seismic Energy Based Fatigue Damage Analysis of Bridge Columns: Part II - Evaluation of Seismic Demand," by G.A. Chang and J.B. Mander, 6/1/94, (PB95-18106, A08, MF-A02).

NCEER-94-0014 "NCEER-Taisei Corporation Research Program on Sliding Seismic Isolation Systems for Bridges: Experimental and Analytical Study of a System Consisting of Sliding Bearings and Fluid Restoring Force/Damping Devices," by P. Tsopelas and M.C. Constantinou, 6/13/94, (PB94-219144, A10, MF-A03).

NCEER-94-0015 "Generation of Hazard-Consistent Fragility Curves for Seismic Loss Estimation Studies," by H. Hwang and J-R. Huo, 6/14/94, (PB95-181996, A09, MF-A02).

NCEER-94-0016 "Seismic Study of Building Frames with Added Energy-Absorbing Devices," by W.S. Pong, C.S. Tsai and G.C. Lee, 6/20/94, (PB94-219136, A10, A03).

NCEER-94-0017 "Sliding Mode Control for Seismic-Excited Linear and Nonlinear Civil Engineering Structures," by J. Yang, J. Wu, A. Agrawal and Z. Li, 6/21/94, (PB95-138483, A06, MF-A02).

NCEER-94-0018 "3D-BASIS-TABS Version 2.0: Computer Program for Nonlinear Dynamic Analysis of Three Dimensional Base Isolated Structures," by A.M. Reinhorn, S. Nagarajaiah, M.C. Constantinou, P. Tsopelas and R. Li, 6/22/94, (PB95-182176, A08, MF-A02).

NCEER-94-0019 "Proceedings of the International Workshop on Civil Infrastructure Systems: Application of Intelligent Systems and Advanced Materials on Bridge Systems," Edited by G.C. Lee and K.C. Chang, 7/18/94, (PB95-252474, A20, MF-A04).

NCEER-94-0020 "Study of Seismic Isolation Systems for Computer Floors," by V. Lambrou and M.C. Constantinou, 7/19/94, (PB95-138533, A10, MF-A03).

NCEER-94-0021 "Proceedings of the U.S.-Italian Workshop on Guidelines for Seismic Evaluation and Rehabilitation of Unreinforced Masonry Buildings," Edited by D.P. Abrams and G.M. Calvi, 7/20/94, (PB95-138749, A13, MF-A03).

NCEER-94-0022 "NCEER-Taisei Corporation Research Program on Sliding Seismic Isolation Systems for Bridges: Experimental and Analytical Study of a System Consisting of Lubricated PTFE Sliding Bearings and Mild Steel Dampers," by P. Tsopelas and M.C. Constantinou, 7/22/94, (PB95-182184, A08, MF-A02).

NCEER-94-0023 "Development of Reliability-Based Design Criteria for Buildings Under Seismic Load," by Y.K. Wen, H. Hwang and M. Shinozuka, 8/1/94, (PB95-211934, A08, MF-A02).

NCEER-94-0024 "Experimental Verification of Acceleration Feedback Control Strategies for an Active Tendon System," by S.J. Dyke, B.F. Spencer, Jr., P. Quast, M.K. Sain, D.C. Kaspari, Jr. and T.T. Soong, 8/29/94, (PB95-212320, A05, MF-A01).

NCEER-94-0025 "Seismic Retrofitting Manual for Highway Bridges," Edited by I.G. Buckle and I.F. Friedland, published by the Federal Highway Administration (PB95-212676, A15, MF-A03).

NCEER-94-0026 "Proceedings from the Fifth U.S.-Japan Workshop on Earthquake Resistant Design of Lifeline Facilities and Countermeasures Against Soil Liquefaction," Edited by T.D. O'Rourke and M. Hamada, 11/7/94, (PB95-220802, A99, MF-E08).

NCEER-95-0001 "Experimental and Analytical Investigation of Seismic Retrofit of Structures with Supplemental Damping: Part 1 - Fluid Viscous Damping Devices," by A.M. Reinhorn, C. Li and M.C. Constantinou, 1/3/95, (PB95-266599, A09, MF-A02).

NCEER-95-0002 "Experimental and Analytical Study of Low-Cycle Fatigue Behavior of Semi-Rigid Top-And-Seat Angle Connections," by G. Pekcan, J.B. Mander and S.S. Chen, 1/5/95, (PB95-220042, A07, MF-A02).

NCEER-95-0003 "NCEER-ATC Joint Study on Fragility of Buildings," by T. Anagnos, C. Rojahn and A.S. Kiremidjian, 1/20/95, (PB95-220026, A06, MF-A02).

NCEER-95-0004 "Nonlinear Control Algorithms for Peak Response Reduction," by Z. Wu, T.T. Soong, V. Gattulli and R.C. Lin, 2/16/95, (PB95-220349, A05, MF-A01).

NCEER-95-0005 "Pipeline Replacement Feasibility Study: A Methodology for Minimizing Seismic and Corrosion Risks to Underground Natural Gas Pipelines," by R.T. Eguchi, H.A. Seligson and D.G. Honegger, 3/2/95, (PB95-252326, A06, MF-A02).

NCEER-95-0006 "Evaluation of Seismic Performance of an 11-Story Frame Building During the 1994 Northridge Earthquake," by F. Naeim, R. DiSulio, K. Benuska, A. Reinhorn and C. Li, to be published.

NCEER-95-0007 "Prioritization of Bridges for Seismic Retrofitting," by N. Basöz and A.S. Kiremidjian, 4/24/95, (PB95-252300, A08, MF-A02).

NCEER-95-0008 "Method for Developing Motion Damage Relationships for Reinforced Concrete Frames," by A. Singhal and A.S. Kiremidjian, 5/11/95, (PB95-266607, A06, MF-A02).

NCEER-95-0009 "Experimental and Analytical Investigation of Seismic Retrofit of Structures with Supplemental Damping: Part II - Friction Devices," by C. Li and A.M. Reinhorn, 7/6/95, (PB96-128087, A11, MF-A03).

NCEER-95-0010 "Experimental Performance and Analytical Study of a Non-Ductile Reinforced Concrete Frame Structure Retrofitted with Elastomeric Spring Dampers," by G. Pekcan, J.B. Mander and S.S. Chen, 7/14/95, (PB96-137161, A08, MF-A02).

NCEER-95-0011 "Development and Experimental Study of Semi-Active Fluid Damping Devices for Seismic Protection of Structures," by M.D. Symans and M.C. Constantinou, 8/3/95, (PB96-136940, A23, MF-A04).

NCEER-95-0012 "Real-Time Structural Parameter Modification (RSPM): Development of Innervated Structures," by Z. Liang, M. Tong and G.C. Lee, 4/11/95, (PB96-137153, A06, MF-A01).

NCEER-95-0013 "Experimental and Analytical Investigation of Seismic Retrofit of Structures with Supplemental Damping: Part III - Viscous Damping Walls," by A.M. Reinhorn and C. Li, 10/1/95, (PB96-176409, A11, MF-A03).

NCEER-95-0014 "Seismic Fragility Analysis of Equipment and Structures in a Memphis Electric Substation," by J-R. Huo and H.H.M. Hwang, (PB96-128087, A09, MF-A02), 8/10/95.

NCEER-95-0015 "The Hanshin-Awaji Earthquake of January 17, 1995: Performance of Lifelines," Edited by M. Shinozuka, 11/3/95, (PB96-176383, A15, MF-A03).

NCEER-95-0016 "Highway Culvert Performance During Earthquakes," by T.L. Youd and C.J. Beckman, available as NCEER-96-0015.

NCEER-95-0017 "The Hanshin-Awaji Earthquake of January 17, 1995: Performance of Highway Bridges," Edited by I.G. Buckle, 12/1/95, to be published.

NCEER-95-0018 "Modeling of Masonry Infill Panels for Structural Analysis," by A.M. Reinhorn, A. Madan, R.E. Valles, Y. Reichmann and J.B. Mander, 12/8/95.

NCEER-95-0019 "Optimal Polynomial Control for Linear and Nonlinear Structures," by A.K. Agrawal and J.N. Yang, 12/11/95, (PB96-168737, A07, MF-A02).

NCEER-95-0020 "Retrofit of Non-Ductile Reinforced Concrete Frames Using Friction Dampers," by R.S. Rao, P. Gergely and R.N. White, 12/22/95, (PB97-133508, A10, MF-A02).

NCEER-95-0021 "Parametric Results for Seismic Response of Pile-Supported Bridge Bents," by G. Mylonakis, A. Nikolaou and G. Gazetas, 12/22/95, (PB97-100242, A12, MF-A03).

NCEER-95-0022 "Kinematic Bending Moments in Seismically Stressed Piles," by A. Nikolaou, G. Mylonakis and G. Gazetas, 12/23/95.

NCEER-96-0001 "Dynamic Response of Unreinforced Masonry Buildings with Flexible Diaphragms," by A.C. Costley and D.P. Abrams," 10/10/96.

NCEER-96-0002 "State of the Art Review: Foundations and Retaining Structures," by I. Po Lam, to be published.

NCEER-96-0003 "Ductility of Rectangular Reinforced Concrete Bridge Columns with Moderate Confinement," by N. Wehbe, M. Saiidi, D. Sanders and B. Douglas, 11/7/96, (PB97-133557, A06, MF-A02).

NCEER-96-0004 "Proceedings of the Long-Span Bridge Seismic Research Workshop," edited by I.G. Buckle and I.M. Friedland, to be published.

NCEER-96-0005 "Establish Representative Pier Types for Comprehensive Study: Eastern United States," by J. Kulicki and Z. Prucz, 5/28/96.

NCEER-96-0006 "Establish Representative Pier Types for Comprehensive Study: Western United States," by R. Imbsen, R.A. Schamber and T.A. Osterkamp, 5/28/96.

NCEER-96-0007 "Nonlinear Control Techniques for Dynamical Systems with Uncertain Parameters," by R.G. Ghanem and M.I. Bujakov, 5/27/96, (PB97-100259, A17, MF-A03).

NCEER-96-0008 "Seismic Evaluation of a 30-Year Old Non-Ductile Highway Bridge Pier and Its Retrofit," by J.B. Mander, B. Mahmoodzadegan, S. Bhadra and S.S. Chen, 5/31/96.

NCEER-96-0009 "Seismic Performance of a Model Reinforced Concrete Bridge Pier Before and After Retrofit," by J.B. Mander, J.H. Kim and C.A. Ligozio, 5/31/96.

NCEER-96-0010 "IDARC2D Version 4.0: A Computer Program for the Inelastic Damage Analysis of Buildings," by R.E. Valles, A.M. Reinhorn, S.K. Kunnath, C. Li and A. Madan, 6/3/96, (PB97-100234, A17, MF-A03).

NCEER-96-0011 "Estimation of the Economic Impact of Multiple Lifeline Disruption: Memphis Light, Gas and Water Division Case Study," by S.E. Chang, H.A. Seligson and R.T. Eguchi, 8/16/96, (PB97-133490, A11, MF-A03).

NCEER-96-0012 "Proceedings from the Sixth Japan-U.S. Workshop on Earthquake Resistant Design of Lifeline Facilities and Countermeasures Against Soil Liquefaction, Edited by M. Hamada and T. O'Rourke, 9/11/96, (PB97-133581, A99, MF-A06).

NCEER-96-0013 "Chemical Hazards, Mitigation and Preparedness in Areas of High Seismic Risk: A Methodology for Estimating the Risk of Post-Earthquake Hazardous Materials Release," by H.A. Seligson, R.T. Eguchi, K.J. Tierney and K. Richmond, 11/7/96.

NCEER-96-0014 "Response of Steel Bridge Bearings to Reversed Cyclic Loading," by J.B. Mander, D-K. Kim, S.S. Chen and G.J. Premus, 11/13/96, (PB97-140735, A12, MF-A03).

NCEER-96-0015 "Highway Culvert Performance During Past Earthquakes," by T.L. Youd and C.J. Beckman, 11/25/96, (PB97-133532, A06, MF-A01).

NCEER-97-0001 "Evaluation, Prevention and Mitigation of Pounding Effects in Building Structures," by R.E. Valles and A.M. Reinhorn, 2/20/97, (PB97-159552, A14, MF-A03).

NCEER-97-0002 "Seismic Design Criteria for Bridges and Other Highway Structures," by C. Rojahn, R. Mayes, D.G. Anderson, J. Clark, J.H. Hom, R.V. Nutt and M.J. O'Rourke, 4/30/97, (PB97-194658, A06, MF-A03).

NCEER-97-0003 "Proceedings of the U.S.-Italian Workshop on Seismic Evaluation and Retrofit," Edited by D.P. Abrams and G.M. Calvi, 3/19/97, (PB97-194666, A13, MF-A03).

NCEER-97-0004 "Investigation of Seismic Response of Buildings with Linear and Nonlinear Fluid Viscous Dampers," by A.A. Seleemah and M.C. Constantinou, 5/21/97, (PB98-109002, A15, MF-A03).

NCEER-97-0005 "Proceedings of the Workshop on Earthquake Engineering Frontiers in Transportation Facilities," edited by G.C. Lee and I.M. Friedland, 8/29/97, (PB98-128911, A25, MR-A04).

NCEER-97-0006 "Cumulative Seismic Damage of Reinforced Concrete Bridge Piers," by S.K. Kunnath, A. El-Bahy, A. Taylor and W. Stone, 9/2/97, (PB98-108814, A11, MF-A03).

NCEER-97-0007 "Structural Details to Accommodate Seismic Movements of Highway Bridges and Retaining Walls," by R.A. Imbsen, R.A. Schamber, E. Thorkildsen, A. Kartoum, B.T. Martin, T.N. Rosser and J.M. Kulicki, 9/3/97.

NCEER-97-0008 "A Method for Earthquake Motion-Damage Relationships with Application to Reinforced Concrete Frames," by A. Singhal and A.S. Kiremidjian, 9/10/97, (PB98-108988, A13, MF-A03).

NCEER-97-0009 "Seismic Analysis and Design of Bridge Abutments Considering Sliding and Rotation," by K. Fishman and R. Richards, Jr., 9/15/97, (PB98-108897, A06, MF-A02).

NCEER-97-0010 "Proceedings of the FHWA/NCEER Workshop on the National Representation of Seismic Ground Motion for New and Existing Highway Facilities," edited by I.M. Friedland, M.S. Power and R.L. Mayes, 9/22/97.

NCEER-97-0011 "Seismic Analysis for Design or Retrofit of Gravity Bridge Abutments," by K.L. Fishman, R. Richards, Jr. and R.C. Divito, 10/2/97, (PB98-128937, A08, MF-A02).

NCEER-97-0012 "Evaluation of Simplified Methods of Analysis for Yielding Structures," by P. Tsopelas, M.C. Constantinou, C.A. Kircher and A.S. Whittaker, 10/31/97, (PB98-128929, A10, MF-A03).

NCEER-97-0013 "Seismic Design of Bridge Columns Based on Control and Repairability of Damage," by C-T. Cheng and J.B. Mander, 12/8/97.

NCEER-97-0014 "Seismic Resistance of Bridge Piers Based on Damage Avoidance Design," by J.B. Mander and C-T. Cheng, 12/10/97.

NCEER-97-0015 "Seismic Response of Nominally Symmetric Systems with Strength Uncertainty," by S. Balopoulou and M. Grigoriu, 12/23/97.

NCEER-97-0016 "Evaluation of Seismic Retrofit Methods for Reinforced Concrete Bridge Columns," by T.J. Wipf, F.W. Klaiber and F.M. Russo, 12/28/97.

NCEER-97-0017 "Seismic Fragility of Existing Conventional Reinforced Concrete Highway Bridges," by C.L. Mullen and A.S. Cakmak, 12/30/97.

NCEER-97-0018 "Loss Asssessment of Memphis Buildings," edited by D.P. Abrams and M. Shinozuka, 12/31/97.

NCEER-97-0019 "Seismic Evaluation of Frames with Infill Walls Using Quasi-static Experiments," by K.M. Mosalam, R.N. White and P. Gergely, 12/31/97.

50272-101

REPORT DOCUMENTATION PAGE	1. REPORT NO. NCEER-97-0019	2.	3. Recipient's Accession No.

4. Title and Subtitle
Seismic Evaluation of Frames with Infill Walls Using Quasi-static Experiments

5. Report Date
December 31, 1997

6.

7. Author(s)
Khalid M. Mosalam, Richard N. White and Peter Gergely

8. Performing Organization Rept. No.

9. Performing Organization Name and Address
Cornell University
School of Civil and Environmental Engineering
Ithaca, NY 14853

10. Project/Task/Work Unit No.
93-3111, 94-3111, 94-3112
95-3111

11. Contract(C) or Grant(G) No.
(C) NSF-BCS 90-25010
(G)

12. Sponsoring Organization Name and Address
National Center for Earthquake Engineering Research
State University of New York at Buffalo
Red Jacket Quadrangle
Buffalo, NY 14261

13. Type of Report & Period Covered

14.

15. Supplementary Notes
This research was conducted at Cornell University and was supported in whole or in part by the National Science Foundation under Grant No. BCS 90-25010 and other sponsors

16. Abstract (Limit: 200 words)

This report treats an experimental investigation of gravity load designed steel frames, ie, steel frames with semi-rigid connections, infilled with unreinforced masonry walls and subjected to slowly applied cyclic lateral loads. An investigation of the mechanical properties of the materials used in constructing the masonry infill walls is included. Various geometrical configurations of the frame and the infill walls, and different material types of the masonry walls, are considered. Based on the results, a hysteresis model for infilled frames is formulated and discussed. All parameters in the model have physical meaning and are calibrated with experimental data.

17. Document Analysis a. Descriptors

Earthquake engineering. Gravity load design. Infilled frames. Steel frames. Unreinforced masonry infill walls. Semi-rigid connections. Cyclic lateral loads. Hysteresis models. Mortar joints. Experimental tests. Quasi-static tests.

b. Identifiers/Open-Ended Terms

c. COSATI Field/Group

18. Availability Statement	19. Security Class (This Report)	21. No. of Pages
Release unlimited	Unclassified	105
	20. Security Class (This Page) Unclassified	22. Price